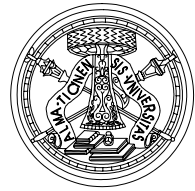




Istituto Universitario
di Studi Superiori



Università degli
Studi di Pavia

EUROPEAN SCHOOL FOR ADVANCED STUDIES IN
REDUCTION OF SEISMIC RISK

ROSE SCHOOL

MODELLING OF FRP-CONFINEMENT OF RECTANGULAR RC SECTIONS

A Dissertation Submitted in Partial
Fulfilment of the Requirements for the Master Degree in

EARTHQUAKE ENGINEERING

by

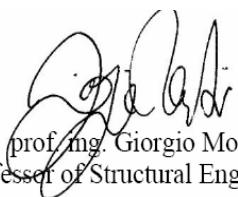
KONSTANTINOS GEORGIOU MEGALOOIKONOMOU

Supervisor: Prof. G.Monti

May, 2007

The dissertation entitled “Modelling of FRP-Confinement of Rectangular RC Sections”, by Konstantinos G.Megalooikonomou, has been approved in partial fulfilment of the requirements for the Master Degree in Earthquake Engineering.

Professor Giorgio Monti



prof. ing. Giorgio Monti
(Professor of Structural Engineering)

Professor Thanasis Triantafillou



*To Professor
S.J.Pantazopoulou
for her trust and support*

ABSTRACT

The behaviour of fiber reinforced polymer (FRP) - confined concrete in circular columns has been extensively studied, but much less is known about concrete in FRP- confined rectangular columns in which the concrete is non-uniformly confined and the effectiveness of confinement is much reduced. In this thesis a mechanistic based and design oriented stress strain model for FRP-confined rectangular columns is presented. To this end, FRP are introduced as innovative materials for retrofitting of existing structures, the confinement effect on concrete is extensively described along with a literature review of existing models of confinement of RC sections. Finally, the model is presented with all the necessary analysis results for a more clear comprehension of the proposed iteration procedure.

Keywords: Confinement; FRP; concrete; column; rectangular; model; stress-strain behaviour

ACKNOWLEDGEMENTS

First of all, I would like to thank sincerely my supervisor Professor Giorgio Monti and his students Andrea Lucchini, Silvia Alessandri and Marc'Antonio Liotta for creating for me a very inspiring environment during my stay in Rome which determinately helped me to reach the results presented in this thesis .In addition, I would like to underline also the contribution of Professor Nicola Nisticó and thank him for his valuable advices. Finally, special thanks should be given to Professor R. Realfonso and the University of Salerno of Italy for the important contribution with necessary experimental results for the verification of the proposed procedure.

TABLE OF CONTENTS

	Page
ABSTRACT	i
ACKNOWLEDGEMENTS	ii
TABLE OF CONTENTS	iii
LIST OF FIGURES	v
LIST OF TABLES	viii
1 INTRODUCTION	1
2 THE MATERIAL: FIBER REINFORCED POLYMERS	3
2.1 Introduction	3
2.2 Retrofit of existing structures with FRP	3
2.3 Benefits & Drawbacks of FRPs	4
2.4 Composition	5
2.4.1 Resins	6
2.4.2 Reinforcements	9
2.5 Reinforcement Forms	13
2.6 Fillers	16
2.6.1 Filler Types	16
2.6.2 Using Fillers in Composites	17
2.7 Additives and Modifiers	18
2.7.1 Additive Functions	18
2.7.2 Catalysts, Promoters, Inhibitors	20
2.8 Adhesives	21
2.9 Codes & Standards	21
2.9.1 Committees	21
2.9.2 Organizations	23

2.9.3 Standards Development	24
2.9.4 Technology Transfer	25
3 LITERATURE REVIEW	27
3.1 Basic characteristics of confinement effect on concrete	27
3.1.1 Behaviour under lateral hydraulic pressure.....	28
3.1.2 Behaviour under Biaxial Stress Condition.....	29
3.1.3 Modeling of concrete under Multi-axial Stresses	29
3.2 Lateral confinement by ties.....	31
3.2.1 Stress-Strain Models under Monotonic Loading	34
3.3 Lateral confinement by FRP jacketing.....	36
3.3.1 FRP-confined concrete in circular sections	38
3.3.2 FRP-confined concrete in rectangular sections.....	43
4 MODEL PROPOSAL.....	50
4.1 Introduction.....	50
4.2 Numerical analysis (FEM).....	51
4.3 Simplified Mechanical Model.....	55
4.4 Proposed Model in MATLAB code with user's interface	68
5 CORRELATION WITH EXPERIMENTAL RESULTS.....	70
5.1 Introduction.....	70
5.2 Experimental Study of University of Salerno of Italy	70
5.3 Experimental Results from the technical report of Department of Transportation of Florida of USA (FDOT)	75
5.4 Conclusions.....	78
6 REFERENCES	80
APPENDIX A.....	1

LIST OF FIGURES

	Page
Figure 2.1. Techniques of structural intervention with FRPs (Aslan FRP- Hughes Brothers)...	4
Figure 2.2 Stress Strain relationship of Matrix, fibers and resulted FRP (CNR-DT200 2004)..	5
Figure 2.3. Epoxy Resins (Edge Structural Composites)	7
Figure 2.4. Carbon Fibers (Aslan FRP- Hughes Brothers).....	11
Figure 2.5. Stress Strain diagram for different reinforcing fibers (CNR DT200 2004)	12
Figure 2.6. Different reinforcement forms (Sika Design Manual)	13
Figure 2.7. Diagram of Stitched Triaxial and Quadraxial Fabrics	14
Figure 2.8. Biaxial & Triaxial Fabrics	15
Figure 2.9. Strength Relation to fiber orientation [Schwartz (1992B)]	15
Figure 3.1. Confinement effect of concrete.	27
Figure 3.2. Axial Stress Strain curve with Lateral confining pressure. (Richart, Brandzaeg and Brown 1928)	28
Figure 3.3. Biaxial concrete strength (Kupfer, Hilsdorf and H. Rush, 1969)	29
Figure 3.4. Ultimate strength surface (CEB State of the art report)	30
Figure 3.5. Test of columns under axial compression (Sugano et al 1985).....	32
Figure 3.6. Fully confined and unconfined parts at the cross-section level and along the length of the member a) circular ties b) rectangular ties (Sheikh and Uzumeri).....	33
Figure 3.7. Test of columns under axial compression (Park and Kent 1971).....	34
Figure 3.8. Confinement model by Mander et al (1988)	35
Figure 3.9. FRP wrapping of concrete cylinder	36
Figure 3.10. Comparison of GFRP, CFRP and steel confined stress-strain concrete behaviour. (Spoelstra & Monti)	37
Figure 3.11. Behaviour of FRP confined circular sections	38

Figure3.12. Stress-strain Behaviour of FRP confined cylinders (Spoelstra&Monti)	39
Figure3.13. Effective confining area used in modelling FRP-confinement of rectangular RC sections. (CNR-DT200 2004)	44
Figure4.1. Confining mechanisms for circular and rectangular sections.....	50
Figure4.2. Transverse section of short square column confined with FRP.	51
Figure4.3. Transverse section of short square column confined with FRP.	51
Figure4.4. Confining stresses (normal) along the diagonal direction in every joint.....	52
Figure4.5. Confining stresses (normal) perpendicular to the diagonal direction in every joint.	52
Figure4.6 Confining stresses (normal) parallel to the sides' directions in every joint	53
Figure4.7 Confining stresses (normal) perpendicular to the sides' directions in every joint ...	53
Figure4.8 Uniaxially and Biaxially confined regions-Check for different thicknesses of FRP Jacketing	54
Figure4.9 Uniaxially and Biaxially confined regions-Check for different radii of the rounded corners.....	54
Figure4.10 Defining the different regions in the section	55
Figure4.11 "Generalized" springs.....	55
Figure4.12 Vertical and lateral behaviour of "Generalized" springs.....	56
Figure4.13 Volumetric Strains to Axial Strains (Pantazopoulou&Mills).....	56
Figure4.14 Volumetric Strains to Axial Stresses (Technical Report FDOT)	58
Figure4.15 Deformed Shape of a rectangular section based only on the diagonal lateral deformation	59
Figure4.16 Diagonal force applied to the lateral springs from the corner of the section	60
Figure4.17 Confinement effectiveness factor (Gebran Karam & Mazen Tabbara (2005)).....	60
Figure4.18 Confining pressures in the different regions	62
Figure4.19 Proposed Iteration Procedure	66
Figure4.20 Proposed Model in MATLAB code with user's interface.....	68
Figure5.1 Specimen Configuration (University of Salerno, Italy)	70
Figure5.2 Comparison with experimental results (University of Salerno, Italy)	72
Figure5.3 Comparison with experimental results (University of Salerno, Italy).....	72
Figure5.4 Comparison with experimental results (University of Salerno, Italy).....	73
Figure5.5 Comparison with experimental results (University of Salerno, Italy).....	73

Figure5.6 Comparison with experimental results (University of Salerno, Italy).....	74
Figure5.7 Comparison with experimental results (University of Salerno, Italy).....	74
Figure5.8 Location of longitudinal and transverse strain gages (Shahawy et al (2003))	75
Figure5.9 Comparison with Experimental Results (Technical Report FDOT)	77
Figure5.10 Comparison with Experimental Results (Technical Report FDOT)	78

LIST OF TABLES

	Page
Table 2.1. Properties of different types of FRPs.....	9
Table 2.2. Comparison between properties of fibers, resins and steel. (typical values).....	12
Table 2.3. Committees for development of structural intervention with FRPs around the world.	21
Table 2.4. FRP Codes around the world.	24
Table 2.5. Organizations & Activities on FRP.	25
Table 3.1. Proposed values for the parameters of the failure criterion of N.S.Ottosen.	31
Table 3.2. Proposed models for FRP-confined concrete (Technical Report FDOT).....	48
Table 3.3. Proposed models for FRP-confined concrete (Technical Report FDOT).....	49
Table 4.1. Proposed values for the parameters of the failure criterion of N.S.Ottosen.	64
Table 4.2. Factor k from existing experimental results (Lam&Teng).	67
Table 5.1. Material Properties.....	71
Table 5.2. Specimen configuration and performance.	71
Table 5.3. Material Properties of Carbon wraps (Shahawy et al (2003))	75
Table 5.4. Specimen Configuration(Shahawy et al (2003))	76

1 INTRODUCTION

Confining wraps or Jackets to rehabilitate and reinforce existing concrete columns represent a principal application of fiber reinforced polymers (FRP). In the last decade multiple research efforts coupled with field applications of FRP wraps as passive confinement to concrete columns have been carried out exploring all the aspects of technique.

Simple models for calculating the strengthening effect have failed to account for two major experimental observations: (1) the apparent average failure strains of the FRP wraps are of the order of 50-80% of the failure strains of tensile coupons made of the same material (Karbhari and Gao 1997; Mirmiran et.al. 1998; Xiao and Wu 2000); and (2) passively confined square and rectangular columns with sharp corners are less efficiently strengthened than circular columns (Mirmiran et.al. 1998; Rochette and Labossiere 2000 ; Pessiki et.al. 2001 ; Yang et.al. 2001; Karam and Tabbara 2002 ; Chaalal et.al. 2003) .

In circular sections the induced by the applied axial load radial lateral displacement (meaning the same displacement around the circumference of the section) activates the confining device and causes radial confining forces or else hydrostatic confining pressure. This pressure results to stress state which is the same in every point of the section. On the other hand, in rectangular sections, the confining device can confine the lateral displacement of corner parts but can not confine the displacement outside the central part of the sides from character of the rectangular section which results to different stress-state in every point of the section.

The effect of FRP wraps is twofold in concrete columns. First, the FRP wrap causes an increase in the confined concrete peak stress with reference to unconfined concrete. This is caused by elastic Poisson's lateral stresses followed by nonlinear dilatational behaviour of concrete due to prepeak cracking. Second, the FRP wrap increases the post peak ductility and ultimate strength of the concrete column developing a pseudo ductile plateau. This is caused by the mechanisms of FRP wraps restraining the movement of discrete concrete blocks after the localization of concrete failure (Issa and Karam 2004).

In rectangular columns the first effect is weak –little increase has been observed in the concrete peak stress with reference to unconfined concrete indicating that little confining stresses have developed. Most of the improvement is observed post peak in the form of

increased ductility and ultimate strength.

Given the relative complexity of treating a generalized rectangular cross section versus a circular cross section, simplified macro structural approaches following Mander et.al. (1988) have been widely used to model the confinement effectiveness in rectangular sections. These approaches use empirical sectional reduction factors (Mander et.al. 1988; Canadian Standards Association 2002; Chung et al. 2002; Campione and Miraglia 2003; Maalej et al 2003 ;) based on two major assumptions:

1. The rectangular cross section can be divided into an unconfined and a confined area. The shape and extent of the unconfined area is derived from the possible arching of the confined material between the confined corners leaving unconfined areas by the flat sides.
2. The confined area is considered to be in a state of uniform biaxial confinement similar to that of the circular cross section, thus allowing the generalization of the formulations derived for circular confinement. The area of the circular cross section is replaced by the reduced area of the rectangle and the confinement level estimated for this equivalent “circular cross section” is deemed applicable to the rectangular cross section.

In the literature, all approaches have concentrated on relating the behaviour of rectangular columns to that of circular columns through the use of geometrically defined efficiency factor, such as described earlier, that allows the use of a unified approach based on the simple and robust formulations developed for the circular section problem.

In this thesis, taking into account all the above considerations, an iteration procedure is being proposed based on the outcome of 3d FEM analysis run by the author that the arching effect doesn't really exist in the case of FRP-confined concrete in rectangular sections. The unconfined “nails” are indeed partially confined so they contribute until their maximum strength (which is much lower than the inner part of the section) to the total strength of the rectangular sections. Based on a system of “generalized springs” but also on well known stress strain laws and a failure criterion, a simplified mechanical model which gives the stress strain behaviour of a rectangular RC section under concentric load is being proposed that can easily be understood and implemented by the designer. It is worthy underlying that its prediction is very close to performed experimental results which are taking into account all the necessary parameters like corner radius effect, rectangularity, type & stiffness of the FRP and concrete strength.

2 THE MATERIAL: FIBER REINFORCED POLYMERS

2.1 Introduction

Fiber Reinforced Polymer (FRP) composites is defined as a polymer (plastic) matrix, either thermo set or thermoplastic, that is reinforced (combined) with a fiber or other reinforcing material with a sufficient aspect ratio (length to thickness) to provide a discernable reinforcing function in one or more directions. FRP composites are different from traditional construction materials such as steel or aluminium. FRP composites are anisotropic (properties only apparent in the direction of the applied load) whereas steel or aluminium is isotropic (uniform properties in all directions, independent of applied load). Therefore, FRP composite properties are directional, meaning that the best mechanical properties are in the direction of the fiber placement. Composites are similar to reinforced concrete where the rebar is embedded in an isotropic matrix called concrete.

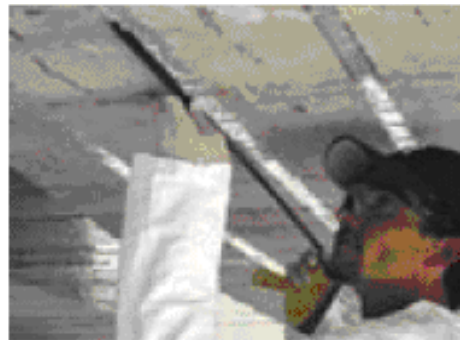
Many terms have been used to define FRP composites. Modifiers have been used to identify a specific fiber such as Glass Fiber Reinforced Polymer (GFRP), Carbon Fiber Reinforced Polymer (CFRP), and Aramid Fiber Reinforced Polymer (AFRP). Another familiar term used is Fiber Reinforced Plastics. In addition, other acronyms were developed over the years and its use depended on geographical location or market use. For example, Fiber Reinforced Composites (FRC), Glass Reinforced Plastics (GRP), and Polymer Matrix Composites (PMC) can be found in many references. Although different, each of aforementioned terms mean the same thing; FRP composites.

2.2 Retrofit of existing structures with FRP

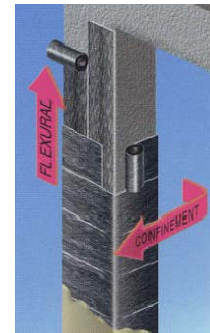
The retrofit of existing reinforced and prestressed concrete structures but also those made of masonry has always been a crucial field where Civil engineering has to give solutions. Despite of the natural aging and damage of structures and materials there are many other reasons that make necessary the structural intervention, like the change of use of a structure, the insufficient initial design or bad performance of design during construction, the environmental effects, the lack of well preservation of the structure and finally and most important random loading like earthquakes or fire or impact effects.

This need for renovation and rehabilitation of structures has lead to seek of new

materials which can make the intervention easier and more effective. FRP belong to this new generation of materials. Generally, we can limit the ways of retrofitting with those materials in two categories. First, are the externally bonded (EBR) FRPs usually in the form of laminates or rovings and second the near surface mounted (NSM), into superficial structural members' grooves, FRPs in the form of bars or laminates.



(a) NSM FRPs



(b) EBR FRPs

Figure 2.1. Techniques of structural intervention with FRPs (Aslan FRP- Hughes Brothers)

2.3 Benefits & Drawbacks of FRPs

FRP composites have many benefits to their selection and use. The selection of the materials depends on the performance and intended use of the product. The composites designer can tailor the performance of the end product with proper selection of materials. It is important for the end-user to understand the application environment, load performance and durability requirements of the product and convey this information to the composites industry professional. A summary of composite material benefits include:

- Light weight
- High strength-to-weight ratio
- Directional strength
- Corrosion resistance
- Weather resistance
- Dimensional stability
- low thermal conductivity
- low coefficient of thermal expansion
- Radar transparency
- Non-magnetic

- High impact strength
- High dielectric strength (insulator)
- Low maintenance
- Long term durability
- Part consolidation
- Small to large part geometry possible
- Tailored surface finish

The drawbacks of the material can be summarized in the following points:

- High Cost
- Brittle materials. Their performance is linear elastic until failure, albeit this happens at a high deformation level.
- The non-compatible coefficient of thermal expansion with this one of concrete and masonry.
- They are vulnerable to fire and generally to high temperatures.
- Reduction of tensile strength and Young Modulus when they are under continuous drench or alkaline environment.

2.4 Composition

Composites are composed of resins, reinforcements, fillers, and additives. Each of these constituent materials or ingredients play an important role in the processing and final performance of the end product. The resin or polymer (matrix) is the “glue” that holds the composite together and influences the physical properties of the end product. The reinforcement provides the mechanical strength. The fillers and additives are used as process or performance aids to impart special properties to the end product.

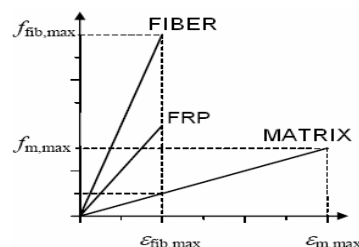


Figure 2.2 Stress Strain relationship of Matrix, fibers and resulted FRP (CNR-DT200 2004)

The mechanical properties and composition of FRP composites can be tailored for their intended use. The type and quantity of materials selected in addition to the manufacturing process to fabricate the product, will affect the mechanical properties and performance. Important considerations for the design of composite products include:

- Type of fiber reinforcement
- Percentage of fiber or fiber volume
- Orientation of fiber (0° , 90° , $\pm 45^\circ$ or a combination of these)
- Type of resin
- Cost of product
- Volume of production (to help determine the best manufacturing method)
- Manufacturing process
- Service conditions

2.4.1 Resins

The primary functions of the resin are to transfer stress between the reinforcing fibers, act as a glue to hold the fibers together, and protect the fibers from mechanical and environmental damage. Resins are divided into two major groups known as thermo set and thermoplastic. Thermoplastic resins become soft when heated, and may be shaped or molded while in a heated semi-fluid state and become rigid when cooled. Thermoset resins, on the other hand, are usually liquids or low melting point solids in their initial form. When used to produce finished goods, these thermosetting resins are “cured” by the use of a catalyst, heat or a combination of the two. Once cured, solid thermo set resins cannot be converted back to their original liquid form. Unlike thermoplastic resins, cured thermo sets will not melt and flow but will soften when heated (and lose hardness) and once formed they cannot be reshaped. Heat Distortion Temperature (HDT) and the Glass Transition Temperature (T_g) is used to measure the softening of a cured resin. Both test methods (HDT and T_g) measure the approximate temperature where the cured resin will soften significantly to yield (bend or sag) under load.

The most common thermosetting resins used in the composites industry are epoxies, unsaturated polyesters, vinyl esters and phenolics. There are differences between these groups that must be understood to choose the proper material for a specific application.



Figure 2.3. Epoxy Resins (Edge Structural Composites)

- **Epoxy**

Epoxy resins have a well-established record in a wide range of composite parts, structures and concrete repair. The structure of the resin can be engineered to yield a number of different products with varying levels of performance. A major benefit of epoxy resins over unsaturated polyester resins is their lower shrinkage. Epoxy resins can also be formulated with different materials or blended with other epoxy resins to achieve specific performance features. Cure rates can be controlled to match process requirements through the proper selection of hardeners and/or catalyst systems. Generally, epoxies are cured by addition of an anhydride or an amine hardener as a 2-part system. Different hardeners, as well as quantity of a hardener produce a different cure profile and give different properties to the finished composite.

Epoxies are used primarily for fabricating high performance composites with superior mechanical properties, resistance to corrosive liquids and environments, superior electrical properties, good performance at elevated temperatures, good adhesion to a substrate, or a combination of these benefits. Epoxy resins do not however, have particularly good UV resistance. Since the viscosity of epoxy is much higher than most polyester resin, requires a post-cure (elevated heat) to obtain ultimate mechanical properties making epoxies more difficult to use. However, epoxies emit little odor as compared to polyesters.

Epoxy resins are used with a number of fibrous reinforcing materials, including glass, carbon and aramid. This latter group is of small in volume, comparatively high cost and is usually used to meet high strength and/or high stiffness requirements. Epoxies are compatible with most composite manufacturing processes, particularly vacuum-bag molding, autoclave molding, pressure-bag molding, compression molding, filament winding and hand lay-up.

- **Polyester**

Unsaturated polyester resins (UPR) are the workhorse of the composites industry and represent approximately 75% of the total resins used. To avoid any confusion in terms, readers should be aware that there is a family of thermoplastic polyesters that are best known for their use as fibers for textiles and clothing. Thermo set polyesters are produced by the condensation polymerization of dicarboxylic acids and difunctional alcohols

(glycols). In addition, unsaturated polyesters contain an unsaturated material, such as maleic anhydride or fumaric acid, as part of the dicarboxylic acid component. The finished polymer is dissolved in a reactive monomer such as styrene to give a low viscosity liquid. When this resin is cured, the monomer reacts with the unsaturated sites on the polymer converting it to a solid thermo set structure.

A range of raw materials and processing techniques are available to achieve the desired properties in the formulated or processed polyester resin. Polyesters are versatile because of their capacity to be modified or tailored during the building of the polymer chains. They have been found to have almost unlimited usefulness in all segments of the composites industry. The principal advantage of these resins is a balance of properties (including mechanical, chemical, and electrical) dimensional stability, cost and ease of handling or processing.

Unsaturated polyesters are divided into classes depending upon the structures of their basic building blocks. Some common examples would be orthophthalic (“ortho”), isophthalic (“iso”), dicyclopentadiene (“DCPD”) and bisphenol A fumarate resins. In addition, polyester resins are classified according to end use application as either general purpose (GP) or specialty polyesters.

Polyester producers have proved willing and capable of supplying resins with the necessary properties to meet the requirements of specific end use applications. These resins can be formulated and chemically tailored to provide properties and process compatibility.

- **Vinyl Ester**

Vinyl esters were developed to combine the advantages of epoxy resins with the better handling/faster cure, which are typical for unsaturated polyester resins. These resins are produced by reacting epoxy resin with acrylic or methacrylic acid. This provides an unsaturated site, much like that produced in polyester resins when maleic anhydride is used. The resulting material is dissolved in styrene to yield a liquid that is similar to polyester resin. Vinyl esters are also cured with the conventional organic peroxides used with polyester resins. Vinyl esters offer mechanical toughness and excellent corrosion resistance. These enhanced properties are obtained without complex processing, handling or special shop fabricating practices that are typical with epoxy resins.

- **Phenolic**

Phenolics are a class of resins commonly based on phenol (carbolic acid) and formaldehyde. Phenolics are a thermosetting resin that cure through a condensation reaction producing water that should be removed during processing. Pigmented applications are limited to red, brown or black. Phenolic composites have many desirable performance qualities including high temperature resistance, creep resistance, excellent thermal insulation and sound damping properties, corrosion resistance and excellent fire/smoke/smoke toxicity properties. Phenolics are applied as adhesives or matrix binders in engineered woods (plywood), brake linings, clutch plates, circuit boards, to name a few.

- **Polyurethane**

Polyurethane is a family of polymers with widely ranging properties and uses, all based on the exothermic reaction of an organic polyisocyanates with a polyols (an alcohol containing more than one hydroxyl group). A few basic constituents of different molecular weights and functionalities are used to produce the whole spectrum of polyurethane materials. The versatility of polyurethane chemistry enables the polyurethane chemist to engineer polyurethane resin to achieve the desired properties.

Polyurethanes appear in an amazing variety of forms. These materials are all around us, playing important roles in more facets of our daily life than perhaps any other single polymer. They are used as a coating, elastomer, foam, or adhesive. When used as a coating in exterior or interior finishes, polyurethane's are tough, flexible, chemical resistant, and fast curing. Polyurethanes as an elastomer have superior toughness and abrasion is such applications as solid tires, wheels, bumper components or insulation. There are many formulations of polyurethane foam to optimize the density for insulation, structural sandwich panels, and architectural components. Polyurethanes are often used to bond composite structures together. Benefits of polyurethane adhesive bonds are that they have good impact resistance, the resin cures rapidly and the resin bonds well to a variety of different surfaces such as concrete.

Table 2.1. Properties of different types of FRPs.

Resins	Density (Kg/m ³)	Tensile Strength (Mpa)	Young's Modulus (Gpa)	Failure strain (%)
Epoxy	1200- 1300	55-130	2.8-4.1	3.0-10.0
Polyester	1100- 1460	35-104	2.1-4.1	<5.0
Vinyl ester	1120- 1320	73-81	3.0-5.5	3.5-5.5

2.4.2 Reinforcements

The primary function of fibers or reinforcements is to carry load along the length of the fiber to provide strength and stiffness in one direction. Reinforcements can be oriented to provide tailored properties in the direction of the loads imparted on the end product. Reinforcements can be both natural and man-made. Many materials are capable of

reinforcing polymers. Some materials, such as the cellulose in wood, are naturally occurring products. Most commercial reinforcements, however, are man-made. Of these, by far the largest volume reinforcement measured either in quantity consumed or in product sales, is glass fiber. Other composite reinforcing materials include carbon, aramid, UHMW (ultra high molecular weight) polyethylene, polypropylene, polyester and nylon. Carbon fiber is sometimes referred to as graphite fiber. The distinction is not important in an introductory text, but the difference has to do with the raw material and temperature at which the fiber is formed. More specialized reinforcements for high strength and high temperature use include metals and metal oxides such as those used in aircraft or aerospace applications.

Early in the development of composites, the only reinforcements available were derived from traditional textiles and fabrics. Particularly in the case of glass fibers, experience showed that the chemical surface treatments or “sizings” required to process these materials into fabrics and other sheet goods were detrimental to the adhesion of composite polymers to the fiber surface. Techniques to remove these materials were developed, primarily by continuous or batch heat cleaning. It was then necessary to apply new “coupling agents” (also known as finishes or surface treatments), an important ingredient in sizing systems, to facilitate adhesion of polymers to fibers, particularly under wet conditions and fiber processing.

Most reinforcements for either thermosetting or thermoplastic resins receive some form of surface treatments, either during fiber manufacture or as a subsequent treatment. Other materials applied to fibers as they are produced include resinous binders to hold fibers together in bundles and lubricants to protect fibers from degradation caused by process abrasion.

- **Glass Fibers**

Based on an alumina-lime-borosilicate composition, “E” glass produced fibers are considered the predominant reinforcement for polymer matrix composites due to their high electrical insulating properties, low susceptibility to moisture and high mechanical properties. Other commercial compositions include “S” glass, with higher strength, heat resistance and modulus, as well as some specialized glass reinforcements with improved chemical resistance, such as AR glass (alkali resistant).

Glass fibers used for reinforcing composites generally range in diameter from 0.00035” to 0.00090” (9 to 23 microns). Fibers are drawn at high speeds, approaching 200 miles per hour, through small holes in electrically heated bushings. These bushings form the individual filaments. The filaments are gathered into groups or bundles called “strands.” The filaments are attenuated from the bushing, water and air cooled, and then coated with a proprietary chemical binder or sizing to protect the filaments and enhance the composite laminate properties. The sizing also determines the processing characteristics of the glass fiber and the conditions at the fiber-matrix interface in the composite.

Glass is generally a good impact resistant fiber but weighs more than carbon or aramid. Glass fibers have excellent characteristics, equal to or better than steel in certain forms. The

lower modulus requires special design treatment where stiffness is critical. Composites made from this material exhibit very good electrical and thermal insulation properties. Glass fibers are also transparent to radio frequency radiation and are used in radar antenna applications.

- **Carbon Fibers**

Carbon fiber is created using polyacrylonitrile (PAN), pitch or rayon fiber precursors. PAN based fibers offer good strength and modulus values up to 85-90 Msi. They also offer excellent compression strength for structural applications up to 1000 ksi. Pitch fibers are made from petroleum or coal tar pitch. Pitch fibers extremely high modulus values (up to 140 Msi) and favorable coefficient of thermal expansion make them the material used in space/satellite applications. Carbon fibers are more expensive than glass fibers, however carbon fibers offer an excellent combination of strength, low weight and high modulus. The tensile strength of carbon fiber is equal to glass while its modulus is about three to four times higher than glass.



Figure 2.4. Carbon Fibers (Aslan FRP- Hughes Brothers)

Carbon fibers are supplied in a number of different forms, from continuous filament tows to chopped fibers and mats. The highest strength and modulus are obtained by using unidirectional continuous reinforcement. Twist-free tows of continuous filament carbon contain 1,000 to 75,000 individual filaments, which can be woven or knitted into woven roving and hybrid fabrics with glass fibers and aramid fibers.

Carbon fiber composites are more brittle (less strain at break) than glass or aramid. Carbon fibers can cause galvanic corrosion when used next to metals. A barrier material such as glass and resin is used to prevent this occurrence.

- **Aramid Fibers (Polyaramids)**

Aramid fiber is an aromatic polyimide that is a man-made organic fiber for composite reinforcement. Aramid fibers offer good mechanical properties at a low density with the added advantage of toughness or damage/impact resistance. They are characterized as having reasonably high tensile strength, a medium modulus, and a very low density as compared to glass and carbon. The tensile strength of aramid fibers are higher than glass fibers and the modulus is about fifty percent higher than glass. These fibers increase the

impact resistance of composites and provide products with higher tensile strengths. Aramid fibers are insulators of both electricity and heat. They are resistant to organic solvents, fuels and lubricants. Aramid composites are not as good in compressive strength as glass or carbon composites. Dry aramid fibers are tough and have been used as cables or ropes, and frequently used in ballistic applications.

Table 2.2. Comparison between properties of fibers, resins and steel. (typical values)

	Young's modulus E	Tensile strength σ_T	Strain at failure ε_T	Coefficient of thermal expansion α	Density ρ
	[GPa]	[MPa]	[%]	[$10^{-6} \text{ } ^\circ\text{C}^{-1}$]	[g/cm^3]
E-glass	70 – 80	2000 – 3500	3.5 – 4.5	5 – 5.4	2.5 – 2.6
S-glass	85 – 90	3500 – 4800	4.5 – 5.5	1.6 – 2.9	2.46 – 2.49
Carbon (high modulus)	390 – 760	2400 – 3400	0.5 – 0.8	-1.45	1.85 – 1.9
Carbon (high strength)	240 – 280	4100 – 5100	1.6 – 1.73	-0.6 – -0.9	1.75
Aramid	62 – 180	3600 – 3800	1.9 – 5.5	-2	1.44 – 1.47
Polymeric matrix	2.7 – 3.6	40 – 82	1.4 – 5.2	30 – 54	1.10 – 1.25
Steel	206	250 – 400 (yield) 350 – 600 (failure)	20 – 30	10.4	7.8

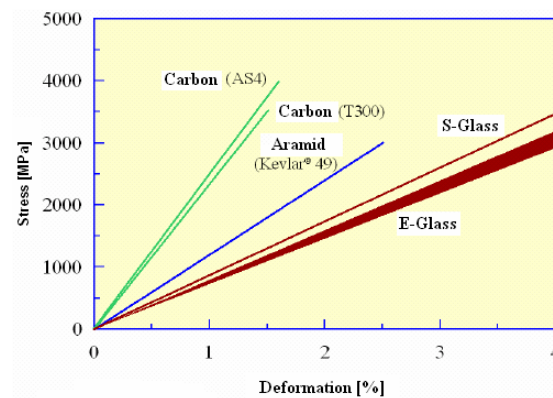


Figure 2.5. Stress Strain diagram for different reinforcing fibers (CNR DT200 2004)

2.5 Reinforcement Forms

Regardless of the material, reinforcements are available in forms to serve a wide range of processes and end-product requirements. Materials supplied as reinforcement include roving, milled fiber, chopped strands, continuous, chopped or thermo formable mat but also bars. Reinforcement materials can be designed with unique fiber architectures and be preformed (shaped) depending on the product requirements and manufacturing process.

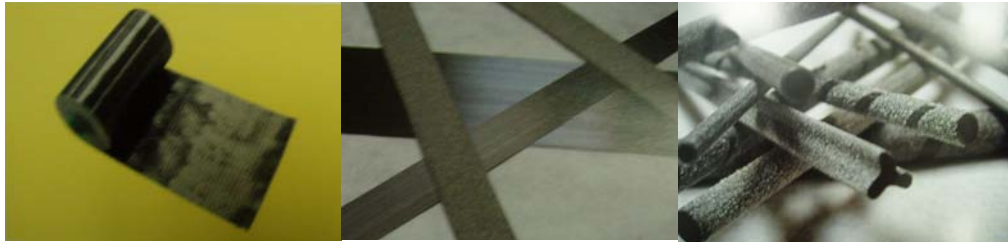


Figure 2.6. Different reinforcement forms (Sika Design Manual)

- **Multi-End and Single-End Rovings**

Rovings are utilized primarily in thermoset compounds, but can be utilized in thermoplastics. Multi-end rovings consist of many individual strands or bundles of filaments, which are then chopped and randomly deposited into the resin matrix. Processes such as sheet molding compound (SMC), preform and spray-up use the multi-end roving. Multi-end rovings can also be used in some filament winding and pultrusion applications. The single-end roving consists of many individual filaments wound into a single strand. The product is generally used in processes that utilize a unidirectional reinforcement such as filament winding or pultrusion.

- **Mats**

Reinforcing mats are usually described by weight-per-unit-of-area. For instance, a 2 ounce chopped strand mat will weigh 2 ounces per square yard. The type and amount of binder that is used to hold the mat together dictate differences between mat products. In some processes such as hand lay-up, it is necessary for the binder to dissolve. In other processes, particularly in compression molding, the binder must withstand the hydraulic forces and the dissolving action of the matrix resin during molding. Therefore, two general categories of mats are produced and are known as soluble and insoluble.

- **Woven, Stitched, Braided & 3-D Fabrics**

There are many types of fabrics that can be used to reinforce resins in a composite. Multidirectional reinforcements are produced by weaving, knitting, stitched or braiding continuous fibers into a fabric from twisted and plied yarn. Fabrics refer to all flat-sheet, roll goods, whether or not they are strictly fabrics. Fabrics can be manufactured utilizing almost any reinforcing fiber. The most common fabrics are constructed with fiberglass, carbon or aramid. Fabrics are available in several weave constructions and thickness (from

0.0010 to 0.40 inches). Fabrics offer oriented strengths and high reinforcement loadings often found in high performance applications.

Fabrics are typically supplied on rolls of 25 to 300 yards in length and 1 to 120 inches in width. The fabric must be inherently stable enough to be handled, cut and transported to the mold, but pliable enough to conform to the mold shape and contours. Properly designed, the fabric will allow for quick wet out and wet through of the resin and will stay in place once the resin is applied. Fabrics, like rovings and chopped strands, come with specific sizings or binder systems that promote adhesion to the resin system.

Fabrics allow for the precise placement of the reinforcement. This cannot be done with milled fibers or chopped strands and is only possible with continuous strands using relatively expensive fiber placement equipment. Due to the continuous nature of the fibers in most fabrics, the strength to weight ratio is much higher than that for the cut or chopped fiber versions. Stitched fabrics allow for customized fiber orientations within the fabric structure. This can be of great advantage when designing for shear or torsional stability.

Woven fabrics are fabricated on looms in a variety of weights, weaves, and widths. In a plain weave, each fill yarn or roving is alternately crosses over and under each warp fiber allowing the fabric to be more drapeable and conform to curved surfaces. Woven fabrics are manufactured where half of the strands of fiber are laid at right angles to the other half (0° to 90°). Woven fabrics are commonly used in boat manufacturing.

Stitched fabrics, also known as non-woven, non-crimped, stitched, or knitted fabrics have optimized strength properties because of the fiber architecture. Woven fabric is where two sets of interlaced continuous fibers are oriented in a 0° and 90° pattern where the fibers are crimped and not straight. Stitched fabrics are produced by assembling successive layers of aligned fibers. Typically, the available fiber orientations include the 0° direction (warp), 90° direction (weft or fill), and $\pm 45^\circ$ direction (bias). The assembly of each layer is then sewn together. This type of construction allows for load sharing between fibers so that a higher modulus, both tensile and flexural, is typically observed. The fiber architecture construction allows for optimum resin flow when composites are manufactured. These fabrics have been traditionally used in boat hulls for 50 years. Other applications include light poles, wind turbine blades, trucks, busses and underground tanks. These fabrics are currently used in bridge decks and column repair systems. Multiple orientations provide a quasi-isotropic reinforcement.

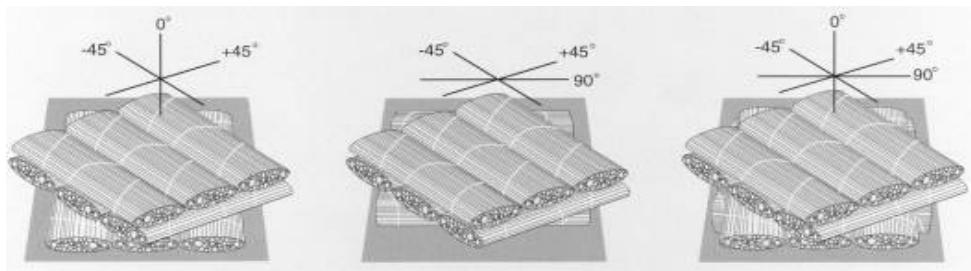


Figure 2.7. Diagram of Stitched Triaxial and Quadraxial Fabrics

Braided fabrics are engineered with a system of two or more yarns intertwined in such a way that all of the yarns are interlocked for optimum load distribution. Biaxial braids provide reinforcement in the bias direction only with fiber angles ranging from $\pm 15^\circ$ to $\pm 95^\circ$. Triaxial braids provide reinforcement in the bias direction with fiber angles ranging from $\pm 10^\circ$ to $\pm 80^\circ$ and axial (0°) direction.

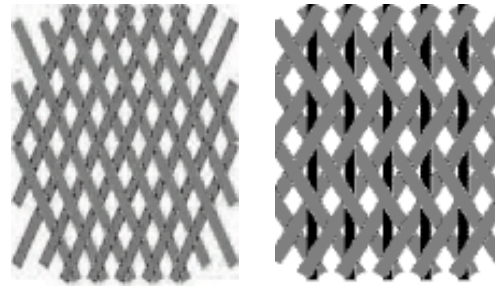


Figure 2.8. Biaxial & Triaxial Fabrics

- **Unidirectional**

Unidirectional reinforcements include tapes, tows, unidirectional tow sheets and rovings (which are collections of fibers or strands). Fibers in this form are all aligned parallel in one direction and uncrimped providing the highest mechanical properties. Composites using unidirectional tapes or sheets have high strength in the direction of the fiber. Unidirectional sheets are thin and multiple layers are required for most structural applications.

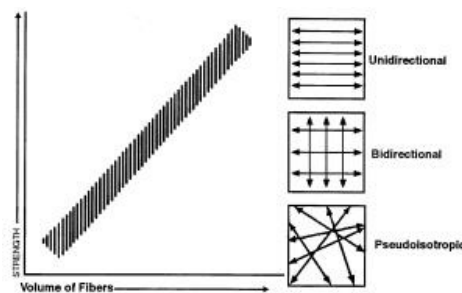


Figure 2.9. Strength Relation to fiber orientation [Schwartz (1992B)]

In some composite designs, it may be necessary to provide a corrosion or weather barrier to the surface of a product. A surface veil is a fabric made from nylon or polyester that acts as a very thin sponge that can absorb resin to 90% of its volume. This helps to provide an extra layer of protective resin on the surface of the product. Surface veils are used to improve the surface appearance and insure the presence of a corrosion resistance barrier for typical composites products such as pipes, tanks and other chemical process equipment. Other benefits include increased resistance to abrasion, UV and other weathering forces. Veils may be used in conjunction with gel coats to provide reinforcement to the resin.

- **Bars**

FRP bars can be produced with a smooth surface or having a deformed surface configuration for bond improvement (indented, grain –coated etc.). In addition to surface shape and treatment, an FRP bar can be produced with different characteristics such as fiber and resin types and fiber ratio. These bars are characterized by high tensile strength, Young's Modulus lower than steel, high durability, light weight and electromagnetic permeability.

- **Prepreg**

Prepregs are a ready-made material made of a reinforcement form and polymer matrix. Passing reinforcing fibers or forms such as fabrics through a resin bath is used to make a prepreg. The resin is saturated (impregnated) into the fiber and then heated to advance the curing reaction to different curing stages. Thermoset or thermoplastic prepregs are available and can be either stored in a refrigerator or at room temperature depending on the constituent materials. Prepregs can be manually or mechanically applied at various directions based on the design requirements.

2.6 Fillers

Use of inorganic fillers in composites is increasing. Fillers not only reduce the cost of composites, but also frequently impart performance improvements that might not otherwise be achieved by the reinforcement and resin ingredients alone. Fillers can improve mechanical properties including fire and smoke performance by reducing organic content in composite laminates. Also, filled resins shrink less than unfilled resins, thereby improving the dimensional control of molded parts. Important properties, including water resistance, weathering, surface smoothness, stiffness, dimensional stability and temperature resistance, can all be improved through the proper use of fillers.

The thermosetting resin segment of the composite industry has taken advantage of the properties of fillers for many years. More recently, the thermoplastic industry has begun to make widespread use of inorganic fillers. Breakthroughs in chemical treatment of fillers that can provide higher filler loadings and improved laminate performance are accelerating this trend.

2.6.1 Filler Types

There are a number of inorganic filler materials that can be used with composites including:

Calcium carbonate is the most widely used inorganic filler. It is available at low cost in a variety of particle sizes and treatments from well-established regional suppliers, especially for composite applications. Most common grades of calcium carbonate filler are derived from limestone or marble and very common in automobile parts.

Kaolin (hydrous aluminum silicate) is the second most commonly used filler. It is known throughout the industry by its more common material name, clay. Mined clays are processed either by air flotation or by water washing to remove impurities and to classify the product for use in composites. A wide range of particle sizes is available.

Alumina trihydrate is frequently used when improved fire/smoke performance is required. When exposed to high temperature, this filler gives off water (hydration), thereby reducing the flame spread and development of smoke. Composite plumbing fixture applications such as bathtubs, shower stalls and related building products often contain alumina trihydrate for this purpose.

Calcium sulfate is a major flame/smoke retarding filler used by the tub/shower industry. It has fewer waters of hydration, and water is released at a lower temperature. This mineral filler offers a low cost flame/smoke retarding filler.

Other commonly used fillers include:

- Mica
- Feldspar
- Wollastonite
- Silica
- Talc
- Glass microspheres
- Flake glass
- Milled glass fibers
- Other micro sphere product

2.6.2 Using Fillers in Composites

When used in composite laminates, inorganic fillers can account for 40 to 65% by weight. They perform a function similar to silica fume in concrete. In comparison to resins and reinforcements, fillers are the least expensive of the major ingredients. These materials are nevertheless very important in establishing the performance of the composite laminate for the following reasons:

- Fillers reduce the shrinkage of the composites part.

- Fillers influences the fire resistance of laminates.
- Fillers lower compound cost by diluting more expensive resin and may reduce the amount of reinforcement required.
- Fillers can influence the mechanical strengths of composites.
- Fillers serve to transfer stresses between the primary structural components of the laminate (i.e., resin and reinforcement), thereby improving mechanical and physical performance.
- Uniformity of the laminate can be enhanced by the effective use of fillers. Fillers help maintain fiber-loading uniformity by carrying reinforcing fibers along with the flow as resin is moved on the mold during compression molding.
- Crack resistance and crack prevention properties are improved with filled resin systems. This is particularly true in sharp corners and resin-rich areas where smaller particles in the filler help to reinforce the resin in these regions.
- The combination of small and medium filler particles helps control compound rheology at elevated temperatures and pressures, thereby helping to ensure that compression molded parts are uniform.
- Low-density fillers are used extensively in marine putty and the transportation industry. They offer the lowest cost of filled systems, without the increases of weight that affect the performance of the final product.

Some fillers are chemically modified by treating the surface area of the particles with a coupling agent. These coupling agents help to improve the chemical bond between the resin and filler and can reduce resin demand.

2.7 Additives and Modifiers

A wide variety of additives are used in composites to modify materials properties and tailor the laminate's performance. Although these materials are generally used in relatively low quantity by weight compared to resins, reinforcements and fillers, they perform critical functions.

2.7.1 Additive Functions

Additive used in thermo set and thermoplastic composites include the following:

- **Low shrink/low profile:** when parts with smooth surfaces are required, a special thermoplastic resin, which moderates resin shrinkage, can be added to thermo set resins.

- **Fire resistance:** Combustion resistance is improved by proper choice of resin, use of fillers or flame retardant additives. Included in this category are materials containing antimony trioxide, bromine, chlorine, borate and phosphorus.
- **Air release:** most laminating resins, gel coats and other polyester resins might entrap air during processing and application. This can cause air voids and improper fiber wet-out. Air release additives are used to reduce such air entrapment and to enhance fiber wet-out.
- **Emission control:** in open mold applications, styrene emission suppressants are used to lower emissions for air quality compliance.
- **Viscosity control:** in many composite types, it is critical to have a low, workable viscosity during production. Lower viscosity in such filled systems is usually achieved by use of wetting and dispersing additives. These additives facilitate the wet-out and dispersion of fillers resulting in lower viscosity (and/or higher filler loading).
- **Electrical conductivity:** most composites do not conduct electricity. It is possible to obtain a degree of electrical conductivity by the addition of metal, carbon particles or conductive fibers. Electromagnetic interference shielding can be achieved by incorporating conductive materials.
- **Toughness:** can be enhanced by the addition of reinforcements. It can also be improved by special additives such as certain rubber or other elastomeric materials.
- **Antioxidants:** plastics are sometimes modified with antioxidants, which retard or inhibit polymer oxidation and the resulting degradation of the polymer.
- **Antistatic agents:** are added to polymers to reduce their tendency to attract electrical charge. Control of static electricity is essential in certain plastics processing and handling operations, as well as in finished products. Static charges on plastics can produce shocks, present fire hazard and attract dust. The effect of static charge in computer/data processing applications, for example, is particularly detrimental.
- **Foaming agents:** are chemicals that are added to polymers during processing to form minute cells throughout the resin. Foamed plastics exhibit lower density, decrease material costs, improve electrical and thermal insulation, increase strength-to-weight ratio and reduce shrinkage and part warping.
- **Plasticizers:** are added to compounds to improve processing characteristics and offer a wider range of physical and mechanical properties.
- **Slip and blocking agents** provide surface lubrication. This results in reduced coefficient of friction on part surfaces and enhances release of parts from the

mold.

- **Heat stabilizers:** are used in thermoplastic systems to inhibit polymer degradation that results from exposure to heat.
- **Ultraviolet stabilizers:** both thermo set and thermoplastic composites may use special materials which are added to prevent loss of gloss, crazing, chalking, discoloration, changes in electrical characteristics, embrittlement and disintegration due to ultraviolet (UV) radiation. Additives, which protect composites by absorbing the UV, are called ultraviolet absorbers. Materials, which protect the polymer in some other manner, are known as ultraviolet stabilizers.

2.7.2 *Catalysts, Promoters, Inhibitors*

In polyesters, the most important additive is catalyst or initiator. Typically, organic peroxide such as methylethylketone peroxide (MEKP) is used for room temperature cured processes, or benzoyl peroxide is added to the resin for heat-cured molding. When triggered by heat, or used in conjunction with a promoter (such as cobalt naphthenate), peroxides convert to a reactive state (exhibiting free radicals), causing the unsaturated resin to react (cross-link) and become solid. Some additives such as TBC (tertiary butyl catechol) are used to slow the rate of reaction and are called inhibitors. Accelerators such as DMA (dimethyl aniline) speed curing.

- **Colorants**

Colorants are often used in composites to provide color throughout the part. Additives can be mixed in as part of the resin or applied as part of the molding process (as a gel coat). Also, a wide range of coatings can be applied after molding.

- **Release Agents**

Release agents facilitate removal of parts from molds. These products can be added to the resin, applied to molds, or both. Zinc stearate is a popular mold release agent that is mixed into resin for compression molding. Waxes, silicones and other release agents may be applied directly to the surface of molds.

- **Thixotropic agents**

In some processes such as hand lay-up or spray-up, thixotropic agents may be used. When “at rest”, resins containing thixotropic agents remain at elevated viscosities. This reduces the tendency of the liquid resin to flow or drain from vertical surfaces. When the resin is subjected to shear, the viscosity is reduced and the resin can be easily sprayed or brushed on the mold. Fumed silica and certain clays are common thixotropic agents.

2.8 Adhesives

Adhesives are used to attach composites to themselves as well as to other surfaces. Adhesive bonding is the method of choice for bonding thermo set composites and is sometimes used for thermoplastic composites. There are several considerations involved in applying adhesives effectively. The joint or interface connection must be engineered to select the proper adhesive and application method to ensure bond strength. Careful surface preparation and cure are critical to bond performance.

Adhesives should be used in a joint design where the maximum load is transferred into the component using the loading characteristics of the adhesive and the composite material. The most common adhesives are acrylics, epoxies, and urethanes. A high-strength bond with high-temperature resistance would indicate the use of an epoxy, whereas a moderate temperature resistance with good strength and rapid cure might use an acrylic. For applications where toughness is needed, urethane might be selected.

2.9 Codes & Standards

2.9.1 Committees

A number of committee activities from professional organizations are addressing the recommended use and specification of FRP composites. Many organizations have published codes, standards, test methods and specifications for FRP composites and their products for the respective products. For example in the FRP pipe market, design standards, test methods, and recommended practices were published by the American Petroleum Institute (API), American Society of Mechanical Engineers (ASME), American Water Works Association (AWWA), Underwriter Laboratories (UL), and others. In the corrosion resistant structural equipment market, ASME published an industry standard called RTP-1. In RTP-1, the document provides purchasers of corrosion-resistant composite equipment with guidelines for the specification of high-quality, cost-effective and high-performance equipment. The American Society of Testing and Materials (ASTM) published recognized industry test methods for FRP composites used in all markets.

Table 2.3. Committees for development of structural intervention with FRPs around the world.

Organization	Committee
American Concrete Institute (ACI)	■ 440 – Composites for Concrete
	■ 440C – State-of-the-art-Report

	<ul style="list-style-type: none"> ■ 440D – Research ■ 410E – Professional Educations ■ 440F – Repair ■ 440G – Student Education ■ 400H – Reinforced Concrete (rebar) ■ 440I – Prestressed Concrete (tendons) ■ 440J – Structural Stay-in-Place Formwork ■ 440K – Material Characterization ■ 400L - Durability
American Society of Civil Engineers (ASCE)	Structural Composites and Plastics
American Society of Testing and Materials (ASTM)	<ul style="list-style-type: none"> ■ ASTM D20.18.01 – FRP Materials for Concrete ■ ASTM D20.18.02 – Pultruded Profiles ■ ASTM D30.30.01 – Composites for Civil Engineering
AASHTO Bridge Subcommittee	T-21 - FRP Composites
International Federation of Structural Concrete (FIB)	Task group on FRP
Canadian Society of Civil Engineers (CSCE)	ACMBS – Advanced Composite Materials for Bridges and Structures
Japan Society of Civil Engineers	Research Committee on Concrete Structures with Externally Bonded Continuous Fiber Reinforcing materials
Transportation Research Board	A2C07 – FRP Composites
National Research Council of Italy	CNR – FRP Sytems
International Federation for Structural Concrete	<i>fib</i> Task Group 9.3 FRP Reinforcement for Concrete Structures

For almost twenty years, the American Society of Civil Engineers (ASCE) has operated a technical committee called Structural Composites and Plastics (SCAP) to address the design and implementation of composites. This committee published a design manual in the early 1980's and is currently working to update this manual to address the many FRP composite products developed over the years.

The American Concrete Institute, and its Committee 440 with ten different subcommittees, address FRP composites in concrete in such topics as state-of-the-art, research, professional and student education, repair, rebar, prestressing, and stay-in-place structural formwork. These highly active committees are focused to produce guidance documents for the engineer. In particular, ACI 440F is developing a document titled “Guide for the Design and Construction of Externally Bonded FRP Systems for Strengthening Concrete Structures”. This landmark publication, reviews the state-of-the-art, provides guidelines for application and selection, design recommendations, and construction techniques for the use of FRP materials to repair, strengthen, or upgrade concrete structures. The ACI 440H committee is developing a similar document of FRP rebar titled “Guide for the Design and Construction of Concrete Reinforced with FRP Bars”. The proposed guideline reviews knowledge based on research and field applications of FRP bars worldwide.

Several ASTM committees are currently working on consensus test methods for the use of rebars, repair materials, and pultruded structural profiles. In ASTM D20.18.01 (FRP Materials for Concrete) committee, industry experts are addressing materials and products to develop standard test methods for FRP rebar and repair materials. In ASTM D20.18.02 is a committee focused on the development of test methods for FRP pultruded profiles and shapes. The ASTM D30.30.01 (Composites for Civil Engineering) committee addresses FRP composites products used construction.

The American Association of State Highway and Transportation Officials (AASHTO) Bridge Committee established a subcommittee in 1997 called “T-21 Composites”. This committee has an ongoing effort to develop design guidelines for the use of composites in bridge applications including FRP reinforced concrete, concrete repair, and vehicular bridge deck panels.

2.9.2 Organizations

The Civil Engineering Research Foundation (CERF), the research arm of the American Society of Civil Engineers is actively engaged with technology transfer of new cutting edge technologies. One of CERF’s programs, Highway Innovation Technology Evaluation Center (HITEC), coordinates product evaluations between the end-user community and industry to produce highway products that meet the needs of the end-user with the program results being shared with all State DOT bridge departments. HITEC has provided the civil engineering community with several product evaluation programs that address the use of composites. One program in particular, FRP Composite Bridge Decks, has developed an evaluation plan for several composites bridge manufacturers for testing, design, and performance of bridge deck panels manufactured with FRP materials.

The Intelligent Sensing for Innovative Structures (ISIS) of the Canadian Network of Centers of Excellence was established to advance civil engineering to a world leadership position through the development and application of FRP composites and an integrated intelligent fiber optic sensing technology to benefit all Canadians through innovative and intelligent infrastructure. ISIS Canada, through its universities, has coordinated a team of professionals dedicated to advancing technology by building better roads, buildings, and

bridges. ISIS has many research projects and field evaluations under study that demonstrate successful implementation of FRP composites with validated design and testing as well as techniques to document the in-field service of new products and systems. ISIS Canada is credited with building the first smart sensing FRP composite bridge and continues to make advancements in the areas of concrete repair, bridge construction with FRP rebars and tendons, and roadways.

Several professional societies from around the world have published design codes for FRP Rebar. In Canada, the civil engineers have documented design procedures in the Canadian Highway Bridge Design Code for the use of FRP rebars. The Japan Society of Civil Engineers has published a code that provides design recommendations for the use of FRP rebars and tendons.

2.9.3 Standards Development

Several global activities are taking place to implement FRP composites materials and products into respective design codes and guidelines. The following summarizes this activity:

Table 2.4. FRP Codes around the world.

Code/Standard	Reference
Canadian Building Code	Design and Construction of Building Components with Fiber Reinforced Plastics
Canadian Highway Bridge Design Code (CHBDC)	Fiber Reinforced Structures (section of code)
International Conference of Building Officials (ICBO)	AC 125: Acceptance Criteria for Concrete and Unreinforced Masonry Strengthening Using Fiber-Reinforced Composite Systems
Japan Society of Civil Engineers (JSCE) Standard Specification for Design and Construction of Concrete Structures	Recommendation for Design and Construction for Reinforced Concrete Structures Using Continuous Fiber Reinforcing Materials
National Research Council (CNR) – Italy Advisory Committee on technical recommendation for construction	Guidelines for design and construction of Externally Bonded FRP systems for strengthening existing structures.

In April 1997, The International Conference of Building Officials (ICBO) published AC125 “Acceptance Criteria for Concrete and Unreinforced Masonry Strengthening Using Fiber-Reinforced Composite Systems”. ICBO has also published individual company product evaluation reports on FRP systems used to strengthen concrete and masonry structural elements such as columns, beams, slabs, and connections of wall to slab.

2.9.4 Technology Transfer

Many academic institutions in the North America, as well as around the world are actively engaged in research involving FRP applications for civil infrastructure. Several universities have distinguished themselves as centers of excellence in specific fields of expertise. Universities and State Departments of Transportation often collaborate on the evaluation and implementation of FRP composites that best meet the needs of the State.

Table 2.5. Organizations & Activities on FRP.

Organization	Activity
American Society of Civil Engineers	<i>Journal of Composites for Construction</i>
Federal Highway Administration (FHWA)	TEA-21 Innovative Bridge Research and Construction Program (IBRC)
Intelligent Sensing for Innovative Structures (ISIS) of the Canadian Network of Centers of Excellence	<ul style="list-style-type: none">• Industry research and collaboration• <i>FRP International</i> (global newsletter)
Market Development Alliance of the FRP Composites Industry	Project Teams and Programs geared towards development of FRP composites for construction applications

The Fed Federal Highway Administration (FHWA) through the TEA-21 Innovative Bridge Research and Construction Program (IBRC) has provided new construction materials the opportunity to meet the goals of reducing maintenance and life-cycle costs of bridge structures. Funds are provided for the Federal share of the cost for repair, rehabilitation, replacement, and new construction of bridges using innovative materials. Each year since the first solicitation in 1998, FRP composites led other innovative construction materials for funding to demonstrate the unique benefits being sought by FHWA to build a better and long-lasting infrastructure.

Many societies, trade associations, academic institutions and organizations worldwide host periodic conferences, trade shows, and seminars in forums that educate as well as transfer state-of-the-art technology to end-users. Some of the conferences are listed below:

- ACMBS Advanced Composites Materials for Bridges and Structures (Canada)
- ASCE Construction and Materials Congress
- PORTS, every three years (2001, 2004)
- Structures Congress
- American Composites Manufacturer's Association (formerly Composites Fabricators Association -CFA) annual conference and exposition, early fall
- FRPRCS Fiber-Reinforced Polymers for Reinforced Concrete Structures (International)
- IBC International Bridge Conference, annual, June
- ICCI International Conference on Composites for Infrastructure
- SAMPE Society for the Advancement of Material and Process Engineering, annual conference and exposition, late spring/early summer.

3 LITERATURE REVIEW

3.1 Basic characteristics of confinement effect on concrete

The stress strain relationship of concrete under short-term monotonically increasing uniaxial compressive loading shows gradual deterioration in stiffness, with strain even at a low stress level, caused by development of micro cracks. The failure of concrete is a result of the continuously increasing rate propagation of those cracks. The presence of passive confining reinforcement has a crucial effect on this behaviour of concrete. This kind of reinforcement can be closed steel stirrups or spiral reinforcement or FRP Jacketing. It is characterized as passive because it doesn't participate directly in carrying the imposed vertical load but raises resistance at the induced from the vertical load expansion of bounded concrete. By doing so, it keeps the cracked pieces of concrete together, limits the progress of expansion and therefore it delays the upcoming failure. The result is that concrete can develop high deformations in the direction of loading without loss of strength (ductility) and the stress strain curve obtains then characteristics similar to those of an elasto-plastic material.

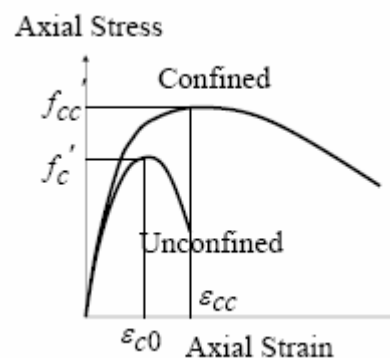


Figure3.1. Confinement effect of concrete.

3.1.1 Behaviour under lateral hydraulic pressure

This improvement through confinement is more intense when the transversal compression stresses are applied actively, like for example by hydraulic pressure. Classical experimental study is the research of Richart, Brandtzaeg and Brown, 1928, at the University of Illinois. The basic result of this research is valid up to nowadays, and has been confirmed theoretically too, albeit the big improvement of the last almost 80 years since that time in the technology and composition of concrete. The increase in the strength and deformability of concrete under hydrostatic pressure is multiple of the transversal compression pressure according to the following equations:

$$f_{cc} = f_{c0} + k_1 \cdot f_l \quad (3.1)$$

$$\varepsilon_{cc} = \varepsilon_{c0} \cdot \left(1 + k_2 \cdot \frac{f_l}{f_{c0}} \right) \quad (3.2)$$

where f_{cc} and ε_{cc} : the maximum concrete stress and the corresponding strain respectively, under the lateral fluid pressure: f_l , f_{c0} & ε_{c0} : unconfined concrete strength and corresponding strain and k_1 , k_2 : coefficients that are function of the concrete mix and the lateral pressure. Richart et al found that the averaged value of the coefficient k_1 is equal to 4.1 and $k_2 = 5k_1$.

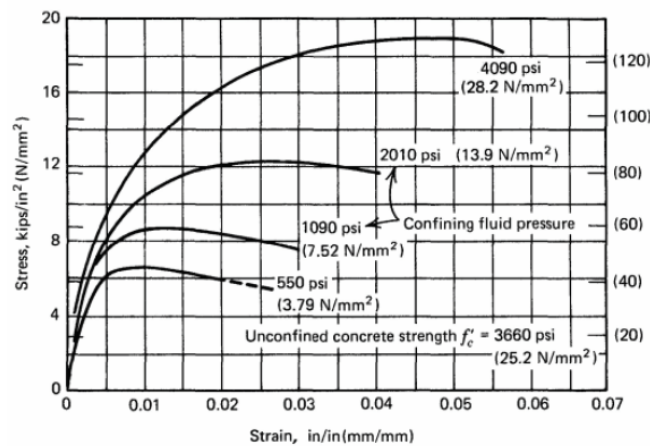


Figure 3.2. Axial Stress Strain curve with Lateral confining pressure. (Richart, Brandtzaeg and Brown 1928)

3.1.2 Behaviour under Biaxial Stress Condition

In the case of bi-directional stress state, concrete compressive strength increases with lateral compressive (confining) stress but decreases with lateral tensile stress. (Kupfer, Hilsdorf and H. Rusch, 1969). The combinations of the principal stresses in the two directions that cause failure of concrete are given in the envelope presented below where the principal stresses are normalized to the unconfined concrete strength. In the diagram the cases of uniaxial compression ($\sigma_1=f_{ck}$, $\sigma_2=0$) and uniaxial tension ($\sigma_1=0$, $\sigma_2=f_{ctk}$) are included. As we can see we can have about 20% increase in case of biaxial compression compared to the uniaxial one, that means when at the same time with the vertical compressive stress there is lateral compressive pressure. In the contrary, the compression strength is reduced dramatically if along with the vertical compression there is lateral tensile stress. This reduction of the compression strength of concrete under the presence of lateral tensile pressure is due to crack propagation after the overcome of the tensile concrete strength. These cracks are perpendicular to the principle tensile stress and so they develop parallel to the principle compressive stress of the specimen.

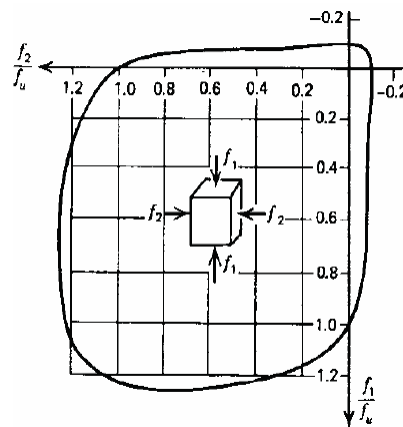


Figure 3.3. Biaxial concrete strength (Kupfer, Hilsdorf and H. Rusch, 1969)

3.1.3 Modeling of concrete under Multi-axial Stresses

Modeling of concrete under multi-axial stresses has been developed by mathematical models that represent the so called “ultimate strength surface”. That means, the locus of all the stress combinations for which a proportionally loaded concrete specimen reaches its maximum load-carrying capacity. In dealing with the modelling of the behaviour of concrete over its complete range of response, the knowledge of the ultimate strength surface is important since it allows identification of regions of stress states beyond which complete failure is reached according to different mechanisms (CEB State of the art report 1996).

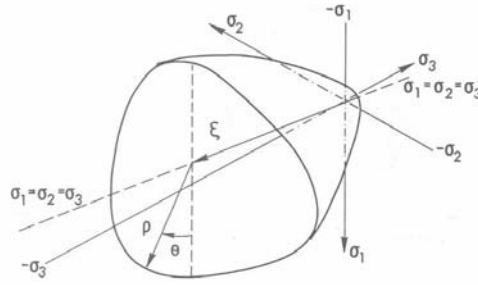


Figure 3.4. Ultimate strength surface (CEB State of the art report)

The behavior of concrete can be conveniently represented in terms of the octahedral normal (hydrostatic) and shear (deviatoric) stresses σ_o and τ_o . Any point in the stress space is described by the coordinates (ξ, ρ, θ) . In which ξ is the projection in the hydrostatic axis ($\sigma_1 = \sigma_2 = \sigma_3$) and (ρ, θ) are the polar coordinates in the deviatoric plane (plane perpendicular to hydrostatic axis).

$$\sigma_o = \frac{1}{3} \cdot (\sigma_1 + \sigma_2 + \sigma_3) \quad (3.3)$$

$$\tau_o = \frac{1}{3} \cdot \sqrt{(\sigma_1 - \sigma_2)^2 + (\sigma_2 - \sigma_3)^2 + (\sigma_3 - \sigma_1)^2} \quad (3.4)$$

One example of failure surface is the one published by N.S.Ottosen (1977). It is an elasticity based model having a Hookean formulation in incremental form. The stiffness tensor is simplified by using three stress strain invariants trying to describe the behaviour of concrete. It corresponds to a smooth convex failure surface with curved meridians, which open in the negative direction of the hydrostatic axis, and the trace in the deviatoric plane changes from nearly triangular to more circular with increasing the hydrostatic pressure.

This failure criterion is given in the following simple form:

$$A \frac{J_{2\sigma}}{f_c^2} + \lambda \frac{\sqrt{J_{2\sigma}}}{f_c} + B \frac{I_{1\sigma}}{f_c} - 1 \geq 0 \quad (3.5)$$

Stress Invariants:

$$I_{1\sigma} = \sigma_1 + \sigma_2 + \sigma_3 \quad (3.6)$$

$$J_{2\sigma} = \frac{((\sigma_1 - \sigma_0)^2 + (\sigma_2 - \sigma_0)^2 + (\sigma_3 - \sigma_0)^2)}{2} \quad (3.7)$$

$$J_{3\sigma} = (\sigma_1 - \sigma_0) \times (\sigma_2 - \sigma_0) \times (\sigma_3 - \sigma_0) \quad (3.8)$$

$$\lambda = K_1 \cdot \cos \left[\frac{1}{3} \cdot \arccos(K_2 \cdot \cos 3\theta) \right] \quad \cos 3\theta \geq 0 \quad (3.9)$$

$$\lambda = K_1 \cdot \cos \left[\frac{\pi}{3} - \frac{1}{3} \cdot \arccos(-K_2 \cdot \cos 3\theta) \right] \quad \cos 3\theta \leq 0$$

$$\cos 3\theta = \frac{3 \cdot \sqrt{3}}{2} \cdot \frac{J_{3\sigma}}{J_{2\sigma}^{3/2}} \quad (3.10)$$

The rest parameters of the model were calibrated by the values proposed in the original paper of Ottosen N.S. (1977) for different ratios of $k=f_t/f_c$.

Table 3.1. Proposed values for the parameters of the failure criterion of N.S.Ottosen.

k	A	B	K₁	K₂
0.08	1.8076	4.0962	14.4863	0.9914
0.1	1.2759	3.1962	11.7365	0.9801
0.12	0.9218	2.5969	9.9110	0.9647

3.2 Lateral confinement by ties

As it is already mentioned the mechanical behavior of concrete (strength, ductility, energy dissipation) increases substantially in the case of triaxial stress state. In practice, in order to develop similar stress state closed stirrups (or spiral reinforcement) are used which in combination with the longitudinal reinforcement are limiting the expansion of concrete. This kind of confinement (passive) affects effectively the behavior of the material after the appearance of the internal cracking which results to the initiation of expansion. Thus it is observed that for low values of deformation the contribution of the confinement is small. In the contrary, it becomes important in the area of the maximum compressive strength and in the descending branch of concrete behavior. In the figure below,

experimental results are presented that exhibit the influence of confinement (shape and percentage of ties) in the mechanical behavior of structural members. It can be concluded that confinement:

- Increases the strength of concrete recovering moreover those losses due to peeling of the section
- Increases the ultimate deformation (ϵ_{cu}) reducing at the same time the inclination of the descending branch (increase of ductility).

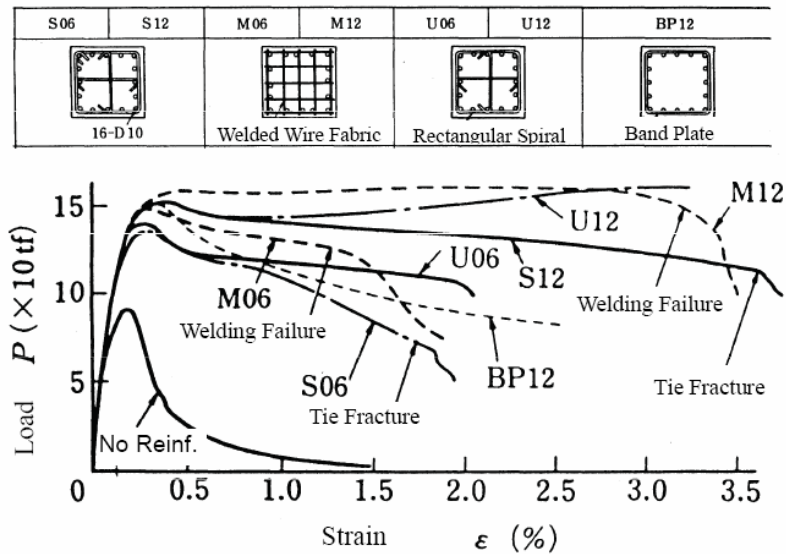


Figure3.5. Test of columns under axial compression (Sugano et al 1985)

It is proven experimentally that confinement with circular spiral is more effective than of that with closed orthogonal or tetragonal ties. This is because circular spirals due to their shape create continuous confining pressure in all the application area. In the contrary, the orthogonal or tetragonal ties allow some expansion of concrete due to flexural behavior of their sides which result to unconfined parts of the section near the central parts of the sides of the specimen. Same unconfined parts are observed also between two successive stirrups.

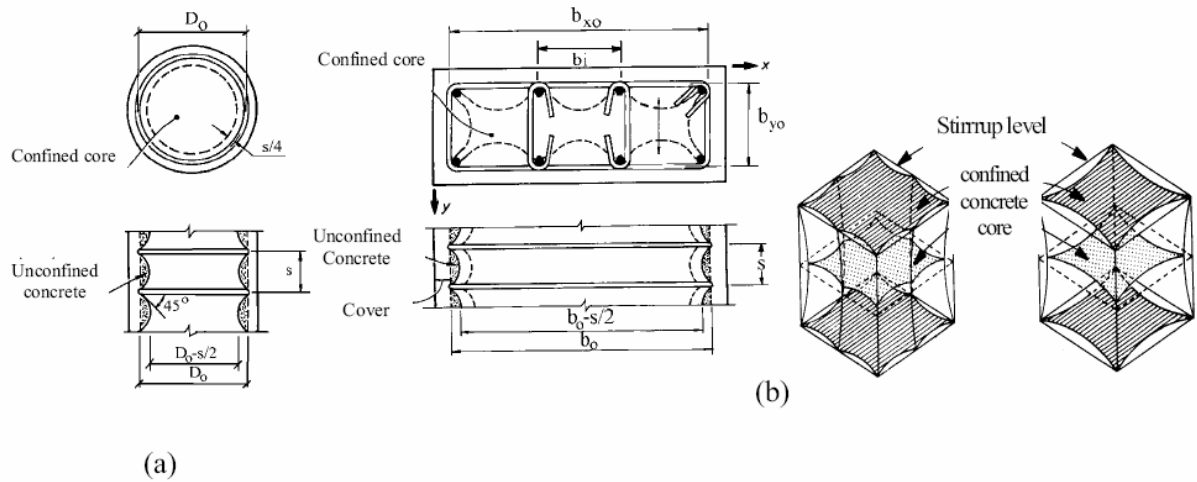


Figure 3.6. Fully confined and unconfined parts at the cross-section level and along the length of the member a) circular ties b) rectangular ties (Sheikh and Uzumeri)

The final shape of the stress strain curve of stirrups-confined concrete depends on various parameters from which the most important are:

- The volumetric ratio (ρ_w) where ρ_w is the fraction of the volume of ties to the volume of the confined core of the section (volume of the solid bounded by the external tie)
- The yield strength of the transversal reinforcement (f_{yw}). Steel stirrups with higher yield strength can impose higher confining forces.
- Spacing of ties (s). Smaller spacing of stirrups increases the imposed confinement due to reduction of the area of the unconfined part of the member. Moreover, lower spacing results to reduced buckling length of the longitudinal under compression reinforcing bars, a problem which is amplified specially in the case of alternated strong loading like earthquakes.
- The shape and the configuration of the stirrups. Depending on the shape and the configuration of the ties used it is possible to reduce to the minimum the unconfined parts of the section which results to increase of the final strength and ductility.
- The longitudinal reinforcement which also contributes to the development of confinement (raise resistance to the lateral expansion of the confined core). This contribution is proportional to the volumetric percentage of the longitudinal reinforcement (ρ_l) and the diameter of the steel bars (Φ_l)
- Concrete strength (f_c). Low strength concrete appears to be more ductile as a material compared to higher strength concrete.
- The type and the rate of loading.

3.2.1 Stress-Strain Models under Monotonic Loading

Various researchers have proposed analytical models for the stress – strain relation of steel stirrups-confined concrete. The most famous are those of Kent and Park (1971), Sheikh and Uzumeri (1980) and Mander, Priestley and Park (1988).

Kent and Park modified the model by Hognestad (1951), and proposed to vary the stiffness of descending branch taking into account the confining effect of concrete by lateral reinforcement.

$$\sigma_c = \sigma_o \cdot \left[2 \cdot \frac{\varepsilon_c}{\varepsilon_o} - \left(\frac{\varepsilon_c}{\varepsilon_o} \right)^2 \right] \quad \varepsilon_c \leq \varepsilon_o \quad (3.11)$$

$$\sigma_c = \sigma_o \cdot [1 - Z \cdot (\varepsilon_c - \varepsilon_o)] \quad \varepsilon_c > \varepsilon_o \quad (3.12)$$

$$\sigma_c \geq 0.2 \cdot \sigma_o \quad (3.13)$$

$$Z = \frac{0.5}{\varepsilon_{50u} + \varepsilon_{50h} - \varepsilon_o} \quad (3.14)$$

$$\varepsilon_{50u} = \frac{0.021 + 0.002 \cdot \sigma_o}{\sigma_o + 6.89} \quad (3.15)$$

$$\varepsilon_{50h} = \left(\frac{3}{4} \right) \cdot p_s \cdot \sqrt{\frac{b''}{s_h}} \quad (3.16)$$

where p_s : ratio of volume of transverse reinforcement to volume of concrete core measured to outside of hoops, b'' : width of confined core measured to outside of hoops, s_h : spacing of hoops. The strain ε_o at maximum stress σ_o is taken as 0.002.

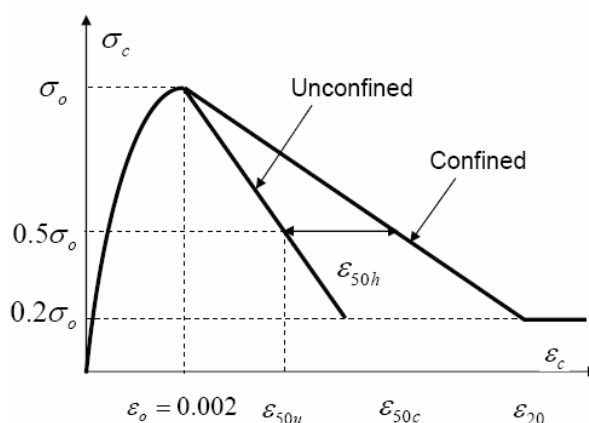


Figure 3.7. Test of columns under axial compression (Park and Kent 1971)

The model of Sheikh-Uzumeri follows the same logic. However, the main difference is that the maximum stress doesn't appear for only one value of strain but for a range of deformations.

In 1988, Mander, Priestley and Park proposed a unified stress-strain approach to predict the preyield and postyield behavior of confined concrete members subjected to axial compressive stresses as shown in the figure below:

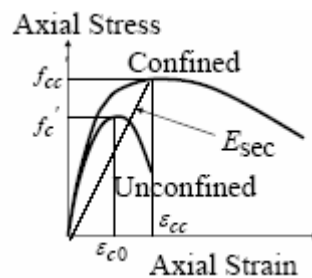


Figure 3.8. Confinement model by Mander et al (1988)

The model utilizes the equation given by Popovic in 1973, originally developed to represent the stress strain response of unconfined concrete. This model is based on a constant confining pressure f_l . The axial stress of the confined concrete f_c for any given strain ϵ_c is related to the peak confined strength f_{cc} as follows:

$$f_c = \frac{f_{cc} \times x \times r}{r - 1 + x^r} \quad (3.17)$$

$$x = \frac{\epsilon_c}{\epsilon_{cc}} \quad (3.18)$$

where ϵ_{cc} the strain at the peak strength f_{cc}

$$r = \frac{E_c}{E_c - E_{sec}} \quad (3.19)$$

where E_c is the tangent elastic modulus of unconfined concrete, and can be estimated as $5000\sqrt{f_c}$ (MPa). E_{sec} is the secant modulus of confined concrete and can be estimated as f_{cc}/ϵ_{cc} .

The peak confined strength f_{cc} is a function of the unconfined strength f_c and the constant confining pressure f_l . A nonlinear relationship is proposed based on the ultimate strength surface developed by Elwi and Murray (1979):

$$f_{cc} = f_{c0} \left(-1,254 + 2,254 \sqrt{1 + \frac{7,94 \times f_l}{f_{c0}}} - 2 \frac{f_l}{f_{c0}} \right) \quad (3.20)$$

The strain at peak confined strength ε_{cc} is given as a function of the strain at peak unconfined strength of concrete ε_{c0} based on the equation of Richart et al (1928):

$$\varepsilon_{cc} = \varepsilon_{c0} \left[1 + 5 \left(\frac{f_{cc}}{f_{c0}} - 1 \right) \right] \quad (3.21)$$

Given a value of the unconfined strength f_c and the constant confining pressure f_l , equation (3.20) can be used to evaluate f_{cc} . The corresponding strain ε_{cc} can be estimated by equation (3.21). Using the ratio r from equation (3.19), the entire stress-strain response of the confined concrete can be determined using (3.17) and (3.18).

3.3 Lateral confinement by FRP jacketing

The use of fiber-reinforced-polymer (FRP) composites for strengthening and rehabilitation of concrete structures is gaining increasing popularity in the civil engineering community. One of the most attractive applications of FRP materials is their use as confining devices for concrete columns, which may result in remarkable increases of strength and ductility. Their use in place of steel for this application offers several advantages. First of all, they have much higher strength (especially the carbon fiber sheets) and they keep imposing confining lateral pressure up to rupture due to their elastic behaviour up to failure contrary to the elasto-plastic behaviour of steel. If the ratio of circumferential to axial fibers is large, the FRP axial modulus is small, allowing the concrete to take essentially the entire axial load; the tensile strength in the circumferential direction is very large and essentially independent from the value of the axial stress; ease and speed of application result from their light weight; their minimal thickness does not produce any change in the shape and size of the strengthened elements; and the good corrosion behaviour of FRP materials makes them suitable for use in coastal and marine structures.



Figure3.9. FRP wrapping of concrete cylinder

Comparing the different types of FRPs, the most commonly used for this kind of application are glass fiber polymer sheets (GFRP), carbon fiber sheets (CFRP) and more rare are the aramid fiber sheets (AFRP). Their main differences are that carbon fiber sheets appear to have higher strength but lower deformability, the opposite happens with glass fiber sheets while aramid sheets combine both deformability and strength.

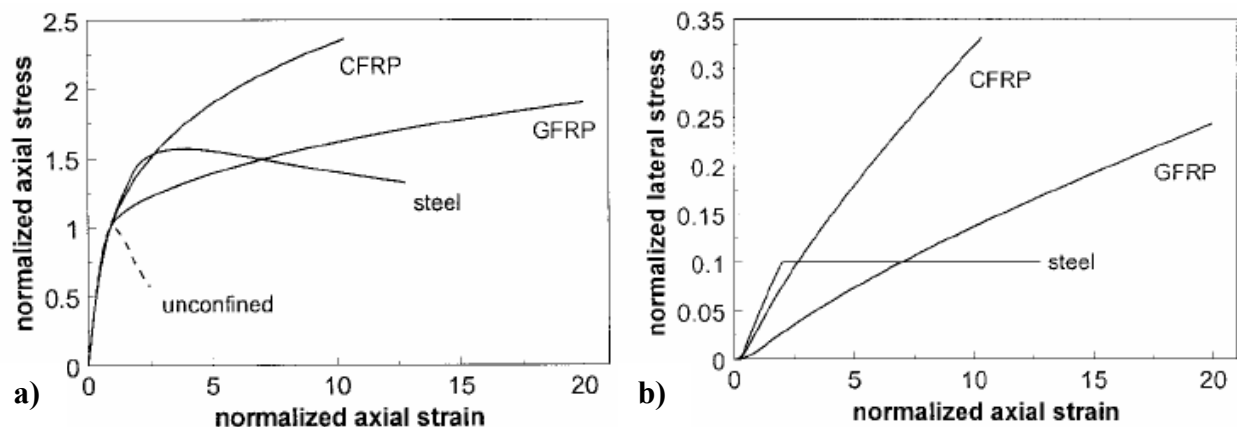


Figure 3.10. Comparison of GFRP, CFRP and steel confined stress-strain concrete behaviour. (Spoelstra & Monti)

As we can see from the figure above after yielding of steel reinforcement the confining pressure becomes constant and independent on the loading level while in the case of FRP the confining pressure is continuously increasing during the loading history due to linear characteristics of the FRP materials.

The confinement of concrete with FRP is based on a well-understood mechanism. When the concrete is subjected to axial compression, it expands laterally. This expansion is resisted by the FRP jacket which provides a confining pressure to the concrete. Eventual failure occurs when the FRP jacket ruptures as a result of tensile stresses in the hoop direction. Confinement effectiveness of fiber reinforced plastics (FRP) jackets in concrete columns depend on several parameters the most important are FRP properties especially stiffness, concrete strength, radius of the rounded corner and shape of the section. Concrete in a circular jacket is uniformly confined, while concrete in a jacket of any other sectional shape is non-uniformly confined. Most existing studies of FRP-confined concrete have been concerned with uniformly confined concrete by testing FRP-confined circular concrete specimens.

3.3.1 FRP-confined concrete in circular sections

In circular sections the induced by the applied axial load radial displacement (meaning the same displacement around the circumference of the section) activates the confining device and causes radial confining forces or else hydrostatic confining pressure. This pressure results to stress state which is the same in every point of the section. It is worthy underlying also that at every point of the circumference the lateral expansion of concrete is equal to the deformation of FRP.

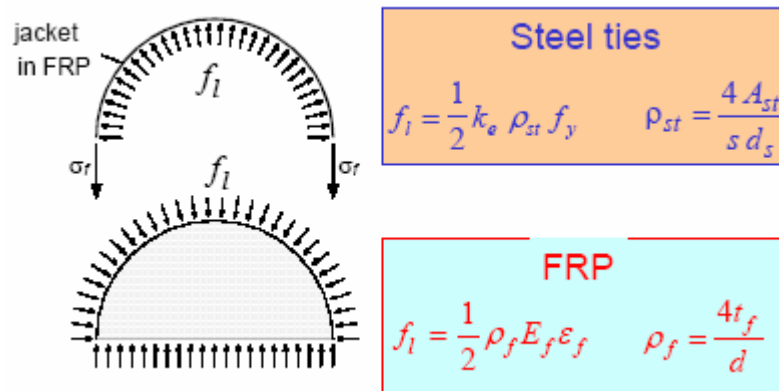


Figure3.11. Behaviour of FRP confined circular sections

The degree of confinement offered by an FRP jacket is commonly represented by the confinement ratio which is defined as the ratio of the maximum confining pressure f_l to the compressive strength of unconfined strength f_{co} . Extensive experimental results have shown that the stress- strain curve of concrete uniformly confined with FRP features a monotonically ascending bi-linear shape (the increasing type) if the FRP-amount exceeds a certain value. For such FRP-confined concrete, both the compressive strength and the ultimate axial strain are reached simultaneously and are significantly enhanced. However, existing tests have also shown that in some cases such a bilinear stress-strain curve cannot be expected, instead the stress-strain curve features a postpeak descending branch and the compressive strength of the confined concrete is reached before the rupture of the FRP jacket.

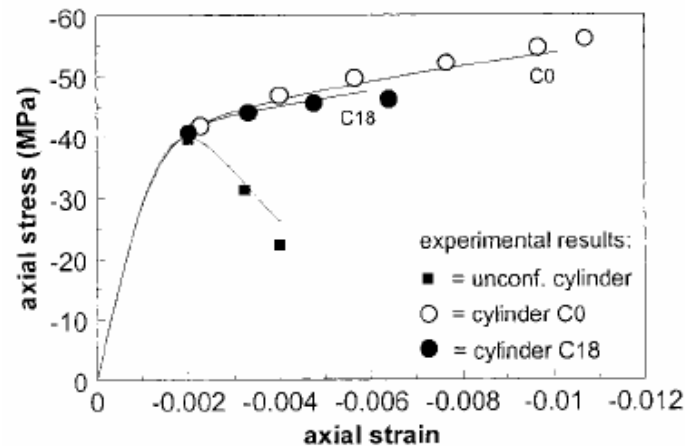


Figure 3.12. Stress-strain Behaviour of FRP confined cylinders (Spoelstra & Monti)

FRP composites have been used for confinement of concrete since the early 1980's, although using commercially available plastic pipes (PVC) filled with concrete was already suggested in the late 1970's (Kurt 1978).

Fardis and Khalili (1981) conducted uniaxial compression tests on 3" x 6" and 4" x 8" concrete cylinders wrapped with different types of CFRP fabrics and reported enhanced strength and ductility due to confinement. They later proposed an analytical hyperbolic model for the compressive strength of confined concrete.

In an attempt to make the confinement model proposed by Ahmed and Shah (1982), usable for concrete confined by FRP spirals, Ahmed et al., (1991) carried out axial compression tests on 33 - 4" x 8" concrete cylinders confined with GFRP spirals and proposed an expression for the peak stress and peak strain of confined concrete.

Saadatmanesh et al. (1994) conducted a parametric analytical study on the behavior of circular and rectangular columns strengthened with external composite procured E-glass or carbon thin straps. They used the confinement model of Mander et al. (1988). Four parameters were considered: the concrete strength, the FRP strap thickness, the strap spacing, and the material of the straps.

Nanni and Bradford (1995) investigated the behavior of 6" x 12" concrete cylinders confined by three types of fiber-wraps: pretensioned braided aramid cables, procured hybrid glass-aramid shells, and glass filament-winding. For the first series, they tested 16 specimens with variable diameter and spacing of the cables. Four specimens were tested in the second series, and 15 in the third series. The cylinders of the third series were made with a central rod, which was then placed on a filament-winding machine, and wrapped with 1, 2, 4, or 8 plies of E-glass fibers and vinylester resin (or polyester for some of the specimens). The strength of concrete core was reported as: 5.2, 6.6 and 5.3 ksi for the three series, respectively. They concluded that the stress-strain response of FRP-encased concrete, in general, could be modeled by a simple bilinear curve with a bend-over point at the peak stress of unconfined concrete, which corresponds to a strain of 0.003. They, however, did not develop a confinement model. Test results were also compared with the confinement models by Mander et al. (1988) and Fardis and Khalili (1982), both of which grossly underestimated the ultimate strain of encased concrete, but compared reasonably well for strength of confined concrete.

Mirmiran and Shahawy (1995) proposed a concrete-filled FRP tube (CFFT), in which the tube acts as a form-work for the encased concrete, hoop and longitudinal reinforcement, and corrosion-resistant casing for the concrete. The CFFT was proposed for bridge columns as well as for pile splicing. The Florida Department of Transportation (FDOT) sponsored a series of projects in order to investigate the behavior of the proposed CFFT. Several parameters were considered in these studies, e.g. the type of loading, the cross-section, the bond, and the length effect.

Bavarian et al. (1996) investigated the effects of externally wrapping concrete cylinders with composite materials. Three sizes of cylinder: 3" x 6", 4" x 8", and 6" x 12"; two types of composite material: S-glass and Kevlar-29, were considered. It was found that the ultimate stress and strain respectively doubled and tripled when using 4 layers of S-glass and 4 layers of Kevlar-29.

Monti and Spoelstra (1997) proposed a confinement model for circular columns wrapped with fiber-reinforced plastics. The procedure is basically the same as the model by Ahmad and Shah (1982). For a certain axial strain a value of axial stress is assumed. The axial stress is then calculated using the confinement model of Mander et al. (1988) as an active confinement model. The lateral strain is then calculated using the expression developed by Pantazopoulou (1995). Knowing the axial stress and the constitutive relationship of the jacket, a new value of axial stress is calculated and compared with the previous value. The procedure is repeated until axial stress converges to a stable value.

Miyauchi and al. (1997) performed uniaxial compression tests on concrete columns reinforced with carbon fiber sheet (CFS) to estimate the strengthening effects. They took into account the compressive strength of the concrete (30 and

50 MPa), the number of layers of CFS (1, 2 and 3 layers) and the dimensions of the column (ϕ 10 x 20cm and ϕ 15 x 30cm). Test results show that: (a) the compressive strength of the concrete strengthened with CFS is enhanced in proportion to the number of layers of CFS, but not the compressive strength of the plain concrete and the dimensions of the specimens; (b) the axial strain at maximum stress of the concrete strengthened with CFS exponentially extends with the number of layers of CFS and is influenced by the compressive strength of plain concrete. Based on these results, a stress-strain relationship, consisting of a parabola and a straight line tangent to the parabola, for the strengthened concrete is proposed and used to perform a time history response analysis for existing bridge piers strengthened with CFS and subjected to earthquake motion. The analytical results show that existing piers strengthened with 2 layers of CFS would be able to withstand an earthquake equal in intensity to the Southern Hyogo Prefecture Earthquake.

Watanabe et al. (1997) investigated experimentally and analytically the confinement effect of FRP sheets on the strength and ductility of concrete cylinders subjected to a uniaxial compression. Plain concrete cylinder specimens with dimensions of ϕ 100 x 200mm retrofitted with FRP sheets were tested under a uniaxial compression. Variables selected for the test and analysis include the type and the number of FRP sheets. Carbon fiber reinforced plastic (CFRP), high stiffness carbon fiber reinforced plastic (HCFRP) and aramid fiber reinforced plastic (AFRP) were used and the number of FRP sheet layers varied from 1 to 4. The analytical procedure used considered a nonlinear 3-Dimensional FEM, which implements Endochronic theory. Comparison of test results with those obtained by the analytical study showed good agreements and the following conclusions were drawn:

- A nonlinear 3-dimensional finite element procedure, which implemented the Endochronic theory proposed by Bazant, can be applicable to predict responses of concrete cylinders under a uniaxial compression.

- The proposed FE analysis procedure can simulate the confinement effect of FRP sheets on the strength and ductility of concrete cylinders under a uniaxial compression.

- If FRP sheets are used to improve the strength and the ductility of concrete cylinder, then the relationship between the Young's modulus and the confinement effect of FRP sheets need to be clarified.

- Compressive strength of concrete cylinders retrofitted with the sheets linearly increased with an increase in the number of plies.

Kono et al. (1998) investigated the confining effects of CFRP. They conducted compressive tests on twenty seven 100 x 200mm concrete cylinders of different mix proportion with different amount of confining (one layer, two layers and three layers) to measure the stress-strain relations. The results showed that the increase in the compressive strength and strain at maximum stress of the cylinder specimens confined by the CFRP sheet vary linearly with the increasing of the

amount and the tensile strength of CFRP sheet.

Kanatharana and Lu (1998) studied the behavior of FRP-reinforced concrete columns under uniaxial compression. Two types of FRP tubes were used in this study; namely the filament-wound FRP (FFRP) and the pultruded FRP (PFRP) tubes. The FFRP has continuous glass fibers winding at 53° and 127° from its circumference, whereas the PFRP has continuous fibers running along its axis. Based on the results obtained from FRP tube tests, 3 configurations of FRP incorporated concrete were selected: Type A configuration simulating a situation similar to a concrete-filled steel tube; Type B configuration simulating a condition similar to an ordinary spiral reinforced concrete column; Type C configuration combining type A and B type configurations. The experimental results showed that significant increases in concrete ductility and FRP strength occurred in all the FFRP specimens but not in the PFRP specimens. Detailed examination revealed that the inclined orientations of the glass fibers provide the FFRP with a circumferential strength necessary for confining concrete, which in turn restrains the FFRP from local instability, and enables strength and ductility gains in the FFRP specimens.

Harmon et al. (1998) investigated the behavior and the failure modes of confined concrete subjected to cyclic axial loading. Composite tubes, 51 mm in diameter and 102 mm long, were fabricated by filament winding, then filled with concrete. The resulting confined cylinders were loaded in uniaxial compression for up to 10,000 cycles. Variables included amplitude, range, fiber type (carbon and glass) and fiber to concrete volume ratio (0, 2, 4 and 6%). The authors reached the following conclusions:

- Cyclic loading increased axial, radial and volume strains for a given range and amplitude. Monotonic loading following cyclic loading rejoined the monotonic stress-strain relationship unless failure occurs first. Cyclic loading at a given amplitude is equivalent to preloading to a higher load which depends on the amplitude, range and number of cycles, followed by unloading to the given amplitude.

- Failure occurred when the circumferential strain in the wrap exceeded the strain capacity of the fiber. The critical threshold can be crossed either by monotonic loading or by cycling loading. Under cyclic loading, the load at failure may be much lower than under monotonic loading. Some evidence suggested that the critical strain threshold may be reduced due to cyclic loading.

- Radial strain tended to stabilize with increasing number of cycles for high wrap stiffness.

- Void compaction increased with load level and decreased with concrete strength and wrap stiffness. Shear slip and void compaction were closely related.

- A reasonable cyclic model for failure and stress-strain behavior can be

constructed from a monotonic model and models for the increase in radial strain, the increase in void compaction and the reduction in the critical threshold level with number of cycles.

3.3.2 FRP-confined concrete in rectangular sections

In case of FRP confined rectangular sections, the concrete is non-uniformly confined and the effectiveness of confinement is much reduced. That's because the confining device can confine the lateral displacement of corner parts but can not confine the displacement outside the central part of the sides from character of the rectangular section which results to different stress-state in every point of the section.

Given the relative complexity of treating a generalized rectangular cross section versus a circular cross section, simplified macro structural approaches following Mander et.al. (1988) have been widely used to model the confinement effectiveness in rectangular sections. These approaches use empirical sectional reduction factors (Mander et.al. 1988; Canadian Standards Association 2002; Chung et al. 2002; Campione and Miraglia 2003; Maalej et al 2003 ;) based on two major assumptions:

- The rectangular cross section can be divided into an unconfined and a confined area. The shape and extent of the unconfined area is derived from the possible arching of the confined material between the confined corners leaving unconfined areas by the flat sides.
- The confined area is considered to be in a state of uniform biaxial confinement similar to that of the circular cross section, thus allowing the generalization of the formulations derived for circular confinement. The area of the circular cross section is replaced by the reduced area of the rectangle and the confinement level estimated for this equivalent "circular cross section" is deemed applicable to the rectangular cross section.

In the literature, all approaches have concentrated on relating the behaviour of rectangular columns to that of circular columns through the use of geometrically defined efficiency factor, based on the figure below, that allows the use of a unified approach based on the simple and robust formulations developed for the circular section problem.

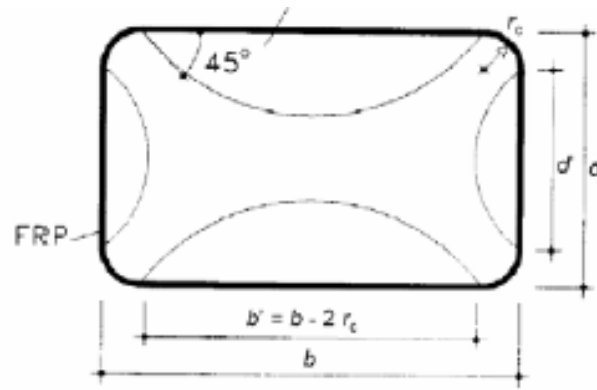


Figure 3.13. Effective confining area used in modelling FRP-confinement of rectangular RC sections. (CNR-DT200 2004)

Rounded corners shown in the figure above are introduced in the case of FRP confinement to improve the effectiveness of FRP jacket. However, due to the presence usually of internal reinforcement the radius of the rounded corner is generally limited to small values.

Picher et al. (1996) examined the effect of the orientation of the confining fibers on the behavior of concrete cylinders wrapped with CFRP composite material. They also evaluated the application of the method to short columns having rectangular and square sections. Twenty-seven short columns in total were wrapped with CFRP material with different fiber orientations, as follows: fifteen 152 x 304 mm - cylinders, eight 152 x 152 x 500 mm square and four 152 x 203 x 500 mm (a x b x h) rectangular prisms. The following observations were reached:

- Confining the cylinders with CFRP greatly improved ductility and compression strength.
- The method can be efficiently applied to prismatic sections, provided the corners are rounded off prior to application of CFRP composite material. The compression capacity enhancement can reach 20% for square sections.
- The variation of wrapping orientation demonstrated that although axial stiffness decreases with an increase of the angle of orientation, ductility remained constant.
- No improvement in failure mode by varying orientations of the confinement was observed.

Restrepo and DeVino (1996) proposed analytical expressions based on Mander's model for the determination of the capacity of axially loaded reinforced concrete columns which are confined by a combination of steel hoops and composite jackets externally applied on the perimeter of the columns. The paper develops equations that can be used to determine the axial compressive load carrying capacity of reinforced concrete rectangular columns, with externally

bonded FRP. The equations take into account the confinement effect due to both steel and FRP jacket.

Hosotani et al. (1997) studied the confinement effect of concrete cylinders by carbon fiber sheets (CFS) for seismic strengthening. They conducted a series of compressive loading test on 600 x 200mm concrete cylinders (10 circular and 12 square) to investigate the stress-strain relation under confinement by CFS. The parameters considered in the tests were the shape of the specimen, the content and the type of CFS (normal and high elastic modulus). Three series of specimens were considered: (a) N-series (cylinders without confinement), (b) S-series (cylinders confined by the CFS with normal elastic modulus - 230GPa), and (c) H-series (cylinders confined by the CFS with high elastic modulus - 392MPa). All the specimens were loaded in axial direction under the displacement control with a loading rate of 0.2 mm/min. The following conclusions were drawn from the test results:

1. At a carbon ratio in the range of 0.05 to 0.15%, the peak axial stress of concrete, $f_{c,}$ and the axial strain of concrete corresponding to the peak stress, $\epsilon_{c,}$ do not increase as the carbon fiber ratio increases, and are almost independent of the cross sectional shape of specimens. However, the deteriorating rate of the axial concrete stress after the peak stress decreases and the axial strain of concrete at rupture of the CFS increases as the carbon fiber ratio increases.
2. At a carbon ratio greater than about 1 %, the axial stress of concrete continues to increase with a change of gradient at an axial concrete strain of 3,000 to 3,500" until failure of CFS.
3. The circumferential strain of the CFS at the peak axial stress of concrete $\epsilon_{cfs,}$ is 1,100 to 2,500 $\mu\epsilon$ for a carbon fiber ratio of 0.056 to 0.16%, while the circumferential strain of the CFS where the gradient changes from the initial value to the second gradient, ϵ_{cft} is 1,800 to 1,900 $\mu\epsilon$ for a carbon fiber ratio of 1.336%; thus, ϵ_{cfs} is quite close to ϵ_{cft} .

Kataoka and al. (1997) studied the ductility improvement of RC columns wrapped with continuous fiber sheets. In order to investigate the restoring strength characteristics of RC columns wrapped by sheets empirically and to propose an evaluation method of structural performance of RC columns wrapped with sheets, Kataoka et al. conducted an experimental program consisting of 3 series of tests:

(a) The objective of the first series was to evaluate the shear strengthening effect of sheets. A total of 15 RC 300 x 300mm square columns with 1100mm clear span length were tested under anti-symmetrical moment condition with constant axial force (cyclic loading controlled by deflection angle). The main parameters selected for this test were the amount of sheets, the type of sheets and the amount of hoops. Four (4) specimens were conventional RC columns (without

wrapping sheets), 10 specimens were sheet-RC columns (wrapped by sheets), and one column was wrapped with sheets after shear failure had occurred, without repair of shear cracks.

(b) The objective of the second series of test was to evaluate the post yielding ductility of RC members wrapped with sheets. A total of 9 RC 300x300mm square columns with clear span length of 900mm were tested. The load was applied similarly to the first series. The main parameters selected for the test were the amount of sheets and the amount of hoops. One specimen was standard column (with 0.13% shear reinforcement ratio and without wrapping sheets), 2 specimens were conventional RC columns (without wrapping sheets), and 6 specimens were sheet-RC columns (wrapped by sheets).

(c) The objective of the third series of test was to investigate the axial compressive behavior of columns wrapped with sheets, empirically. A total of 10 specimens were tested. The dimensions of the columns were the same as those of the second series. The main parameters selected for the test were the amount of sheets and the amount of hoops. One specimen was standard, one was conventional RC column, and 8 were sheet-RC columns. In this last series, two types of tests were carried out: one was normal monotonic axial compression test and the other was axial compression test to investigate the axial compression capacity of the columns which had already failed under lateral loading in the second series.

From the test results over the three series of test, the following conclusions were achieved: (i) the sheet-wrapping method can enhance the seismic behavior, the capacity as well as the ductility, of existing RC columns; (ii) structural performance of RC columns wrapped with sheets can generally be evaluated using the effective shear reinforcement ratio.

Harries et al. (1998) presented the results of an extensive experimental investigation on the axial behavior of reinforced concrete columns retrofit with FRPC jackets. Initially, 152 x 610 mm plain concrete cylinders and 152 x 152 x 610 mm square concrete prisms having FRPC jackets were tested under monotonically increasing concentric axial compression. These tests were aimed at addressing some of the issues raised in previous studies.

Following these tests, 8 full-scale, 508mm diameter circular and 457mm square reinforced concrete columns confined with external FRPC jackets were tested under monotonically increasing concentric axial compression. Reinforcing details of the columns were typical of those designed prior to 1971. In these tests, 3 different FRPC materials were used: (a) A stitched multi-directional E-Glass fabric with 50% of the fibers oriented at 0° with respect to the circumferential direction of the column and 25% of the fibers oriented at each of $\pm 45^\circ$; (b) A woven unidirectional E-Glass fabric oriented in the circumferential direction of

the column; and (c) A unidirectional carbon fiber tow sheet oriented in the circumferential direction of the column. The results of this study showed that external FRPC jackets retrofits increase axial force capacity and axial deformation capacity and suggested that practical retrofit measures will provide confinement equivalent to that provided by closely spaced, well detailed, conventional transverse reinforcement. The stiffness of the applied FRPC jacket was found to be the key parameter in the design of external jacket retrofits. The results of this study suggested that there was no significant scale effect where jackets with similar confinement capacity were provided.

The following tables summarized the described the models:

Table 3.2. Proposed models for FRP-confined concrete (Technical Report FDOT)

Authors	Models	Comments
Fardis and Khalili (1981)	$f'_c = \frac{E_c \epsilon_c}{1 + \epsilon_c \left[\frac{E_c}{f'_c} - \frac{1}{\epsilon_{cc}} \right]} \quad (2.6)$ $\epsilon_{cc} = 0.002 + 0.001 \frac{E_j t_j}{D f'_c}$	<p>E_j, t_j modulus of elasticity and thickness of FRP jacket.</p> <p>E_c = initial tangent modulus of concrete.</p>
Ahmad et al. (1991)	$f'_{cc} = f'_c \left(1 + \frac{k}{4^{n S_{sp}}} \right)$ $\epsilon_{cc} = \epsilon_{co} \left[1 + \frac{k}{4^{n S_{sp}}} \right]$	<p>k and n are functions of f'_c</p> <p>S_{sp} = spacing of FRP spirals.</p>
Monti and Spoe Istra (1997)	$\frac{f'_{cc}}{f'_{co}} = 2.254 \sqrt{1 + 7.94 \frac{f_t}{f'_{co}}} - 2 \frac{f_t}{f'_{co}} - 1.254$ $f'_c = \frac{f'_{cc} \cdot x \cdot r}{r - 1 + x^r}$ $\epsilon_t(\epsilon_c, f_t) = \frac{E_c \epsilon_c - f'_c(\epsilon_c, f_t)}{2 \beta f'_c(\epsilon_c, f_t)}$ $f_t = \frac{1}{2} \rho_j f_j = \frac{1}{2} \rho_j E_j \epsilon_{j-t} \quad \text{with} \quad \rho_j = \frac{4 t_j}{d_j}$	
Samaan, Mirmiran and Shahawy (1998)	<p>(a) Model for axial strains (see Fig. 3.2)</p> $f'_c = \frac{(E_1 - E_2) \epsilon_c}{\left[1 + \left(\frac{(E_1 - E_2) \epsilon_c}{f_o} \right)^n \right]^{\frac{1}{n}}} + E_2 \epsilon_c \quad (2.11)$ $f'_{cu} = f'_c + 3.38 f_r^{0.7} \quad (2.12)$	<ul style="list-style-type: none"> See definitions of $f'_c, E_1, E_2, \epsilon_c, f_o, f'_{cu}$ in Fig. 3.2. f_j, E_j and t_j = tensile strength, modulus of elasticity and thickness of FRP wrap.

Table 3.3. Proposed models for FRP-confined concrete (Technical Report FDOT)

Authors	Models	Comments
	$f_r = \frac{2f_j t_j}{D}$ $E_1 = 47.586\sqrt{1,000f'_c}$ $E_2 = 52.4111f'_c{}^{0.2} + 1.3456\frac{E_j t_j}{D}$ $f_o = 0.872f'_c + 0.371f_r + 0.908$ $\epsilon_{cu} = \frac{f'_{cu} - f_o}{E_2}$	<ul style="list-style-type: none"> D = diameter of column n = curve shape parameter (n = 1.5 for circular). E 1 and E2 in ksi
	<p>(b) Model for lateral strains (see Fig. 3.3)</p> $f_c = \frac{(E_{1r} - E_{2r})\epsilon_r}{\left[1 + \left(\frac{(E_{1r} - E_{2r})\epsilon_r}{f_{or}}\right)^{nr}\right]^{\frac{1}{nr}}} + E_{2r}\epsilon_r$ $E_{1r} = \frac{E_1}{V}$ $\mu = \frac{d\epsilon_r}{d\epsilon_c}$ $\mu = -0.187Ln\left(\frac{2E_j t_j}{f'_c D}\right) + 0.881 \quad (2.21)$ $E_{2r} = \frac{E_2}{\mu_u} \quad (2.22)$ $n_r = \frac{n}{\mu_n} \quad (2.23)$ $f_{or} = 0.636f'_c + 0.233f_r + 0.661 \quad (2.24)$ $\epsilon_{ru} = \frac{f'_{cu} - f_{or}}{E_{2r}} \quad (2.25)$	<ul style="list-style-type: none"> r denotes lateral (radial) direction v = Poisson's ratio μ = dilation rate ε_{ru} = ultimate radial strain

4 MODEL PROPOSAL

4.1 Introduction

As described in previous chapter the behaviour of fiber reinforced polymer (FRP) - confined concrete in circular columns has been extensively studied, but much less is known about concrete in FRP- confined rectangular columns in which the concrete is non-uniformly confined and the effectiveness of confinement is much reduced. In this chapter a mechanistic based and design oriented stress strain model for FRP-confined rectangular columns is presented.

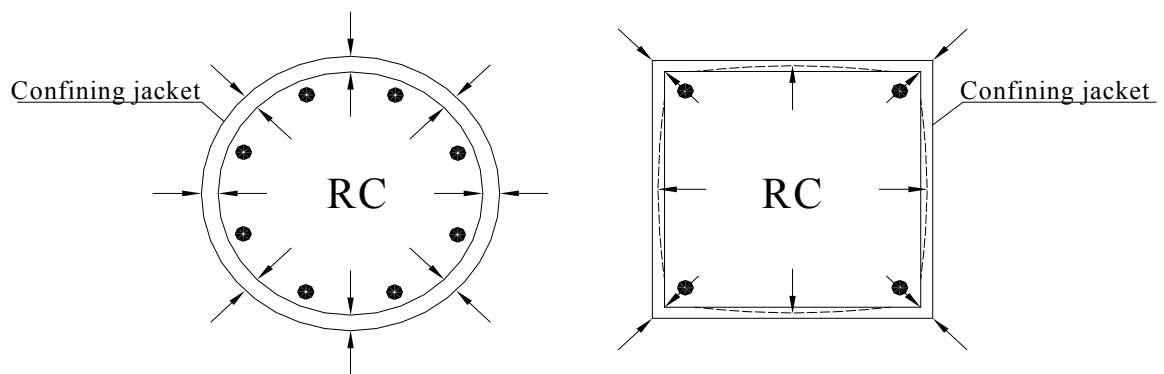


Figure4.1. Confining mechanisms for circular and rectangular sections.

In the circular sections their main characteristic is the radial lateral displacement caused by the applied axial load. That means the same displacement around the circumference of the section which causes radial confining forces or else hydrostatic confining pressure. This pressure results to stress state which is the same in every point of the section. On the other hand, in the rectangular sections, the confining device can confine the lateral displacement of corner parts but can not confine the displacement outside in the central part of the sides from character of the rectangular section which results to different stress states in the section.

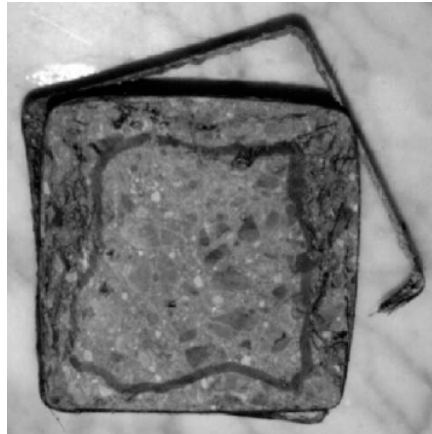


Figure4.2. Transverse section of short square column confined with FRP.

4.2 Numerical analysis (FEM)

In the paper of G.Campione & N.Miraglia (2003) the above picture is included. The figure is related to the transverse cross-section and shows the effective concrete core after FRP failure at the corner. Uneven damage can be observed throughout the section. Two different regions can be identified having different confinement stress state. In order, to specify the path of the confining stresses and examine better the borders of those regions in the section a 3D FEM in SAP 2000 (linear range) has been developed.

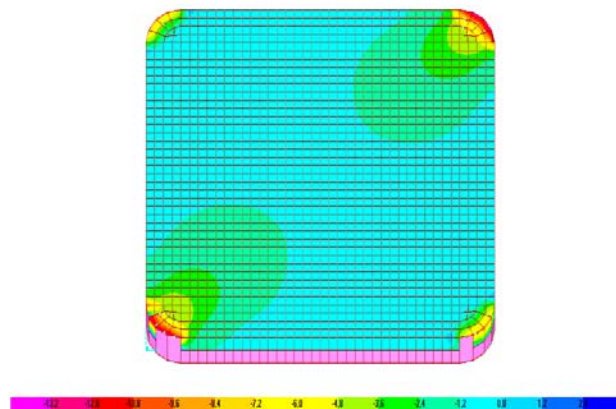


Figure4.3. Transverse section of short square column confined with FRP.

The model includes a square section 200x200 mm with rounded corners given initially a radius of 20 mm. Just a slice of a column was simulated having a height of 10 mm. A mesh of 5 mm space has been used. Solid elements of concrete are modeling the section while in the circumference shell elements of FRP are attached on the solid elements modeling the confining device. For every thickness tested, easily the thickness of the shell element was changed and for different stiffnesses of FRP the properties of the material given to the shell elements were changed. The joints of the elements at the base were restrained, the same happened at the top where moreover the displacements corresponding to a specific level of deformations were applied.

From the results obtained from the program some 3d plots were performed to study the stress field. Firstly, the normal stresses were plotted so a sense of direction of the confining forces can be recognized. In the plot below the origin of the coordinate system is moved in the corner of $\frac{1}{4}$ of the section, in one axis the length of the section is plotted, in the other axis the width and finally in the z axis the level of stresses is presented. The points of the rounded corner are excluded where a concentration of very high stresses is observed. In the case presented below, the joints' local axes in the model were rotated so one of them to be parallel to the diagonal and the other perpendicular to that. Firstly, the normal stresses parallel to the diagonal are presented and then those in the perpendicular direction.

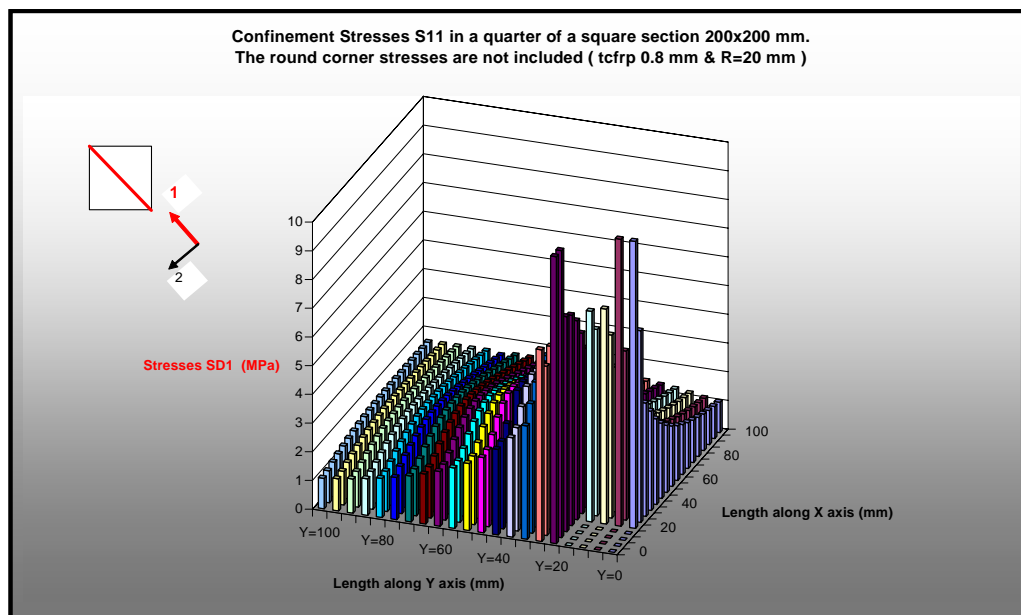


Figure4.4.Confining stresses (normal) along the diagonal direction in every joint.

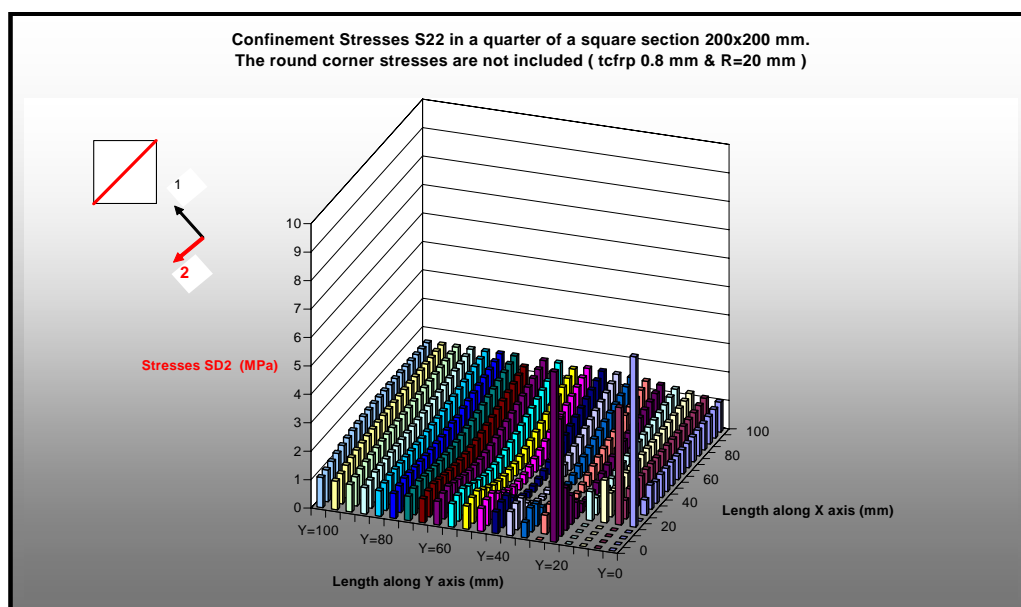


Figure4.5.Confining stresses (normal) perpendicular to the diagonal direction in every joint.

The same plots have been produced also for coordinate system in the joints of the FEM parallel to the sides:

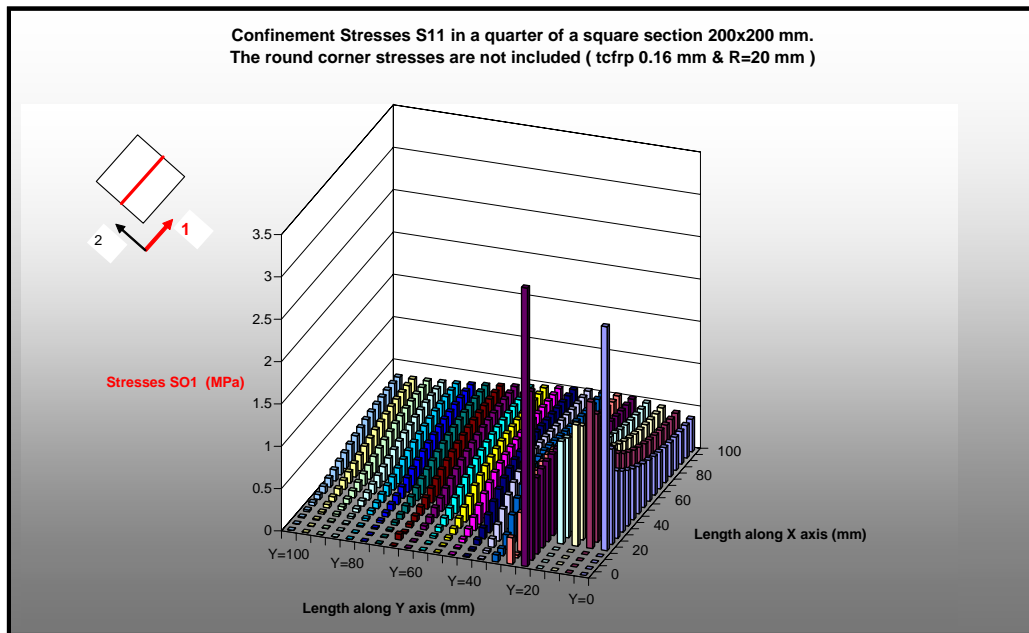


Figure4.6 Confining stresses (normal) parallel to the sides' directions in every joint

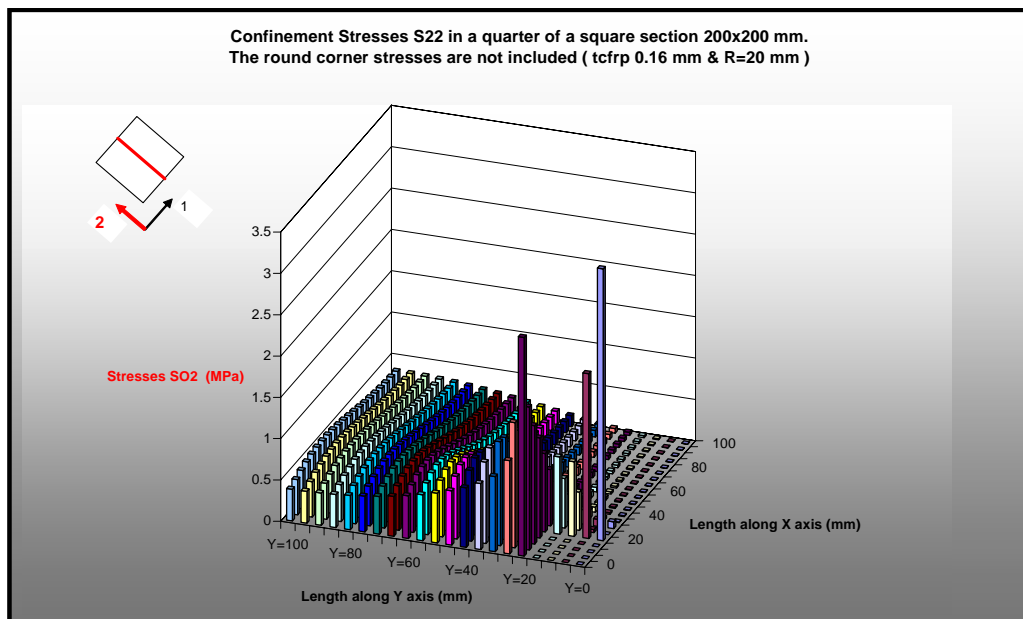


Figure4.7 Confining stresses (normal) perpendicular to the sides' directions in every joint

Observing the above plots the following important remarks can be produced:

- There is no arching effect as many models are assuming. The central parts near the sides are confined from forces coming from the corners and moving parallel to the sides.
- The confining forces in the vicinity of the perimeter have strong directionality

(uniaxial confinement) and on the other hand in the vicinity of the center become almost equal (biaxial confinement)

Under the use of some tolerance the regions where a biaxial and a uniaxial confinement exist can easily be defined based on the ratio of the principal stresses of the two directions in the joints of the FEM.

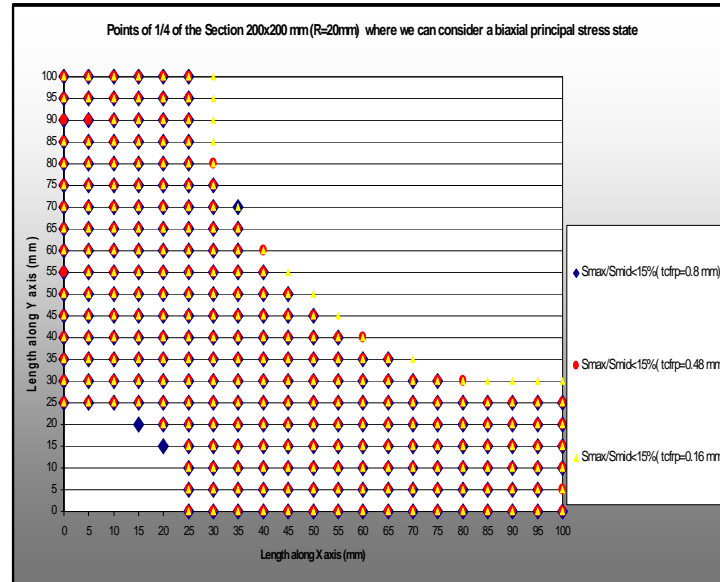


Figure4.8 Uniaxially and Biaxially confined regions-Check for different thicknesses of FRP Jacketing

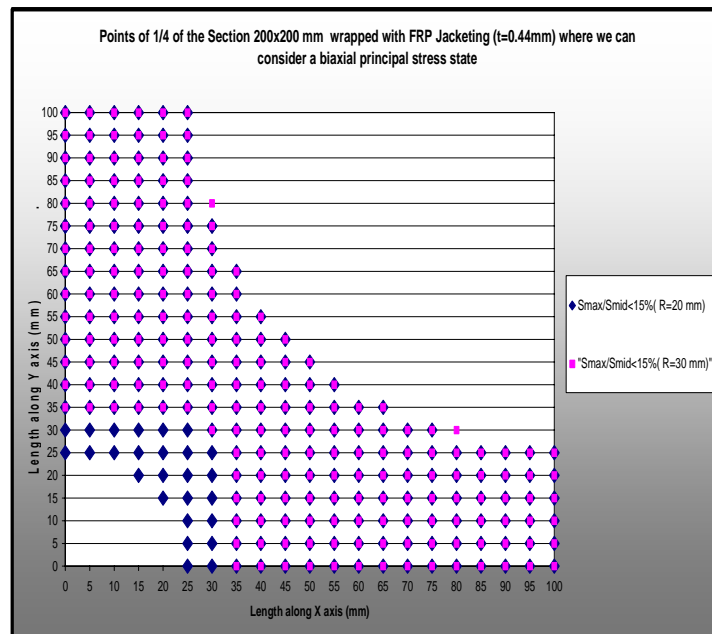


Figure4.9 Uniaxially and Biaxially confined regions-Check for different radii of the rounded corners.

Apparently, for a specific tolerance (ratio of confining stresses less than 15%) the height of the biaxial stress state region is independent of the stiffness of the FRP. Moreover the radius corner is affecting more the diagonal dimension of this region but parallel to the sides the height remains the same. According to those results the width of the uniaxially confined region can be calculated simply by the following equation (W=width, H=height of the section). The dimensions of the regions are easily then related and determined according to this height.

$$h1_{biaxial} = \frac{W}{8} \quad h2_{biaxial} = \frac{H}{8} \quad (4.1)$$

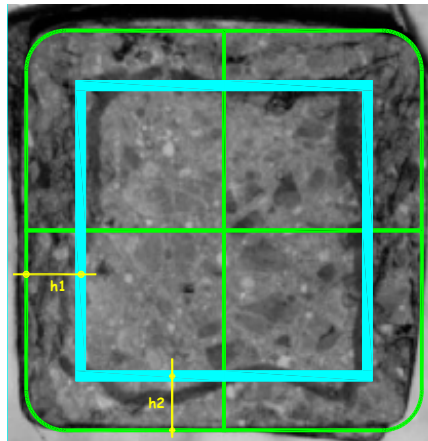


Figure4.10 Defining the different regions in the section

4.3 Simplified Mechanical Model

A series of “generalized” springs is used to describe the following confining behavior. Compressed concrete expands laterally according to its confinement state. Such expansion activates the confining device. The confining forces are applied at the section corner and directed along the diagonal. According to these thoughts the following figures are presented:

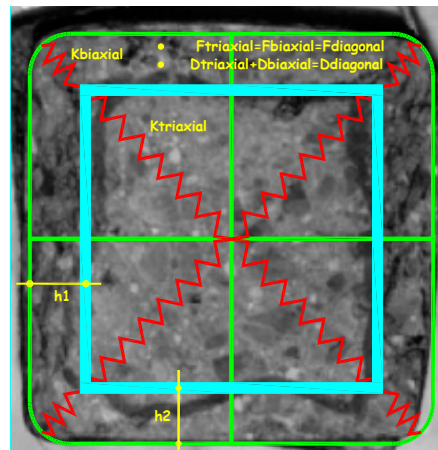


Figure4.11 “Generalized” springs

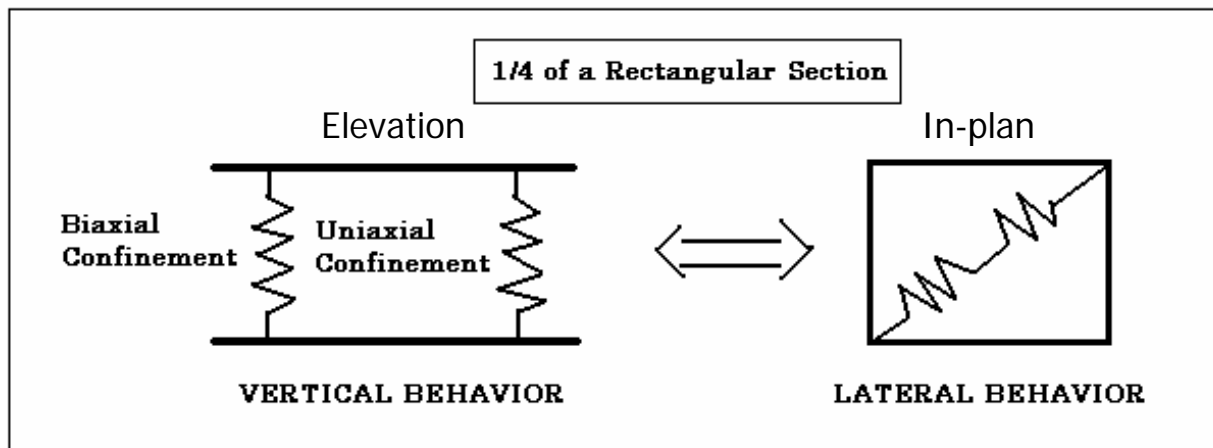


Figure4.12 Vertical and lateral behaviour of “Generalized” springs

For the constitutive law used to describe the behavior of these “generalized springs” the model of Pantazopoulou&Mills (1995) has been taken as a basis. The model which relates the volumetric strains to axial strains describes the following behavior shown in the figure. (Volumetric strains are simply the summation of lateral strains in the two directions with the vertical one).

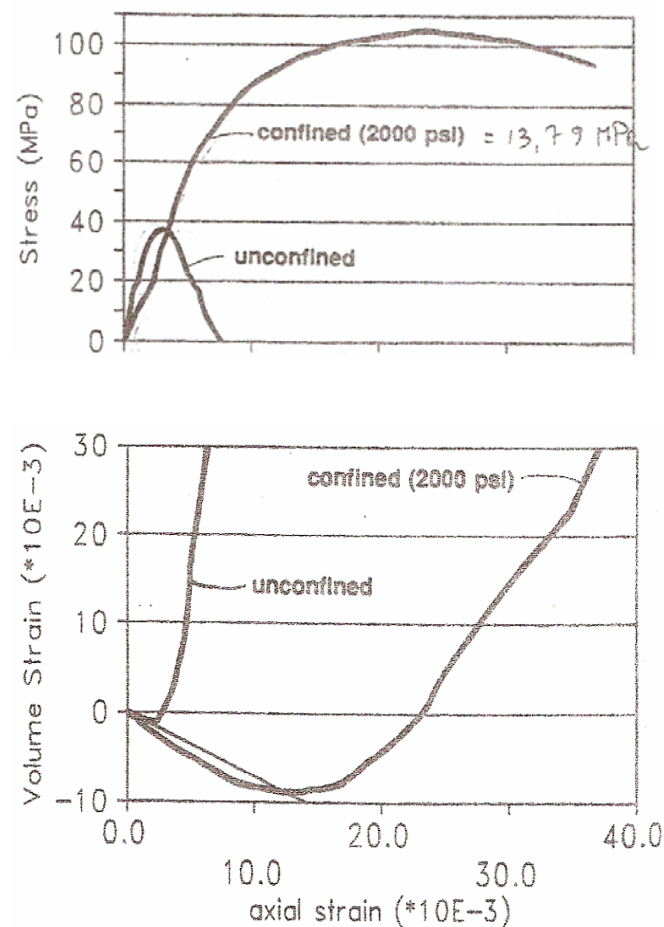


Figure4.13 Volumetric Strains to Axial Strains (Pantazopoulou&Mills)

Confinement is known to delay loss of stiffness and strength and to increase the deformability of the material; these features are evident in the stress strain curve above. Therefore, the higher internal stress and higher deformability developed by confined concrete simply imply a delay in the onset of unstable crack propagation. Evidently confinement provides the necessary lateral kinematic restraint that prevents volumetric dilation and keeps the concrete fragments together, to the extent that failure can be delayed, or even altered, to resemble plastic flow. This point is manifest in the relationship between volume strain ε_v and axial strain ε_c plotted in the figure above. The initial slope of the curve representing unconfined concrete in an idealized elastic condition is $(1-2\nu)$. Again both curves deviate from this line; however, the curve for confined concrete does so at a much slower rate than the unconfined one, and it reaches a minimum (point of reversal of ε_v at a higher level of axial strain. In tests under very high confining stresses, it has been observed that in some cases the $\varepsilon_v - \varepsilon_c$ diagram may not even cross the ε_c axis.

As stated above prior to apparent surface cracking, the $\varepsilon_v - \varepsilon_c$ relationship is almost linear, with lateral strain being $\varepsilon_l = \nu \varepsilon_c$ (ν is the ASTM-based value in the range of 0.15-0.25). Beyond the axial strain value $\varepsilon_c = \varepsilon_c^{\text{lim}}$ that corresponds to lateral strain ε_l in excess of the tensile cracking of concrete ε_{cr} , the $\varepsilon_v - \varepsilon_c$ relationship shows profound deviation from the idealized linear response, and appears to be well approximated by a parabolic expression. The model of Pantazopoulou and Mills (1995) of confined concrete under uniaxial load is as follows:

$$\begin{aligned} \varepsilon_v &= (1 - 2 \cdot \nu) \cdot \varepsilon_c & \varepsilon_c \leq \varepsilon_l^{\text{lim}} &= -\frac{\varepsilon_{cr}}{\nu} \\ \varepsilon_v &= (1 - 2\nu) \cdot \alpha \cdot \varepsilon_{co} \left[\frac{\varepsilon_c}{\alpha \cdot \varepsilon_{co}} - b \left(\frac{\varepsilon_c - \varepsilon_l^{\text{lim}}}{\alpha \cdot \varepsilon_{co} - \varepsilon_l^{\text{lim}}} \right)^c \right] & \varepsilon_c > \varepsilon_l^{\text{lim}} \end{aligned} \quad (4.2)$$

Parameter $\alpha \varepsilon_{co}$ represents the compressive axial strain at the instant of zero volumetric strain, which for normal strength concrete commonly occurs at strains 0.002 to 0.0035, i.e., at 80 to 100 of the strain at peak stress ε_{co} . ε_c is the compressive axial strain variable, usually controlling the load application in uniaxial tests. Constant b can be used to reflect the degree of passive confinement of concrete, the value of 1 corresponding to uniaxially loaded, unconfined concrete; lower values would be required as higher passive confining pressures are applied. Constants α and c would be increased for higher strength concretes; it appears that α increases with nominal strength towards the value of 1, where as the post peak response becomes more brittle. (c tends towards or exceeds 3).

The same behavior (linear and parabolic part) has been observed also in the relationship between volumetric strains and axial stresses.

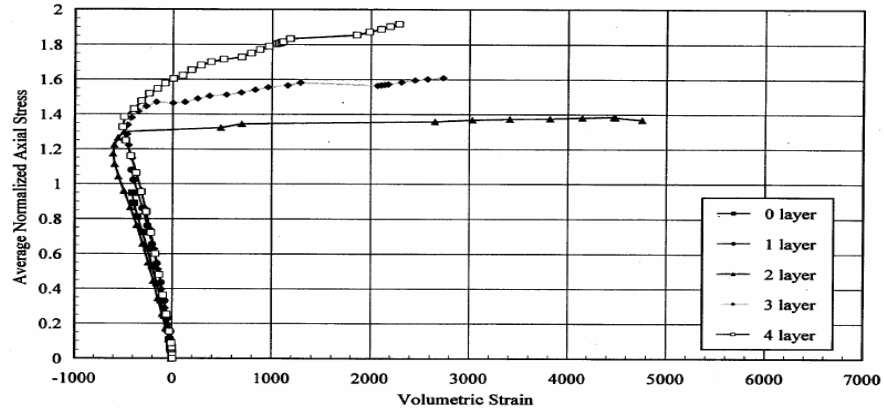


Figure 4.14 Volumetric Strains to Axial Stresses (Technical Report FDOT)

Initially, volume change is in the form of compaction and is almost linear up to the critical stress of $0.7f_{co}$ (unconfined concrete strength) until which the Poisson's ratio ν remains in the range of 0.15-0.25. At this point, direction of volume change is reversed resulting in a volumetric expansion called dilatancy near or at peak strength. The expansion becomes unstable at the crushing phase of concrete that is beyond the peak strength.

In order to comply with the mechanical model of the “generalized” springs and the differently confined regions the model of Pantazopoulou and Mills has been modified so it can relate the volumetric strains with the axial stresses according to the following equation:

$$\varepsilon_v = -(1-3\nu) \cdot 10^{-4} \cdot f_c \quad f_c \leq \alpha f_{co} \quad (4.3)$$

$$\varepsilon_v = -(1-3\nu) \cdot 10^{-4} \cdot b \cdot f_{co} \left[\frac{f_c}{b f_{co}} - \left(\frac{f_c - \alpha f_{co}}{b f_{co} - \alpha f_{co}} \right)^c \right] \quad f_c > \alpha f_{co}$$

where

- **Poisson's ratio** is given an initial value of $\nu=0.2$
- **Factor α** indicates the point where tensile cracking of concretes starts and therefore a change of Poisson's coefficient is observed. Usually that happens when $\alpha=0.7$ (for this limit also the initial Young Modulus of concrete is also usually determined).
- **Factor b** indicates the point where the volumetric strain becomes zero. The value of 1.2 has been determined for this point which is the ultimate strength of the uniaxially confined region (biaxial stress state). After the deterioration of this region expansion rate of concrete becomes higher than the compression rate of the specimen due to less effective resulted confinement.

- **Factor c** indicates the expansion rate of concrete after the tensile cracking. The value of 2 is given knowing that the right inclination will be adjusted through the proposed iteration procedure.

In the model of Pantazopoulou&Mills the axial strains are considered negative by keeping the same base after determining the volumetric strain from the above equation the area strain can be easily determined as the difference between the volumetric strain ε_V and the axial strain ε_c :

$$\varepsilon_A = \varepsilon_V - \varepsilon_c \quad (4.4)$$

Now assuming that the diagonal lateral deformation is the most critical one in a rectangular section the following deformed shape can be produced:

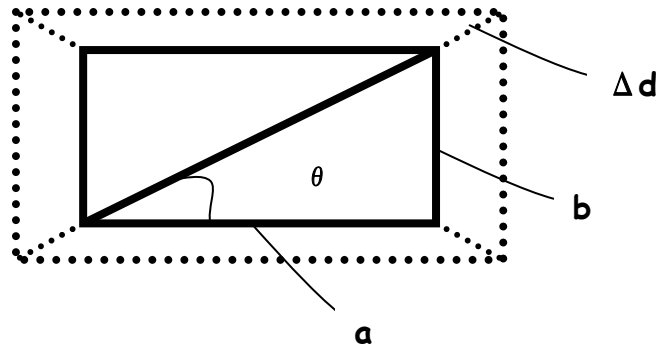


Figure4.15 Deformed Shape of a rectangular section based only on the diagonal lateral deformation

Based on that figure the elongation strain of the sides can be calculated easily as follows:

$$\varepsilon_A = \frac{\Delta A}{A} = \frac{(\alpha + \Delta\alpha) \cdot (b + \Delta b) - a \cdot b}{a \cdot b} = \frac{(\alpha + \varepsilon_a \cdot \alpha) \cdot (b + \varepsilon_b \cdot b) - a \cdot b}{a \cdot b} = (1 + \varepsilon_a) \cdot (1 + \varepsilon_b) - 1 \quad (4.5)$$

$$\frac{\varepsilon_a}{\varepsilon_b} = \frac{\Delta_a \cdot b}{\Delta_b \cdot a} = \frac{\Delta_d \cdot \cos \theta \cdot b}{\Delta_d \cdot \sin \theta \cdot a} = 1 \quad (4.6)$$

$$\varepsilon_A = (1 + \varepsilon_{elongation})^2 - 1 \Rightarrow \varepsilon_{elongation} = \sqrt{\varepsilon_A + 1} - 1 \quad (4.7)$$

According to the above calculations a very important conclusion can come up. The fact that in a circular section the lateral elongation is the same around the section doesn't provoke any objection. However, this is not the case if is proposed the same for a rectangular section. Apparently, based on the above considerations even in a rectangular section the elongation of the side is the same, a conclusion that allows us to consider only the deformation of one of the two sides and calculate it based on the area stains as previously described.

Based on a usually applied assumption of no friction between FRP jacket and concrete section the elongation strain of the sides and the jacket strain can be equated. Therefore the diagonal force of the jacket applied laterally from the corners to the springs can be determined by projection:

$$F_{diagonal} = \sqrt{2} \cdot E_j \cdot \varepsilon_{elongation} \cdot t_j \cdot k_e \quad (4.8)$$

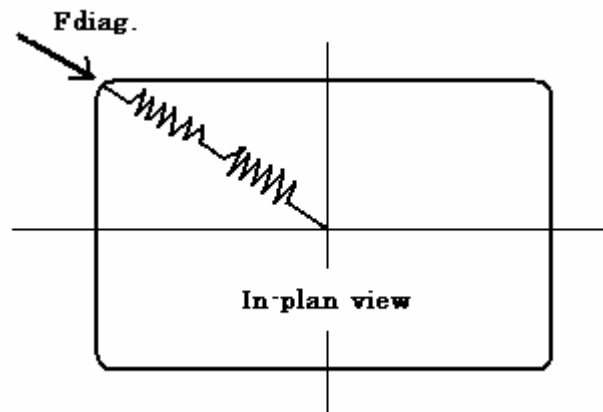


Figure4.16 Diagonal force applied to the lateral springs from the corner of the section

The factor k_e is a confinement efficiency factor by Gebran Karam & Mazen Tabbara (2005) which takes into account the fact that confinement effectiveness is increasing by increasing the corner radius and is decreasing by increasing the rectangularity of the section. The following figures show the considerations made to end up to this factor.

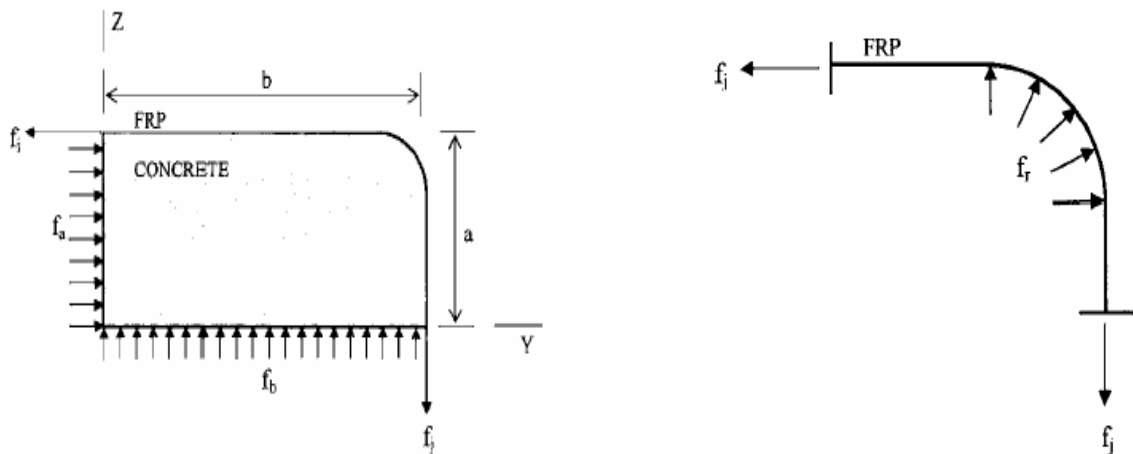


Figure4.17 Confinement effectiveness factor (Gebran Karam & Mazen Tabbara (2005))

In the figure in the left side a confining FRP wrap is shown acting on a generic

rectangular section with short side $2a$, a long side $2b$ and radius of the rounded corner R following the simple approach for circular sections. The concrete is assumed to be subjected to average (uniform) confining stresses at its middle sections with f_a acting along the short side and f_b acting along the long side as shown in the figure. The relationship between the f_a , f_b and the jacket tensile stress f_j is determined from statics:

$$t \cdot f_j = \alpha \cdot f_a = b \cdot f_b \quad (4.9)$$

where t = thickness of the FRP wrap. In the figure in the right hand, the FRP wrap is assumed to act as a cable around the corner similarly to a pulley. Assuming no friction the relationship between f_j and the confining stresses at the corner f_r is also found from statics:

$$t \cdot f_j = \alpha \cdot f_a = b \cdot f_b \quad (4.10)$$

Using the equations (4.7) and (4.8) the following equations can be written:

$$\frac{f_b}{f_a} = \frac{\alpha}{b} \quad \frac{f_r}{f_a} = \frac{a}{R} \quad (4.11)$$

Hence the sharper the corner radius, the higher the confining stress at the corner with respect to the average confining stress inside the cross section. This is supported by the finite element analysis of Parvin and Wang (2001) and published experimental results Cole and Belarbi 2001; Yang et al. 2001a; de Paula and da Silva 2002; Parvin and Wang 2002; Chaallal et al. 2003.

Based to the above considerations it is possible to define a geometric confinement effectiveness factor as the average confinement stress over the whole cross section divided by the maximum confinement stress attained in the cross section. In a typical rectangular cross section the maximum confinement stress can be taken as equal to the average of the two uniform confining stresses acting at the center of the cross section $(f_a + f_b)/2$. The confinement effectiveness factor can be then calculated as:

$$k_e = \frac{f_a + f_b}{2 \cdot f_r} = \frac{R}{\alpha} \cdot \frac{1}{2} \cdot \left(1 + \frac{\alpha}{b} \right) \quad (4.12)$$

It is clear that $k_e = 1$ for a circular cross section and $k_e = R/a$ for a square cross section. For the case of an elongated cross rectangular cross section with semicircular ends $b \gg a$ and $R = a$, k_e tends asymptotically to 0.5, which corresponds to confinement along one direction in the cross-sectional plane.

After the determination of the diagonal force applied to the lateral springs in series from the corners also the lateral pressures for each region can be easily determined.

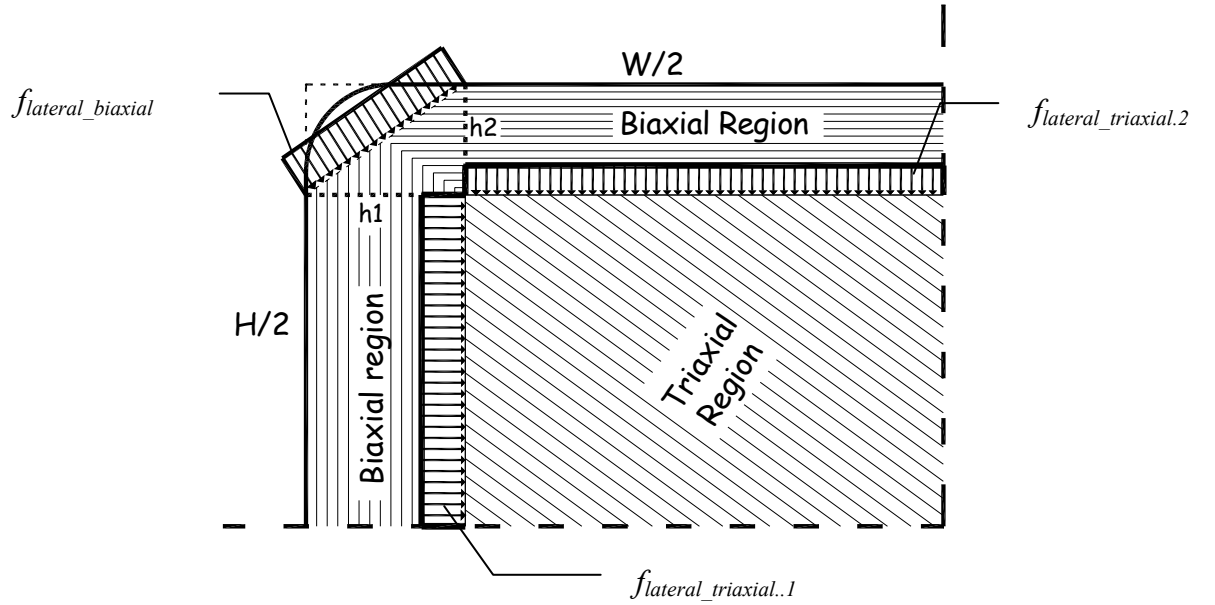


Figure 4.18 Confining pressures in the different regions

The springs are in series so they “feel” the same force. For the biaxial stress state region the force starts from the corners and moves to the directions parallel to the sides. Therefore the confining pressure (assumed uniform) can easily be determined by the following equation:

$$h = \sqrt{h_1^2 + h_2^2} \quad (4.13)$$

$$f_{lateral_biaxial} = \frac{F_{diagonal}}{h} \quad (4.14)$$

For the triaxial stress state region the uniform confining pressures on the sides of the section can be easily determined based on the geometry of the region as follows:

$$f_{lateral_triaxial}^1 = \frac{F_{diagonal}}{0.5 \cdot H - h_{2_biaxial}} \quad f_{lateral_triaxial}^2 = \frac{F_{diagonal}}{0.5 \cdot W - h_{1_biaxial}} \quad (4.15)$$

Based on the lateral pressures calculated above the corresponding vertical stress can be easily determined by the use of a biaxial or a triaxial stress strain model corresponding to the confinement stress state of each region:

- **Triaxial stress-state region:** The stress-strain model of Popovic modified by

Mander et al is used to describe the behavior of this region. The model is described extensively in the previous chapter. The equation of maximum vertical stress f_{cc} is not used in this case due to the fact that it describes the performance of hydrostatic confining pressure. In order to comply with the above modeling of the triaxial stress-state region where the confining pressures are different in the two directions (only in the case of a square section are the same) a failure criterion where all the cases can be considered is applied. To be more specific the failure surface of Ottosen is used.

The failure criterion of Ottosen although described in the previous chapter is given again here for completeness of the proposed model. As already mentioned it is an elasticity based model having a Hookean formulation in incremental form. The stiffness tensor is simplified by using three stress strain invariants trying to describe the behaviour of concrete. It corresponds to a smooth convex failure surface with curved meridians, which open in the negative direction of the hydrostatic axis, and the trace in the deviatoric plane changes from nearly triangular to more circular with increasing the hydrostatic pressure.

The following equations describe the surface. Having the lateral confining pressures of this region through iteration the value of maximum vertical stress f_{cc} can be reached that makes the surface equal to the unit value.

$$A \frac{J_{2\sigma}}{f_c^2} + \lambda \frac{\sqrt{J_{2\sigma}}}{f_c} + B \frac{I_{1\sigma}}{f_c} - 1 \geq 0 \quad (4.16)$$

where:

$$I_{1\sigma} = \sigma_1 + \sigma_2 + \sigma_3 \quad (4.17)$$

$$\sigma_1 = -f_{cc_triaxial} \quad \sigma_2 = -f_{lateral_triaxial.1} \quad \sigma_3 = -f_{lateral_triaxial.2} \quad (4.18)$$

$$\sigma_0 = \frac{1}{3} \cdot (\sigma_1 + \sigma_2 + \sigma_3) \quad (4.19)$$

$$J_{2\sigma} = \frac{((\sigma_1 - \sigma_0)^2 + (\sigma_2 - \sigma_0)^2 + (\sigma_3 - \sigma_0)^2)}{2} \quad (4.20)$$

$$J_{3\sigma} = (\sigma_1 - \sigma_0) \times (\sigma_2 - \sigma_0) \times (\sigma_3 - \sigma_0) \quad (4.21)$$

$$\lambda = K_1 \cdot \cos \left[\frac{1}{3} \cdot \arccos(K_2 \cdot \cos 3\theta) \right] \quad \cos 3\theta \geq 0 \quad (4.22)$$

$$\lambda = K_1 \cdot \cos \left[\frac{\pi}{3} - \frac{1}{3} \cdot \arccos(-K_2 \cdot \cos 3\theta) \right] \quad \cos 3\theta \leq 0$$

$$\cos 3\theta = \frac{3 \cdot \sqrt{3}}{2} \cdot \frac{J_{3\sigma}}{J_{2\sigma}^{3/2}} \quad (4.23)$$

The rest parameters of the model were calibrated by the values proposed in the original paper of Ottosen N.S. (1977) for different ratios of $k=f_t/f_c$.

Table 4.1. Proposed values for the parameters of the failure criterion of N.S.Ottosen.

k	A	B	K₁	K₂
0.08	1.8076	4.0962	14.4863	0.9914
0.1	1.2759	3.1962	11.7365	0.9801
0.12	0.9218	2.5969	9.9110	0.9647

Based on the f_{cc} determined above the stress-strain law of Mander et.al is applied. The following equations describe the model's behavior:

$$f_{c_triaxial} = \frac{f_{cc_triaxial} \times x \times r}{r - 1 + x^r} \quad (4.24)$$

$$r = \frac{E_c}{E_c - E_{sec}} \quad (4.25)$$

$$\varepsilon_{cc} = \varepsilon_{c0} \left[1 + 5 \left(\frac{f_{cc_triaxial}}{f_{c0}} - 1 \right) \right] \quad (4.26)$$

$$E_{sec} = \frac{f_{cc_triaxial}}{\varepsilon_{cc}} \quad x = \frac{\varepsilon_c}{\varepsilon_{cc}} \quad (4.27)$$

- **Biaxial Stress-state region:** The model for concrete under biaxial stress of Liu et al (1972) is used for the biaxial region:

$$f_{c_biaxial} = \frac{\varepsilon_c \cdot E_c}{(1 - \nu\alpha_1) \left[1 + \left(\frac{E_c}{f_{cp}'(1 - \nu\alpha_1)} - \frac{2}{\varepsilon_{cp} + 0.005} \right) \cdot \varepsilon_c + \left(\frac{\varepsilon_c}{\varepsilon_{cp} + 0.005} \right)^2 \right]} \quad (4.28)$$

$$\alpha_1 = \frac{f_{lateral_biaxial}}{f_{c_biaxial}} \quad (4.29)$$

where:

$$\alpha_1 < 0.2 \quad f_{cp1}' = \left(1 + \frac{\alpha_1}{1.2 - \alpha_1}\right) \cdot f_c' \quad (peak\ stress) \quad (4.30)$$

$$1.0 \geq \alpha_1 \geq 0.2 \quad f_{cp1}' = 1.2 \cdot f_{co}' \quad (4.31)$$

Note: For $\alpha_1 > 1$ the $f_{c_biaxial}$ is kept constant to the value of $1.2f_{co}$

$$\alpha_1 \leq 1 \quad \varepsilon_{cp1} = 0.0025 \quad (peak\ strain) \quad (4.32)$$

Based on the areas of the different regions we can have the total averaged vertical stress of the section.

$$A_{biaxial} = (0.5 \cdot W) \cdot h_2 + (0.5 \cdot H) \cdot h_1 - h_1 \cdot h_2 \quad (4.33)$$

$$A_{triaxial} = (0.5 \cdot H - h_{2_biaxial}) \cdot (0.5 \cdot W - h_{1_biaxial}) \quad (4.34)$$

$$A_{total} = H \cdot W \quad (4.35)$$

$$f_{c_total} = \frac{4 \cdot A_{biaxial}}{A_{total}} \cdot f_{c_biaxial} + \frac{4 \cdot A_{triaxial}}{A_{total}} \cdot f_{c_triaxial} \quad (4.36)$$

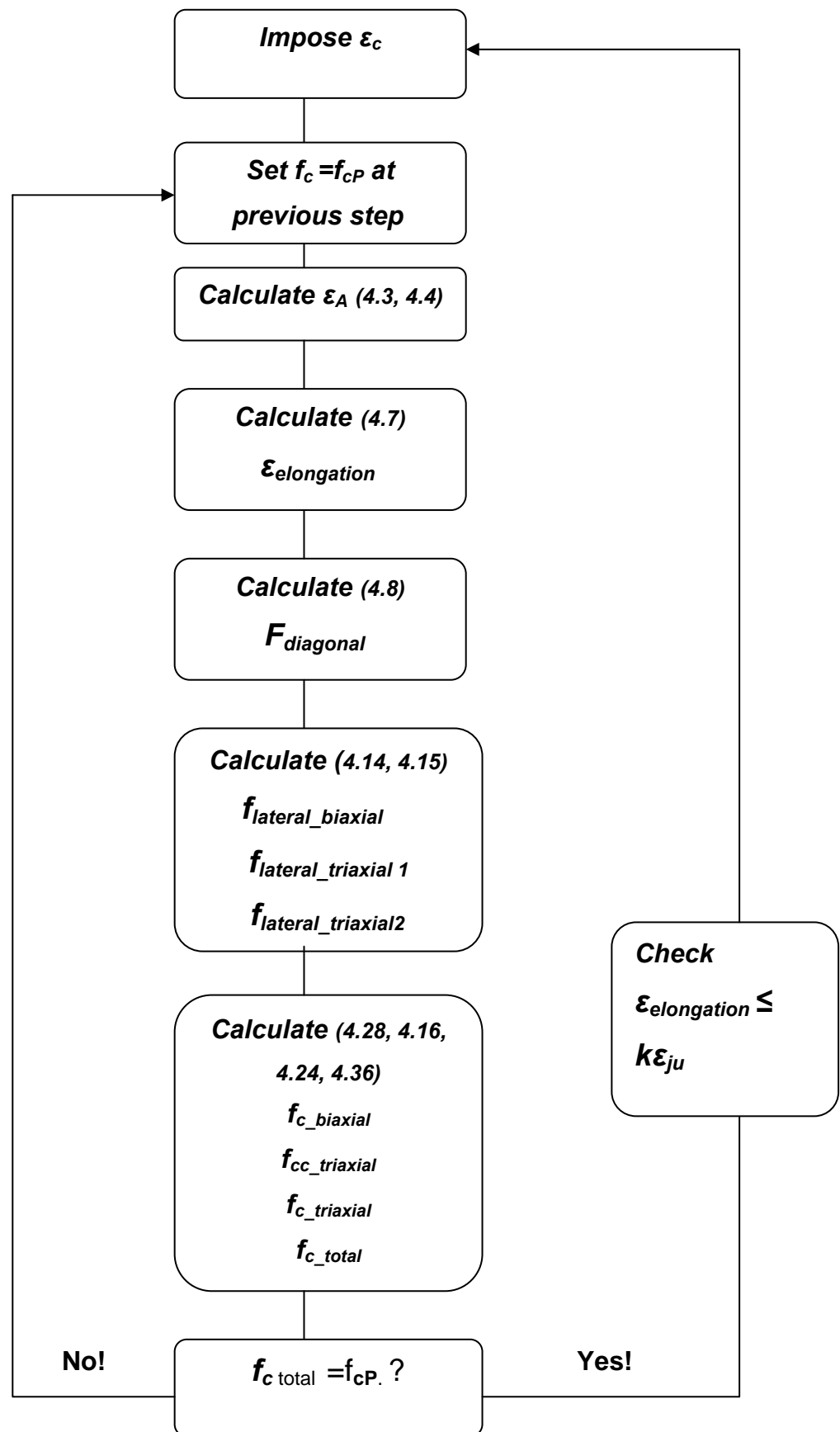


Figure4.19 Proposed Iteration Procedure

After converging the assumed vertical stress with the one calculated with the above considerations, the resulted elongation strain through the iteration procedure should be compared to the ultimate rupture strain of the jacketing. It has been observed from experimental results that the average failure strains of the FRP wraps are of the order of 50-80% of the failure strain of the tensile coupons made from the same material and tested before the application of the material. This actual value of factor k (ranging between 50-80%) depends on the type of FRP used. In the following tables published by Lam&Teng this factor is reported in the column (k_e):

Table 4.2. Factor k from existing experimental results (Lam&Teng).

No.	B (mm)	H (mm)	Length (mm)	R_c (mm)	f'_{co} (MPa)	Type of FRP	t (mm)	f_{frp} (MPa)	E_{frp} (MPa)	ϵ_{lu} (%)	f'_{cc}/f'_{co}	$\epsilon_{cu}/\epsilon_{co}$	f_{cr} (MPa)	$\epsilon_{cc}/\epsilon_{co}$	k_e	$k_1 k_e$	$k_2 k_e^{1.45}$
Square Specimens																	
Demers and Neale [24]																	
1	152	152	505	5	32.3	GFRP	1.05	220	10500	–	0.985	5.25	24.0	1.50	5.30	30.46	
2	152	152	505	5	32.3	GFRP	1.05	220	10500	–	1.022	4.50	22.0	1.50	5.30	30.46	
3	152	152	305	5	32.3	CFRP	0.9	380	25000	–	1.056	12.25	28.0	2.00	5.67	34.91	
4	152	152	305	5	42.2	CFRP	0.9	380	25000	–	1.090	7.00	32.0	1.75	5.67	34.91	
5	152	152	305	5	42.2	CFRP	0.9	380	25000	–	1.083	12.50	28.0	1.75	5.67	34.91	
Rochette and Labossiere [16]																	
6	152	152	500	5	42.0	CFRP	0.9	1265	82700	0.23	0.940	3.45	25.2	1.25	0.575	1.95	6.41
7	152	152	500	25	42.0	CFRP	0.9	1265	82700	0.56	0.990	4.70	41.6	4.70	0.575	1.95	6.41
8	152	152	500	25	42.0	CFRP	0.9	1265	82700	0.63	1.030	4.45	42.4	4.45	0.575	1.95	6.41
9	152	152	500	38	42.0	CFRP	0.9	1265	82700	0.71	1.130	5.40	47.5	5.40	0.575	1.95	6.41
10	152	152	500	38	42.0	CFRP	0.9	1265	82700	1.61	1.200	5.80	49.1	5.80	0.575	1.95	6.41
11	152	152	500	5	43.9	CFRP	1.5	1265	82700	0.44	1.000	5.10	32.0	1.75	0.575	1.95	6.41
12	152	152	500	25	43.9	CFRP	1.2	1265	82700	0.59	1.160	6.75	50.9	6.75	0.575	1.95	6.41
13	152	152	500	25	35.8	CFRP	1.2	1265	82700	0.70	1.460	10.20	52.3	10.2	0.575	1.95	6.41
14	152	152	500	25	35.8	CFRP	1.5	1265	82700	0.65	1.610	10.60	57.6	10.6	0.575	1.95	6.41
15	152	152	500	38	35.8	CFRP	1.2	1265	82700	0.89	1.660	9.60	59.4	9.60	0.575	1.95	6.41
16	152	152	500	38	35.8	CFRP	1.5	1265	82700	0.86	1.920	11.95	68.7	11.95	0.575	1.95	6.41
17	152	152	500	5	43.0	AFRP	1.26	230	13600	0.79	1.180	5.30	23.7		0.557	1.90	11.20
18	152	152	500	5	43.0	AFRP	2.52	230	13600	1.30	1.200	7.45	28.4		0.557	1.90	11.20
19	152	152	500	5	43.0	AFRP	3.78	230	13600	1.48	1.250	10.40	34.8	1.25	0.557	1.90	11.20
20	152	152	500	5	43.0	AFRP	5.04	230	13600	0.90	1.260	6.20	46.9		0.557	1.90	11.20
21	152	152	500	25	43.0	AFRP	1.26	230	13600	1.12	1.190	3.95	30.5	1.30	0.557	1.90	11.20
22	152	152	500	25	43.0	AFRP	2.52	230	13600	1.27	1.190	4.85	44.3	1.30	0.557	1.90	11.20
23	152	152	500	25	43.0	AFRP	3.78	230	13600	0.94	1.240	5.50	49.9	1.30	0.557	1.90	11.20
24	152	152	500	25	43.0	AFRP	5.04	230	13600	1.04	1.280	6.30	57.2	1.30	0.557	1.90	11.20
Rectangular Specimens																	
Rochette and Labossiere [16]																	
51	152	203	500	25	42.0	CFRP	0.9	1265	82700	0.74	1.000	3.95	29.4		0.575	1.95	6.41
52	152	203	500	38	42.0	CFRP	0.9	1265	82700	0.68	1.040	4.25	42.0		0.575	1.95	6.41
53	152	203	500	5	43.9	CFRP	1.5	1265	82700	0.43	1.010	4.90	27.2		0.575	1.95	6.41
54	152	203	500	25	43.9	CFRP	1.2	1265	82700	0.53	1.010	4.65	42.1		0.575	1.95	6.41
Shehata et al. [27]																	
55	94	188	300	10	23.7	CFRP	0.165	3550	235000		1.089				0.801	2.66	
56	94	188	300	10	23.7	CFRP	0.33	3550	235000		1.401				0.801	2.66	
57	94	188	300	10	29.5	CFRP	0.165	3550	235000	0.50	1.085	3.95	27.0	1.00	0.801	2.66	6.05
58	94	188	300	10	29.5	CFRP	0.33	3550	235000	0.50	1.312	3.75	28.0	1.25	0.801	2.66	6.05

4.4 Proposed Model in MATLAB code with user's interface

The previously described iteration procedure was written in a MATLAB code so the necessary results can be easily obtained. For an easier manner of inputting the data the following interface has been created:

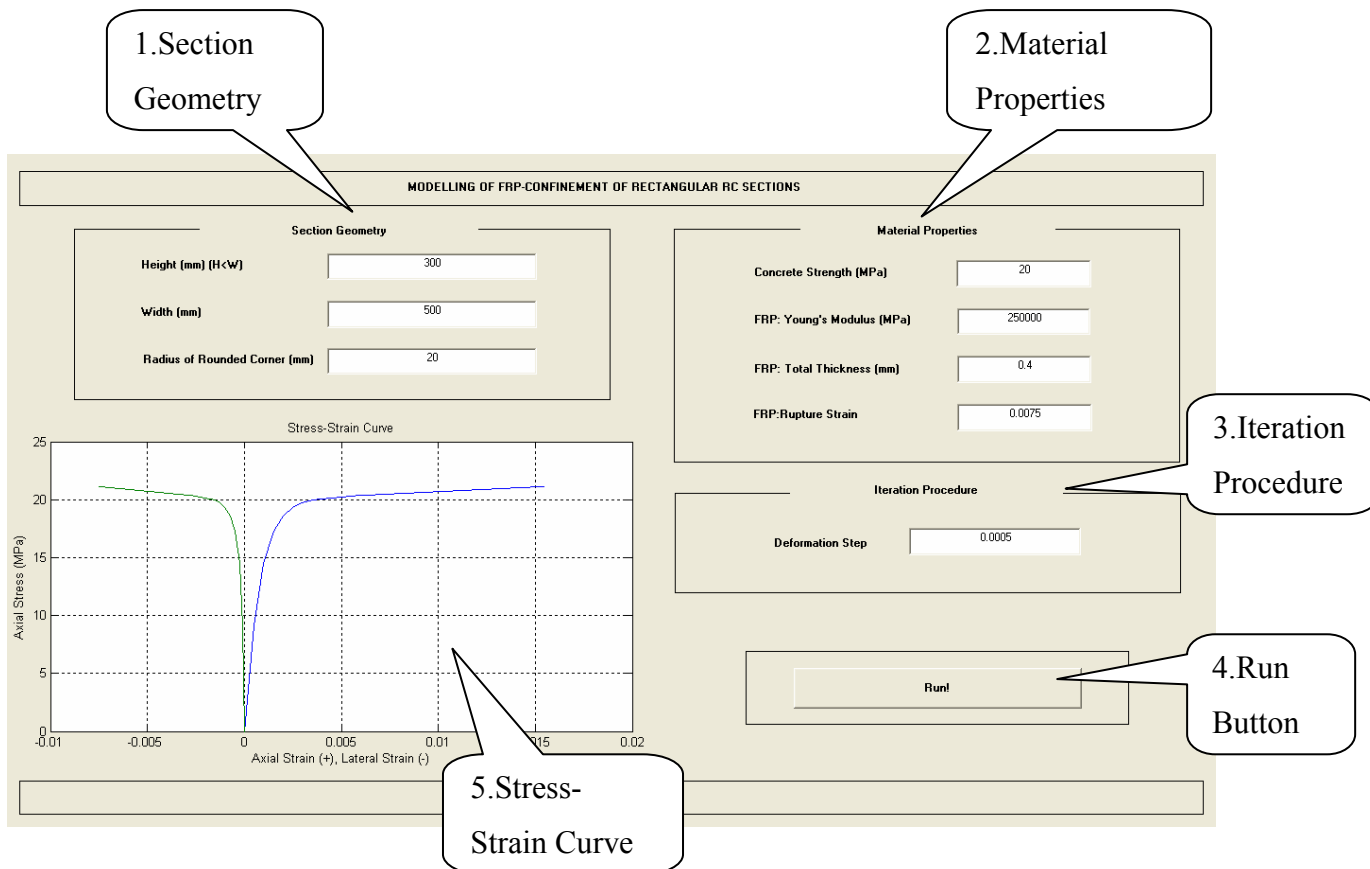


Figure 4.20 Proposed Model in MATLAB code with user's interface.

- In the first table as shown above the geometry of the rectangular section is asked. The Height in mm, the width and the radius of the rounded corner are the necessary input data of the table.
- In the second table the properties of the materials used are asked as input. The concrete strength in MPa and then the Elastic Modulus, the total thickness and the rupture strain of the FRP are the information needed. It has to be considered for the case of the rupture strain the penalty of the factor k previously described.
- In the third and the last table of the input the deformation step that the user would like the iteration procedure to run with is asked. Of course, lower step results to more time needed for the iteration procedure to reach the final

results.

- After the run button is clicked the iteration procedures starts. At the end in the command window of MATLAB are plotted all the input along with all the necessary results of confinement. The elapsed time needed for the iteration procedure is also printed.
- Finally the most important result of the procedure which is the axial stress plotted against the axial and the lateral strain of the section under concentric load is printed on the screen of the interface.

5 CORRELATION WITH EXPERIMENTAL RESULTS

5.1 Introduction

For the correlation of the model with experiments two series of experimental results has been used that contain all the necessary parameters for the verification of the model. The first series are from University of Salerno of Italy and include square short columns under compression where a GFRP jacketing was applied and the number of layers and the radius of the rounded corner were the parameters to study in the experiments. The second series are square and rectangular short columns confined with CFRP jacketing reported in the technical report of department of transportation of the state of Florida (USA) where the parameters to study in the experiments were the number of layers, the rectangularity of the section and the concrete strength. The experimental studies are carefully described in this chapter and at the end the prediction of the model is compared with those results.

5.2 Experimental Study of University of Salerno of Italy

The figures below show the specimen and the experimental configuration of the strain gages applied on the short column:

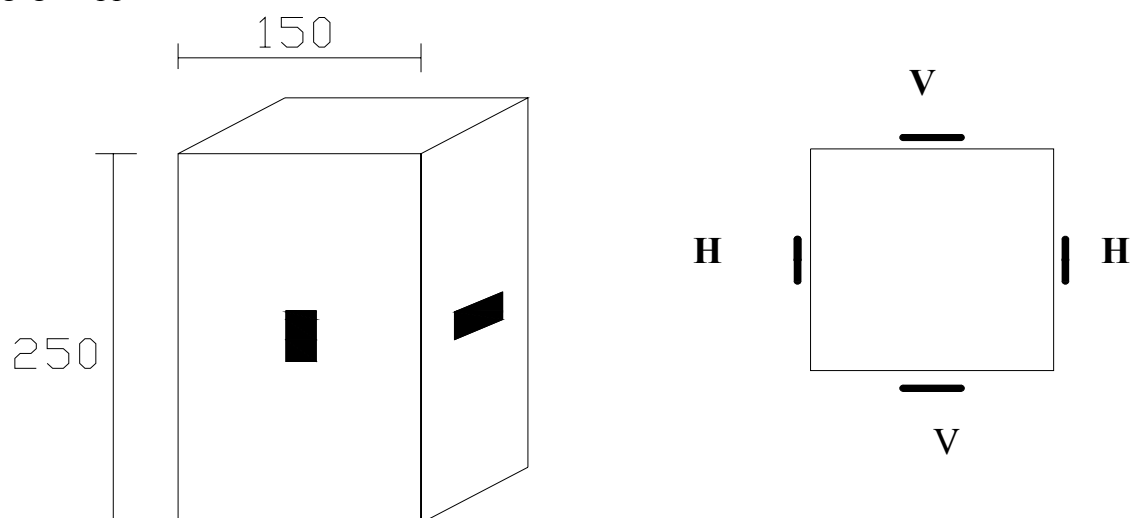


Figure 5.1 Specimen Configuration (University of Salerno, Italy)

The material properties and the details of the specimens along with their performance are summarized in the following tables:

Table 5.1. Material Properties.

Concrete Strength [MPa]	30
GFRP	
E_f (MPa)	80700
ε_{ju}	0.035
t_f (mm)	0.48
n_f	1
	2

Table 5.2. Specimen configuration and performance.

Specimen Configuration		Number of Layers	Rc (mm)	N_u (KN)	f_{cc} (MPa)
Specimen Code	Tag				
P3N1R10E0	P3*	1	10	719.81	32.115
P4N1R10E0	P4	1	10	727.872	32.474
P3N1R20E0	P5	1	20	920.278	41.536
P4N1R20E0	P6	1	20	754.487	34.053
P3N1R30E0	P7	1	30	909.779	41.875
P4N1R30E0	P8*	1	30	845.07	38.897
P11N2R10E0	P9	2	10	952.875	42.512
P12N2R10E0	P10	2	10	1104.138	49.261
P11N2R20E0	P11	2	20	1135.270	51.240
P12N2R20E0	P12	2	20	1171.408	52.871
P11N2R30E0	P13	2	30	1275.302	58.699
P12N2R30E0	P14	2	30	1206.812	55.547

The plots that follow show the comparison of the model prediction with the results of the experimental study described above. For the proper evaluation of the results it is reminded that the iteration procedure stops when the rupture strain of the FRP is exceeded. Therefore, the maximum transversal strain reported from the strain gages on the FRP jacket is given to the model for each case.

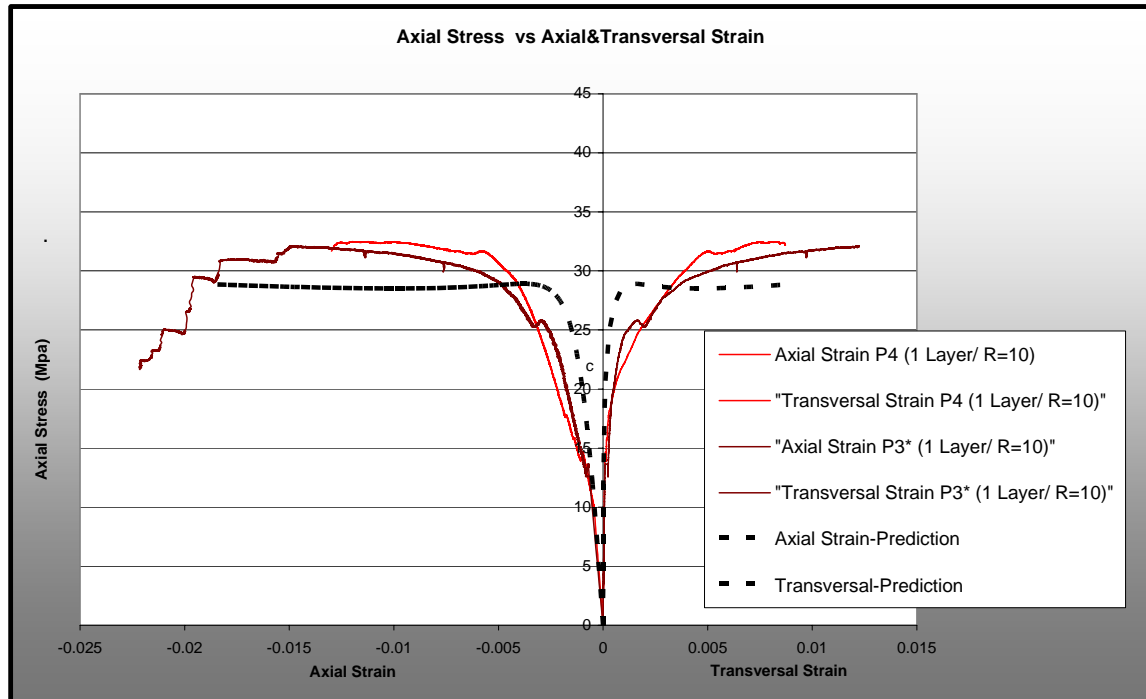


Figure 5.2 Comparison with experimental results (University of Salerno, Italy)

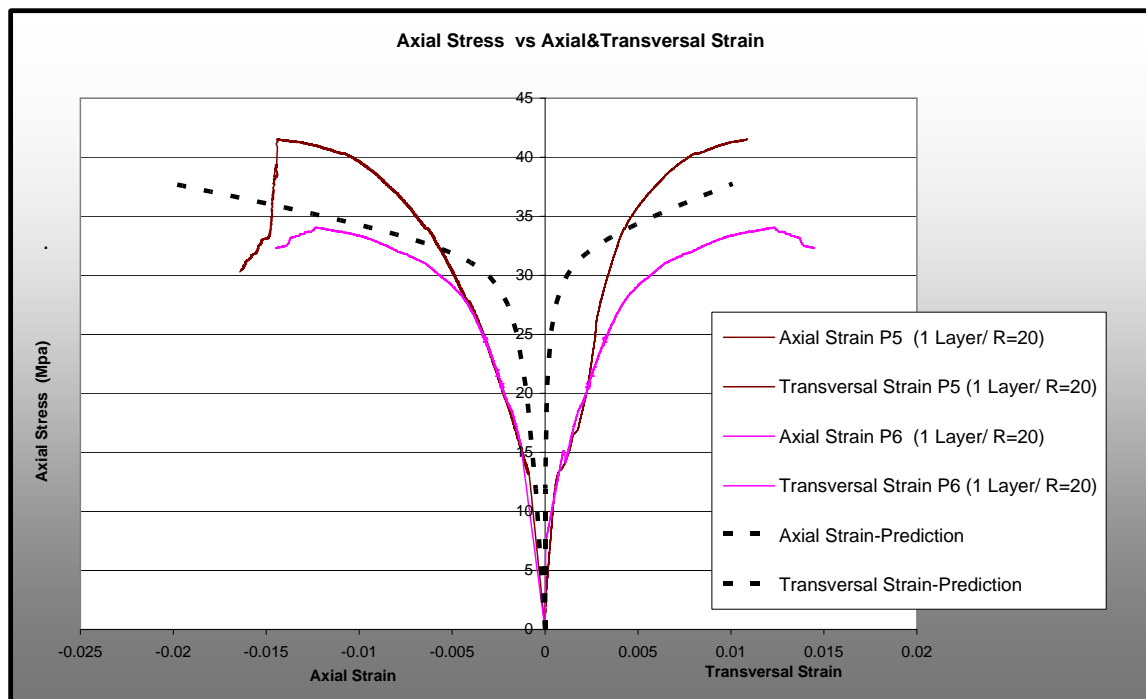


Figure 5.3 Comparison with experimental results (University of Salerno, Italy)

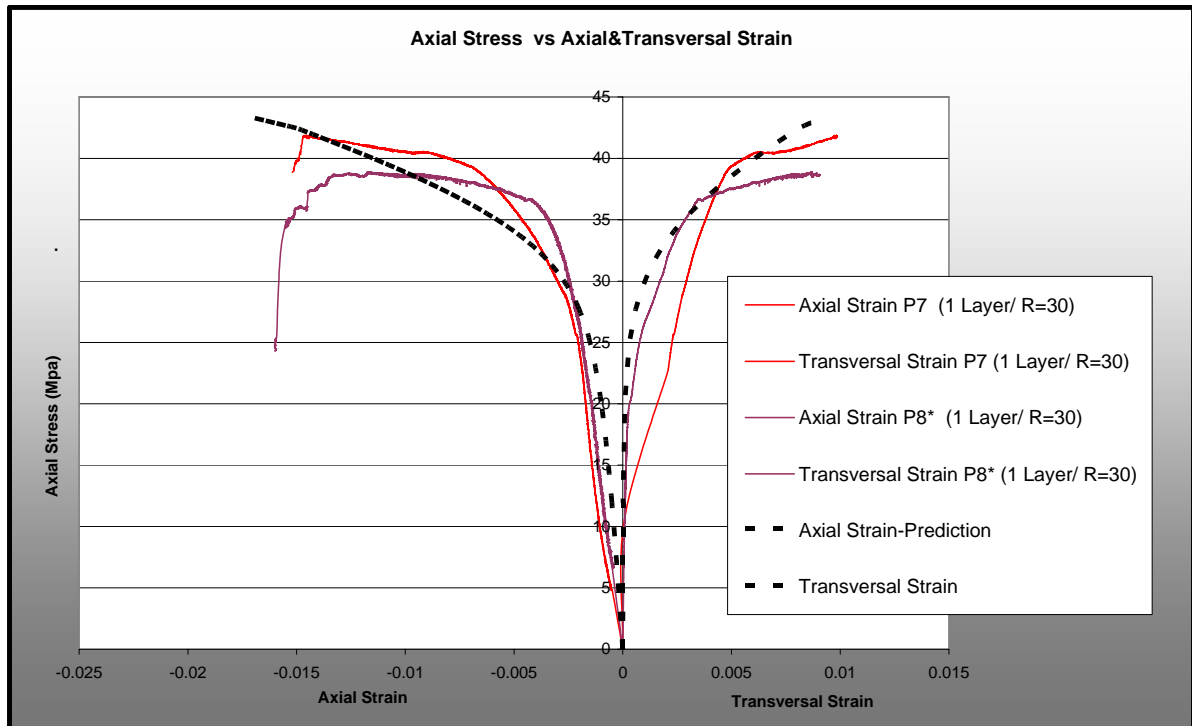


Figure 5.4 Comparison with experimental results (University of Salerno, Italy)

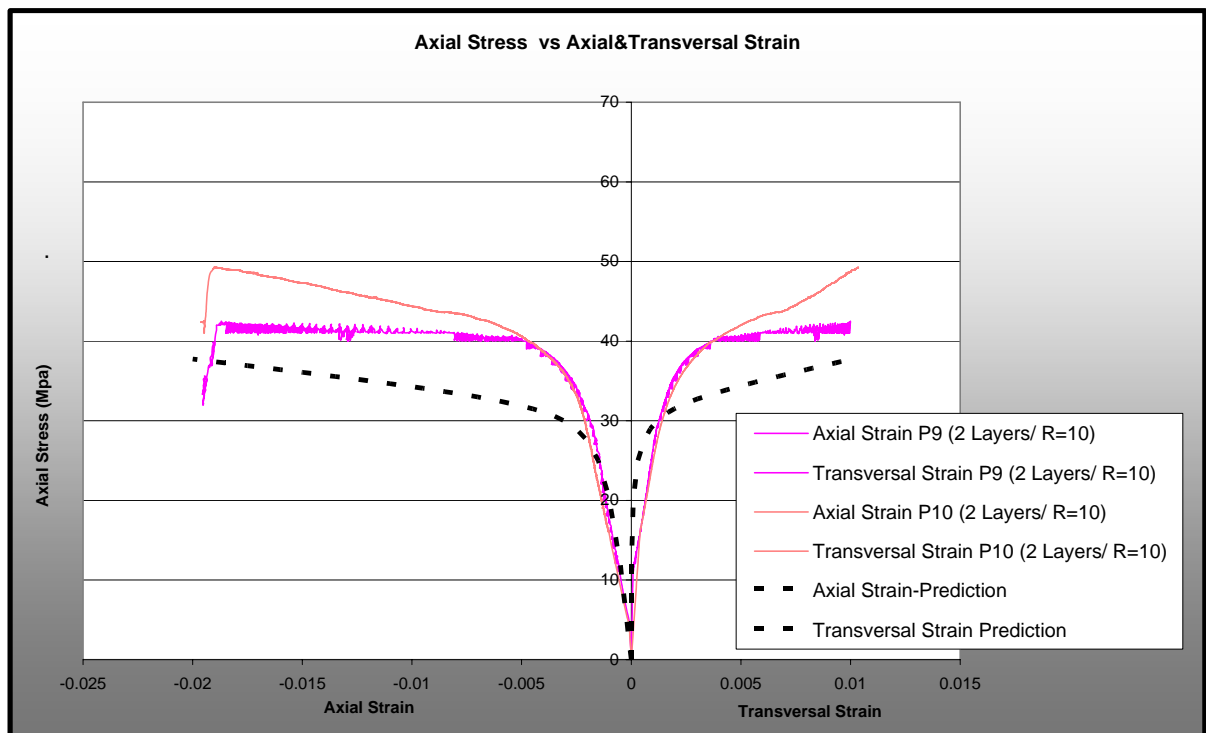


Figure 5.5 Comparison with experimental results (University of Salerno, Italy)

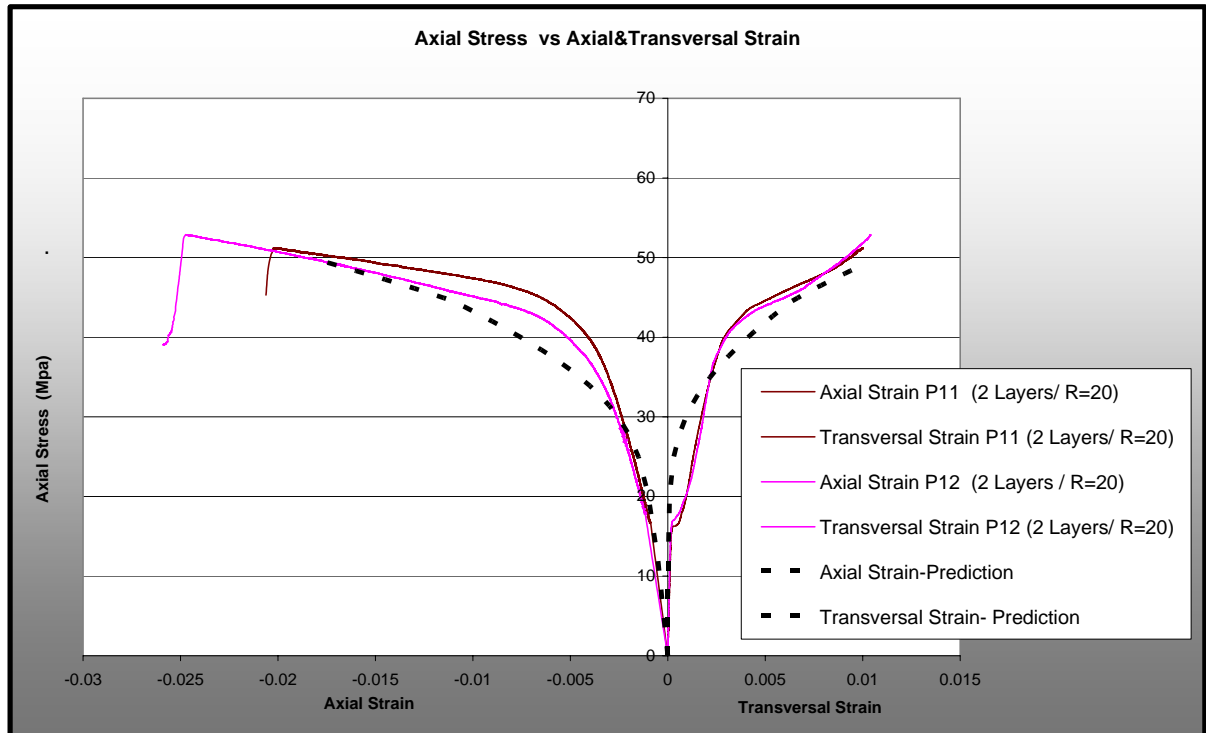


Figure5.6 Comparison with experimental results (University of Salerno, Italy)

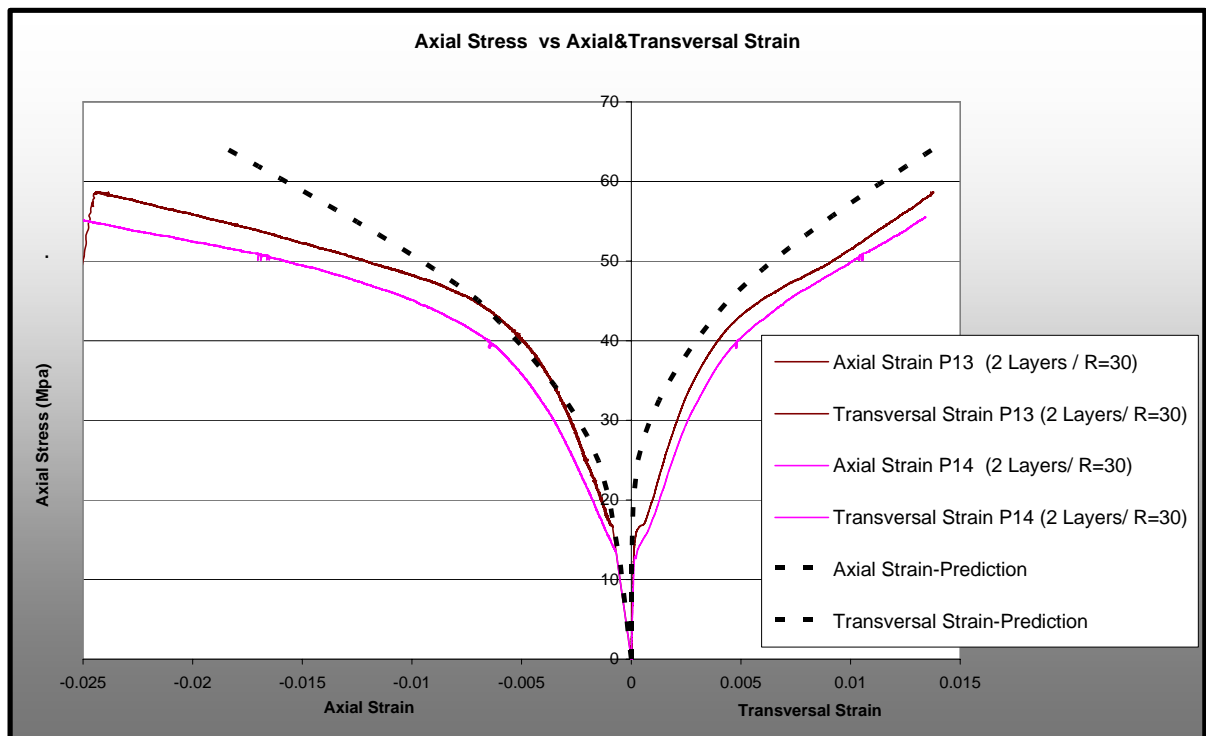


Figure5.7 Comparison with experimental results (University of Salerno, Italy)

Apparently from the plots above the model can predict adequately the curves' development but also the level of maximum axial stress and the corresponding axial strain. It is necessary to be noted that in each of the above plots are presented two of the specimens with the same configuration so to underline the fact that there is an important range in the experimental results that always should be taken into account in case of comparison.

5.3 Experimental Results from the technical report of Department of Transportation of Florida of USA (FDOT)

The experimental study presents results of a comprehensive experimental investigation on the behaviour of axially loaded short rectangular columns strengthened with CFRP wrap. Six series, a total of 90 specimens, of uniaxial compression tests are conducted on rectangular short columns. The behaviour of the specimens is investigated in the axial and transverse directions. The parameters considered in this study are: (a) concrete strength (targeted strengths 3 ksi and 6 ksi (1 ksi = 6.8948 MPa)), aspect ratio ($a/b=0.5, 0.65$ and 1) and number of CFRP layers (0, 1, 2, 3 and 4). The following tables and figures summarize the experimental study:

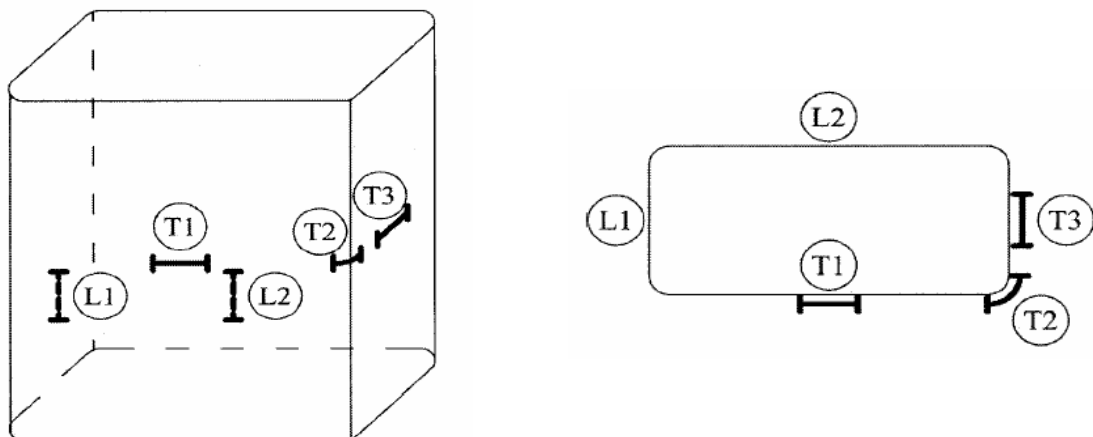


Figure 5.8 Location of longitudinal and transverse strain gages (Shahawy et al (2003))

Table 5.3. Material Properties of Carbon wraps (Shahawy et al (2003))

Description	Manufacturer's data ^a
Tensile strength	530 ksi (3.65 GPa)
Tensile modulus of elasticity	33,500 ksi (231 GPa)
Ultimate tensile elongation	1.4%
Filament diameter	7 μm
Filaments/yarn	12,000

^aReported for carbon fabric only.

Thickness of layer: 0.5 mm

Table 5.4. Specimen Configuration(Shahawy et al (2003))

Series	Specimen number	$a \times b$ (in.)	Number of CFRP layers	Number of specimens
(a) 3 ksi concrete				
1	SC-0L3-1.0	5.25×5.25	0	3
	SC-1L3-1.0	5.25×5.25	1	3
	SC-2L3-1.0	5.25×5.25	2	3
	SC-3L3-1.0	5.25×5.25	3	3
	SC-4L3-1.0	5.25×5.25	4	3
2	SC-0L3-0.7	4.25×6.5	0	3
	SC-1L3-0.7	4.25×6.5	1	3
	SC-2L3-0.7	4.25×6.5	2	3
	SC-3L3-0.7	4.25×6.5	3	3
	SC-4L3-0.7	4.25×6.5	4	3
3	SC-0L3-0.5	3.75×7.5	0	3
	SC-1L3-0.5	3.75×7.5	1	3
	SC-2L3-0.5	3.75×7.5	2	3
	SC-3L3-0.5	3.75×7.5	3	3
	SC-4L3-0.5	3.75×7.5	4	3
(b) 6 ksi concrete				
4	SC-0L6-1.0	5.25×5.25	0	3
	SC-1L6-1.0	5.25×5.25	1	3
	SC-2L6-1.0	5.25×5.25	2	3
	SC-3L6-1.0	5.25×5.25	3	3
	SC-4L6-1.0	5.25×5.25	4	3
5	SC-0L6-0.7	4.25×6.5	0	3
	SC-1L6-0.7	4.25×6.5	1	3
	SC-2L6-0.7	4.25×6.5	2	3
	SC-3L6-0.7	4.25×6.5	3	3
	SC-4L6-0.7	4.25×6.5	4	3
6	SC-0L6-0.5	3.75×7.5	0	3
	SC-1L6-0.5	3.75×7.5	1	3
	SC-2L6-0.5	3.75×7.5	2	3
	SC-3L6-0.5	3.75×7.5	3	3
	SC-4L6-0.5	3.75×7.5	4	3

Note: 1 ksi= 6.8948 MPa.

1 in= 25.4mm

Height of specimens: 12 in.

The effect of high concrete strength has been already tested from the previous series of experiments. Moreover, the comparison with the model's prediction for the case of square specimens has already been done. Therefore, the series of concrete strength 3 ksi (20.7 MPa) has been chosen for correlation with the model for two different aspect ratio of $a/b=0.5$, 0.65 so the effect of rectangularity of the specimen can be also tested. The following plots are reported for comparison with these experimental results. Please note again that the maximum transversal strain of the Jacket was given to the iteration procedure as input for each case. In addition should be underlined the fact that values shown in the plot are average of the 3 specimens tested for each case and that transversal strains are the average of the strains measured from the long side short side and corner side of the section.

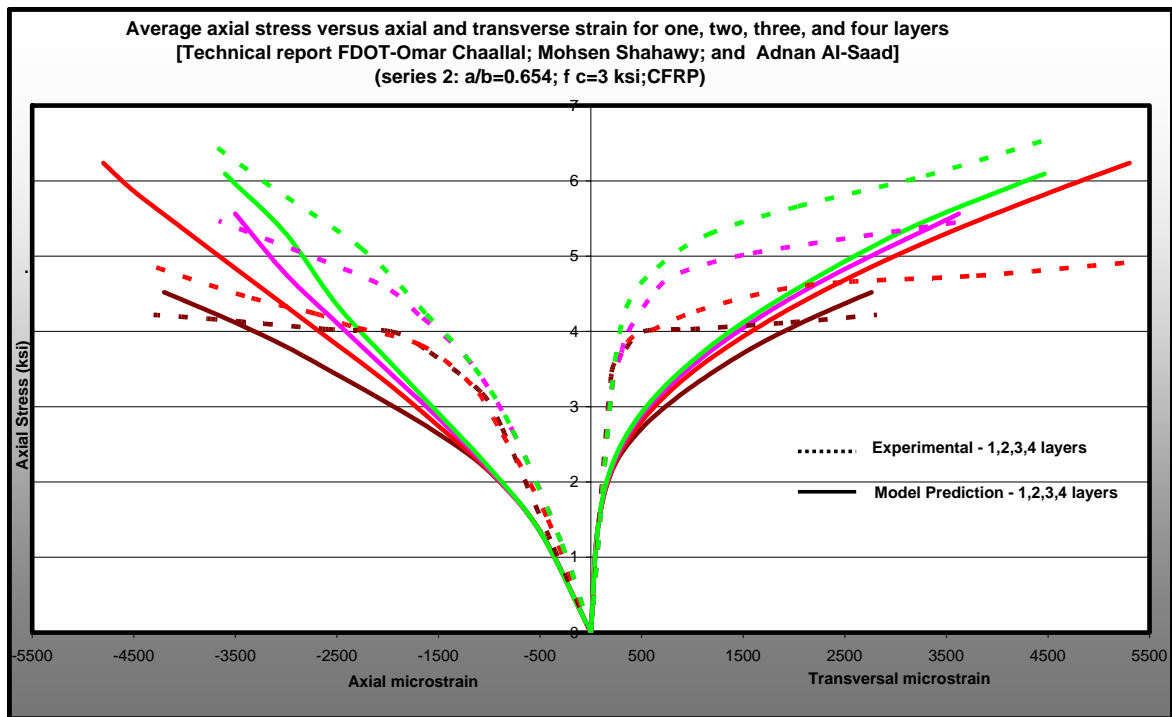


Figure 5.9 Comparison with Experimental Results (Technical Report FDOT)

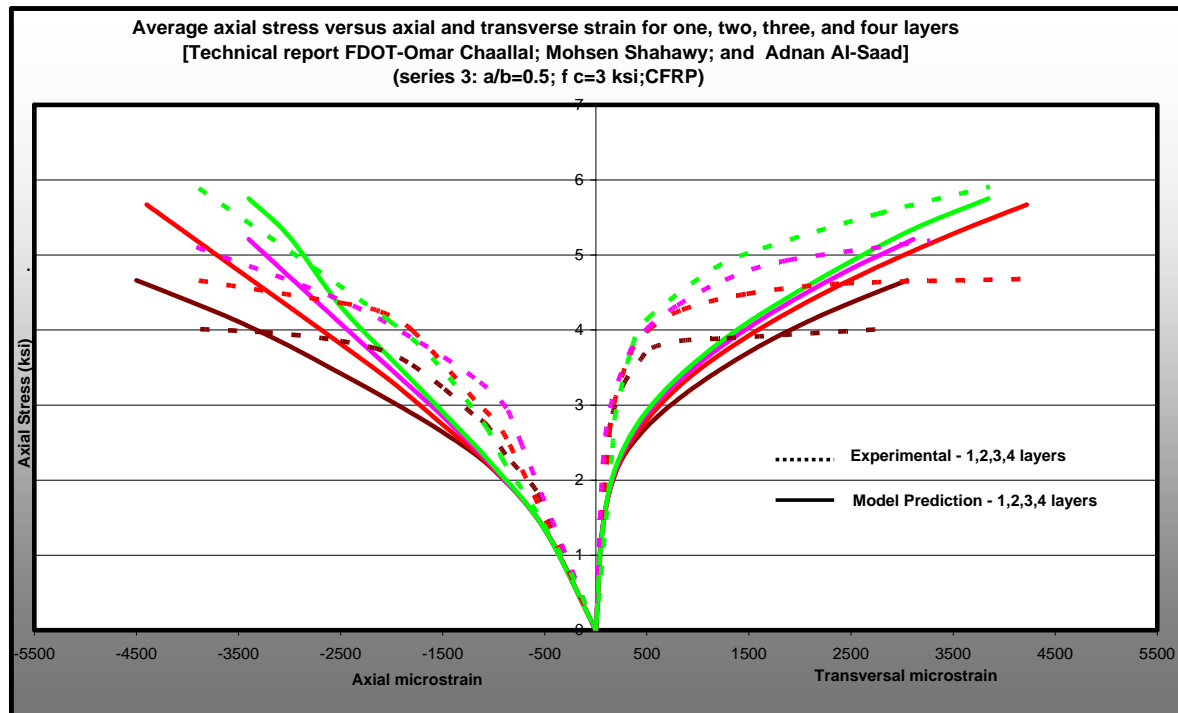


Figure 5.10 Comparison with Experimental Results (Technical Report FDOT)

Here the comparison turns out to be less satisfactory. The development of the curves seems to have more differences here but in terms of level of axial stress and maximum axial strain the curves agree adequately. Finally, the fact that those curves present the average out of the 3 specimens tested for each case should be also taken into account.

5.4 Conclusions

After comparing the proposed iteration procedure with the experimental results the following conclusions can come up:

No unconfined concrete ‘nails’ are observed, as assumed in many models. The central parts near the sides are confined from forces coming from the corners and moving parallel to the sides. Therefore, the areas where arching effect is assumed in the section are indeed partially confined so they contribute until their maximum strength (which is much lower than the inner part of the section) to the total strength of the rectangular sections. Thus, there are two different regions with different confining stress-state.

The two regions are uniaxially and biaxially confined. Therefore, the contribution of each region on the final strength can be modeled by a system of parallel springs and their strengths are added based on the corresponding strength of biaxial or triaxial stress state. By using stress-strain laws that describe these two stress states the averaged total strength can be captured adequately.

The lateral behavior can be concentrated in the diagonals of the section based on a system of springs in series. By doing so, it can be proved that the lateral strain of the sides of the rectangular section is the same. The reacting force of the confining device applied from the corners can be shared among the regions based on the path of the confining forces and the geometry of the regions. The resulted uniform pressures lead to the corresponding strength of the regions.

Correlation with experimental results turns out to be satisfactory, especially in terms of ultimate strength which is the key element for the designer. However, the necessity of comparison with more experimental results that could test more the validity of the model should be underlined.

6 REFERENCES

- Ahmad, S.H., and Shah, S.P. [1982a.] "Complete triaxial stress-strain curves for concrete", *Proceedings, ASCE*, Vol. 108, No.ST4, pp. 728-742.
- Ahmad, S.J., Khaloo, A.R. and Irshaid, A. [1991]. 'Behavior of concrete spirally confined by fiberglass filaments': *Mag. of Concrete Research*, Vol.43, No.156, pp.143-148.
- Bavarian, B., Shively, R., Ehr Gott, R., and DiJulio, R., [1996], "External Support of Concrete Structures Using Composite Materials, " *Proceedings of the First International Using Composites in Infrastructure*, ICCI '96, H. Saadatmanesh and M. R. Ehsani, Editors, Tucson, Arizona, pp. 917-928.
- Campione, G., Miraglia, N., [2003]. "Strength and strain capacities of concrete compression members reinforced with FRP." *Cem. Concr. Compos.* 25, pp.31–41.
- Canadian Standards Association _CSA_. [2002]. "Design and construction of building components with fiber-reinforced polymers." *S806-02*, Toronto.
- Chaallal, O., Shahawy, M., and Hassan, M. [2003]. "Performance of axially loaded short rectangular columns strengthened with carbon fiber reinforced polymer wrapping." *J. Compos. Constr.*, Vol.7, No.3, pp. 200–208.
- Chaallal, O., Shahawy, M., Adnan Al-Saad [2000] "Behaviour of Axially loaded short Rectangular Columns strengthened with CFRP Composite Wrapping" *Technical Report FDOT Structures Research Center*
- Chung, H. S., Yang, K. H., Lee, Y. H., and Eun, H. C. [2002]. "Stress–strain curve of laterally confined concrete." *Cem. Concr. Compos.*, 24, pp.1153–1163.
- Demers, M. and Neale, K.W. [1994]. "Strengthening of Concrete Columns with Unidirectional Composite Sheets", In: Mufti, A.A., Bakht, B. and Jaeger, L.G. (eds), *Development in Short and Medium Span Bridge Engineering '94, Proceedings of the Fourth International Conference on Short and Medium Span Bridges*, pp. 895–905, Canadian Society for Civil Engineering, Montreal, Canada.
- Elwi, A.A., and Murray, D.W. [1979]. "A 3D Hypoelastic Concrete Constitutive Relationship ". *J. Eng. Mech.* 105, pp. 623-641.
- Fardis, M. N., and Khalili, H. H. [1981]. "Concrete encased in fiberglass-reinforced plastic". *ACI J.*, Vol.78, No.6, pp. 440-446.

- Harmon, T.G., Gould, P.L., Wang, E. and Ramakrishnan, S., [1998], "Behavior of Confined Concrete Under Cyclic Loading, " *Proceedings of the Second International on Composites in Infrastructures, ICCI'98*, H. Saadatmanesh and M.R. Ehsani, Editors, Tucson, Arizona, pp. 398-409.
- Harries, K.A., Kestner, J., Pessiki, S., Sause, R., and Ricles, J., [1998], "Axial Behavior of Reinforced Concrete Columns Retrofit with FRPC Jackets," *Proceedings of the First International Using Composites in Infrastructure, ICCI '98*, H. Saadatmanesh and M. R. Ehsani, Editors, Tucson, Arizona, pp. 411-425.
- Hollaway, Leonard (Editor), [1994], *Handbook of Polymer Composites for Engineers*, Woodhead Publishing, Cambridge, England.
- Hosotani, M., Kawashima, K. and Hoshikima, J., [1997], "A study on Confinement Effect of Concrete Cylinders by Carbon Fiber Sheets," Non metallic (FRP) Reinforcement for Concrete Structures, *Proceedings of the Third International Symposium*, Vol. 1, Sapporo, Japan, pp, 209-216.
- Issa, C., and Karam, G. [2004]. "Compressive strength of concrete cylinders with variable widths CFRP wraps." *Proc., 4th International Conf. on Advanced Composite Materials in Bridges and Structures*, ACMBS-IV, Calgary, Alberta, Canada.
- Kanatharana, J. and Lu, L.-W., [1998], "Strength and Ductility of Concrete Columns Reinforced with FRP Tubes," *Proceedings of the Second International on Composites in Infrastructure., ICCI '98*, H. Saadatmanesh and M. R. Ehsani, Editors, Tucson, Arizona, pp. 370-384.
- Karam, G., and Tabbara, M. [2002]. "Corner effects on the efficiency of rectangular concrete columns with FRP confining wraps." *Proc., 3rd Middle East Symp. on Structural Composites for Infrastructure Applications MESC-3*, Aswan, Egypt.
- Karam, G., Tabbara, M., [2005], "Confinement Effectiveness in Rectangular Concrete Columns with Fiber Reinforced Polymer Wraps", *Journal of Composites for Construction, ASCE, Vol.9, No.5, pp.388-396*
- Karbhari, V. M., and Gao, Y. [1997]. "Composite jacketed concrete under axial compression—Verification of simple design equations." *J.Mater. Civ. Eng.*, Vol.9, No.4, pp. 185–193.
- Kataoka, T. et al. [1997], "Ductility of Retrofitted RC Columns with Continuous Fiber Sheets," Non metallic (FRP) Reinforcement for Concrete Structures, *Proceedings of the Third International Symposium*, Vol. 1, Sapporo, Japan, pp.547-554.
- Kaw, Autar K., [1997], *Mechanics of Composites Materials*, CRC Press, New York, NY.
- Kent, D. C., and R. Park, [1971] "Flexural Members with Confined Concrete," *Journal, Structural Division, ASCE*, Vol. 97, ST 7, pp. 1969-1990.
- Kono, S. Inazumi, M. and Kaku, T., [1998], "Evaluation of Confining Effects of CRFP Sheets on Reinforced Concrete members," *Proceedings of the Second International on Composites in Infrastructure, ICCI '98*, H. Saadatmanesh and M. R. Ehsani, Editors, Tucson, Arizona, pp. 343-355.
- Kupfer, H., H. K. Hilsdorf, and H. Rusch, [1969] "Behavior of Concrete Under Bi-axial Stress," *Journal, American Concrete Institute*, Vol. 66, No. 8, pp. 656-666

- Kurt, C.E., [1978]. "Concrete-filled structural plastic columns". *J. Struct. Div., ASCE*, Vol.104, No.1, pp. 55-63
- L.Lam , J.G.Teng [2003], "Design-oriented Stress-Strain model for FRP-confined concrete in rectangular columns" *Journal of reinforced plastics and composites*, Vol.22 , No.13,pp. 1149-1186.
- Liu C. Y., Nilson A. H., Slate F. O. [1972]. "Biaxial Stress-Strain Relations for Concrete", *J. struct.*, ASCE, Vol.5,pp. 1025-1034
- Maalej, M., Tanwongsva, S., and Paramasivam, P. [2003]. "Modelling of rectangular RC columns strengthened with FRP." *Cem. Concr. Compos.*,25, 263–276.
- Mander J.B., Priestley M.J.N., Park R. [1988] "Observed stress-strain behavior of confined concrete."ASCE Journal of Structural Engineering, Vol. 114, No. 8, pp 1827-1849
- Miller, Tara, [1998], *Introduction to Composites, 4th Edition*, Composites Institute, Society of the Plastics Industry, New York, NY.
- Mirmiran, A., Shahawy, M., Samaan, M., El Echary, H., Mastrapa, J. C.,and Pico, C.[1998] Effect of column parameters on FRP-confined concrete." *J. Compos. Constr.*, Vol.2, No.4,pp. 175–185.
- Miyaushi, K., Nishibayashi, S. and Inoue, S., (1997), "Estimation of Strengthening Effects with Carbon Fiber Sheet for Concrete column," Non metallic (FRP) Reinforcement for Concrete Structures, *Proceedings of the Third International Symposium*, Vol. 1, Sapporo, Japan, pp.217-232.
- Murphy, John, [1998], *Reinforced Plastics Handbook*, Elsevier Science, Oxford, England.
- N.S.Ottosen [1977] "A failure criterion for concrete" *Journal of the Engineering Mechanics Division*, Vol.103, No. EM4, pp. 527-533
- Nanni, A., and Bradford, M.N. [1995]. "FRP jacketed concrete under uniaxial compression". *Constr. & Bldg. Mater.*, Vol.9, No.2, pp.115-124.
- Pantazopoulou, S.J., and Mills, R. H. (1995). "Microstructural aspects of the mechanical response of plain concrete." *ACI Mat. J.*, 92(Nov.–Dec.), pp. 605–616.
- Parvin, A., and Wang, W. [2001]. "Behavior of FRP jacketed concrete columns under eccentric loading." *J. Compos. Constr.*, Vol. 5, No.3, pp. 146–152.
- Parvin, A., and Wang, W. [2002]. "Tests on concrete square columns confined by composite wraps." *Proc., 3rd International Conf. on Composites in Infrastructure ICCI'02*, San Francisco
- Pessiki, S., Harries, K. A., Kestner, J. T., Sause, R., and Ricles, J. M. [2001] "Axial behavior of reinforced concrete columns confined with FRP jackets." *J. Compos. Constr.*, Vol.5, No.4, pp. 237–245.
- Picher, F., Rochetter, P. and Labossiere, p. [1996], "Confinement of Concrete Cylinders with CFRP, " *Proceedings of the First International Conference on Composites in Infrastructure, ICCI '96*, Edited by Saadatmanesh and Ehsani, Tucson, Arizona, pp. 829-841.
- Popovics, S. [1973]. "A numerical approach to the complete stress-strain curves for concrete." *Cem.*

- Concr. Res., Vol.3, No.5, pp.583–599.*
- Restrepol, III. I., and DeVino, B., [1996]. 'Enhancement of the Axial Load Carrying Capacity of Reinforced Concrete Columns by Means of Fiberglass-Epoxy Jackets, "*Advanced Composite Materials in Bridges and Structures, Second International Conference*, Canadian Society of Engineering, M.M. El-Badry, Editor, pp. 547-553.
- Richardson, Terry, [1987], *Composites: A Design Guide*, Industrial Press, New York, NY.
- Richart F.E., Brandtzaeg A. And Brown R.L. [1928] A study of the failure of concrete under combined compressive stresses. Engineering Experiment Station Bulletin No. 185, University of Illinois, Urbana
- Rochette, P., and Labossière, P. [2000] "Axial testing of rectangular column models confined with composites." *J. Compos. Constr.*, Vol.4, No.3, pp.129–136.
- Rosato, Dominick V., [1997], *Designing with Reinforced Plastics*, Hanser/Gardner, Cincinnati, Ohio.
- Saadatmanesh M., Ehsani, M. R., Limin Jin, [1996], 'Behavior of Concrete Retrofitted with Fiber Composite Straps Under Cyclic Loading' . Fiber Composites Infrastructure. *Proceedings of the First International Conference on Composites in Infrastructures, ICCI '96*, H. Saadatmanesh and M.R. Ehsani, Editors, Tucson, Arizona, U.S.A., pp. 842-856.
- Schwarz, M.M., [1992], *Composite Materials Handbook*, McGraw Hill, Inc., New York.
- Shehata, I.A.E.M., Carneiro, L.A.V. and Shehata, L.C.D. [2002]. "Strength of Short Concrete Columns Confined with CFRP Sheet", *Materials and Structures*, Vol.35, No.1, pp. 50–58.
- Sheikh SA, Uzumeri SM.[1980] "Strength and ductility of tied concrete columns. *J Struct Div*;106(ST5):pp.1079–112.
- Spoelstra, M. R., and Monti, G. [1999] "FRP-confined concrete model." *J. Compos. Constr.*, Vol. 3, No.3, pp.143–150.
- Suter, R. and Pinzelli, R. [2001]. "Confinement of Concrete Columns with FRP Sheets", *Proceedings, Fifth International Conference on Fibre Reinforced Plastics for Reinforced Concrete Structures*, pp.793–802, Cambridge, U.K.
- Watanabe, K., and al. [1997], "Confinement Effect of FRP Sheet on Strength and Ductility of Concrete Cylinders Under Uniaxial Compression," Non metallic (FRP) Reinforcement for Concrete Structures, *Proceedings of the Third International Symposium*, Vol. 1, Sapporo, Japan, pp.233-238.
- Xiao, Y., and Wu, H. [2000]. "Compressive behavior of concrete confined by carbon fiber composite jackets." *J. Mater. Civ. Eng.*, Vol.12, No.2, pp.139–146.
- Yang, X., Nanni, A., and Chen, G. [2001a]. "Effect of corner radius on the performance of externally bonded FRP reinforcement." *Proc., 5th International Symp. on Fiber Reinforced Polymer for Reinforced Concrete Structures FRPRCS-5*, Cambridge, U.K., 197–204.

APPENDIX A

CODES IN MATLAB FOR THE ITERATION PROCEDURE

MAIN CODE

```
tic;%Starts clock
H= Height
W=Width
R=Radius
fc=Concrete_strength
Ej=FRP_Elastic_Modulus
tj=FRP_thickness
eju=FRP_ultimate_strain
step=Deformation_step
assumption=1;

%Section Geometry
A=H*W;
%Regions
%Biaxial Region
Hb=H/2;
hb=Hb/4;
Wb=W/2;
wb=Wb/4;
Ab=Wb*hb+Hb*wb-hb*wb;
Bb=sqrt(hb^2+wb^2);
%Triaxial Region
Ht=Hb-hb;
Wt=Wb-wb;
At=Ht*Wt;
%Concrete
ft=fc/10;
v=0.2;
Ec=5000*sqrt(fc);
eco=0.002;
```

```
%Confinement efficiency factor by Gebran Karam & Mazen Tabbara
ke=R/Hb*0.5*(1+Hb/Wb);
%Volumetric Strain-parameters
a=0.7;
b=1.2;
c=2;
%Vertical deformation - ITERATION
fc0=assumption;
P=zeros(5000,11);
for r=1:5000
    ec=r*step;
    fc_initial=fc0;
    %Calculation of Volumetric strains
    if fc_initial <= a*fc
        eV=-(1-3*v)*10^-4*fc_initial;
    elseif fc_initial >a*fc
        eV=-(1-3*v)*10^-4*b*fc*((fc_initial/(b*fc))-((fc_initial-a*fc)/(b*fc-a*fc))^c);
    end
    %Calculation of Area Strains
    eA=eV+ec;
    %Calculation of elongation Strains
    el=sqrt(eA+1)-1;
    %Diagonal Lateral force applied in the corners
    Fl=Ej*el*tj*sqrt(2)*ke;
    %Lateral Pressures in the different regions
    fl_biaxial=Fl/Bb;
    fl_1triaxial=(Fl/Ht);
    fl_2triaxial=Fl/Wt;
    %Verical Stresses
    fcc_triaxial=ottosen(-fc,ft,-fl_1triaxial,-fl_2triaxial); %Maximum Vertical stress for triaxial stress
    state by ottosen -the function is included in a seperate file
    fc_triaxial=mander(Ec,fc,ec,eco,-fcc_triaxial); %Vertical stress for triaxial stress state by Mander-
    the function is included in a seperate file
    fc_biaxial=liu(Ec,ec,fc,v,fl_biaxial);%Vertical Stress for bixial stress state by Liu-the function is
    included in a seperate file
    fc_total=fc_triaxial*4*At/A+fc_biaxial*4*Ab/A;% Sumation based on the areas of the different
    regions
    fc0=fc_total; %Correction of the initial assumption
    while abs(fc_total-fc_initial)>0.01
        fc_initial=fc0;
        if fc_initial <= a*fc
            eV=-(1-3*v)*10^-4*fc_initial;
        elseif fc_initial >a*fc
            eV=-(1-3*v)*10^-4*b*fc*((fc_initial/(b*fc))-((fc_initial-a*fc)/(b*fc-a*fc))^c);
```



```
end
eA=eV+ec;
el=sqrt(eA+1)-1;
Fl=Ej*el*tj*sqrt(2)*ke;
fl_biaxial=Fl/Bb;
fl_1triaxial=Fl/Ht;
fl_2triaxial=Fl/Wt;
fcc_triaxial=ottosen(-fc,ft,-fl_1triaxial,-fl_2triaxial);
fc_triaxial=mander(Ec,fc,ec,eco,-fcc_triaxial);
fc_biaxial=liu(Ec,ec,fc,v,fl_biaxial);
fc_total=fc_triaxial*4*At/A+fc_biaxial*4*Ab/A;
fc0=fc_total; %Correction of the initial assumption
end
fc0=fc_total; %Correction of the initial assumption
%Results are saved in Matrix P
P(r,1)=ec;
P(r,2)=eV;
P(r,3)=eA;
P(r,4)=el;
P(r,5)=fc_total;
P(r,6)=fl_biaxial;
P(r,7)=fc_biaxial;
P(r,8)=fl_1triaxial;
P(r,9)=fl_2triaxial;
P(r,10)=-fcc_triaxial;
P(r,11)=fc_triaxial;
if el>eju
    break
end
end
%takes out the zero elements of P
m=1;
while P(m,1)>0
    m=m+1;
end
k=m-1;
K=P(1:k,:); %Contains all the results
%Results
Vertical_Strain=[0 ; K(:,1)]
Lateral_Strain=[0 ; K(:,4)]
Vertical_Stress=[0; K(:,5)]
Biaxial_Lateral_stress=[0 ; K(:,6)]
Biaxial_Vertical_stress=[0 ; K(:,7)]
Triaxial_one_Lateral_stress=[0 ; K(:,8)]
Triaxial_two_Lateral_stress=[0 ; K(:,9)]
```

```
Triaxial_Maximum_Vertical_stress_fcc=[0 ; K(:,10)]
Traxial_Vertical_stress=[0 ; K(:,11)]
if max(Vertical_Stress)>Vertical_Stress(length(Vertical_Stress))
    Maximum_Vertical_Stress=max(Vertical_Stress)
    Ultimate_Vertical_Stress=Vertical_Stress(length(Vertical_Stress))
end
if max(Vertical_Stress)==Vertical_Stress(length(Vertical_Stress))
    Maximum_Vertical_Stress=Vertical_Stress(length(Vertical_Stress))
end
Maximum_Lateral_Strain=Lateral_Strain(length(Lateral_Strain))
q=1;
if max(Vertical_Stress)>Vertical_Stress(length(Vertical_Stress))
    while K(q+1,5)>K(q,5)
        q=q+1;
    end
    Strain_at_Peak_Stress=K(q,1)
    Ultimate_Vertical_Strain=Vertical_Strain(length(Vertical_Strain))
end
if max(Vertical_Stress)==Vertical_Stress(length(Vertical_Stress))
    Maximum_Vertical_Strain=Vertical_Strain(length(Vertical_Strain))
end
% Create plot
plot(Vertical_Strain,Vertical_Stress,-Lateral_Strain,Vertical_Stress);
grid
xlabel('Axial Strain (+), Lateral Strain (-)');
ylabel('Axial Stress (MPa)');
title('Stress-Strain Curve');
toc;%stops clock
```

ACCOMPANYING FUNCTIONS

function fcc=ottosen(fc,ft,s2,s3)

```
fcc0=fc;
fcc=fcc0;
w=1;
k=(ft)/abs(fc);
I1=fcc+s2+s3;
sigma_oct=1/3*I1;
ss1=fcc-sigma_oct;
ss2=s2-sigma_oct;
ss3=s3-sigma_oct;
J2=0.5*(ss1^2+ss2^2+ss3^2);
J3=1/3*(ss1^3+ss2^3+ss3^3);
taf_oct=sqrt(2/3*J2);
A = 222*k^2 - 66.545*k + 5.7104; %Equation based on the points of the original paper
```

```
B= 375.87*k^2 - 112.66*k + 10.703; %Equation based on the points of the original paper
K1=1157.6*k^2 - 345.91*k + 34.75; %Equation based on the points of the original paper
K2=-5.125*k^2 + 0.3575*k + 0.9956;
lamda_t=1153.4*k^2 - 345.69*k + 34.746;
lamda_c=522.87*k^2 - 156.71*k + 16.974;
cos3theta=3*sqrt(3)/2*J3/(J2^1.5);
if cos3theta>=0
    lamda=K1*cos(1/3*acos(K2*cos3theta));
end
if cos3theta<0
    lamda=K1*cos(pi/3-1/3*acos(-K2*cos3theta));
end
S=A*J2/(abs(fc)^2)+lamda*sqrt(J2)/abs(fc)+B*I1/abs(fc);
while abs(S-1)>0.00001
    w=w+1;
    fcc=fcc0-0.00001*w;
    I1=fcc+s2+s3;
    sigma_oct=1/3*I1;
    ss1=fcc-sigma_oct;
    ss2=s2-sigma_oct;
    ss3=s3-sigma_oct;
    J2=0.5*(ss1^2+ss2^2+ss3^2);
    J3=1/3*(ss1^3+ss2^3+ss3^3);
    taf_oct=sqrt(2/3*J2);
    A = 222*k^2 - 66.545*k + 5.7104;
    B= 375.87*k^2 - 112.66*k + 10.703;
    K1=1157.6*k^2 - 345.91*k + 34.75;
    K2=-5.125*k^2 + 0.3575*k + 0.9956;
    lamda_t=1153.4*k^2 - 345.69*k + 34.746;
    lamda_c=522.87*k^2 - 156.71*k + 16.974;
    cos3theta=3*sqrt(3)/2*J3/(J2^1.5);
    if cos3theta>=0
        lamda=K1*cos(1/3*acos(K2*cos3theta));
    end
    if cos3theta<0
        lamda=K1*cos(pi/3-1/3*acos(-K2*cos3theta));
    end
    S=A*J2/(abs(fc)^2)+lamda*sqrt(J2)/abs(fc)+B*I1/abs(fc);
end

function fc_tri axial=mander(Ec,fc,ec,eco,fcc)
ecc=eco*(1+5*(fcc/fc-1));
x=ec/ecc;
Esec=fcc/ecc;
r=Ec/(Ec-Esec);
```

```
fc_triaxial=(fcc*x*r)/(r-1+x^r);
```

```
function fc_biaxial=liu(Ec,ec,fc,v,s2)
```

```
q=1;
```

```
a0=0.00001;
```

```
a=a0;
```

```
if a<0.2
```

```
    fcp=(1+a/(1.2-a))*fc;
```

```
end
```

```
if a>=0.2 & a<=1
```

```
    fcp=1.2*fc;
```

```
end
```

```
if a<=1
```

```
    ecp=0.0025;
```

```
end
```

```
x=s2/a;
```

```
fc_biaxial=(ec*Ec)/((1-v*a)*(1+(Ec/(fcp*(1-v*a))-2/(ecp+0.005))*ec+(ec/(ecp+0.005))^2));
```

```
while abs(fc_biaxial-x)>0.1
```

```
    q=q+1;
```

```
    a=a0+q*0.000001;
```

```
    if a<=1
```

```
        if a<0.2
```

```
            fcp=(1+a/(1.2-a))*fc;
```

```
        end
```

```
        if a>=0.2 & a<=1
```

```
            fcp=1.2*fc;
```

```
        end
```

```
        if a<=1
```

```
            ecp=0.0025;
```

```
        end
```

```
        x=s2/a;
```

```
        fc_biaxial=(ec*Ec)/((1-v*a)*(1+(Ec/(fcp*(1-v*a))-2/(ecp+0.005))*ec+(ec/(ecp+0.005))^2));
```

```
    end
```

```
    if a>1
```

```
        break %When a>1 the descending branch of the stress-strain law starts-this part is excluded  
        keeping constant the strength
```

```
    end
```

```
end
```

```
if a>1
```

```
    fc_biaxial=1.2*fc;
```

```
end
```